UNIVERSITÀ
DEGLI STUDI
DI PADOVA

University of Padova

Department of Surgery, Oncology and Gastroenterology

PhD course in Clinical and Experimental Oncology and Immunology

29th series

THE ENDOCYTIC ADAPTOR DAB2 CONTROLS THE MACROPHAGE-ASSISTED METASTATIC PROCESS

Coordinator: Prof. Paola Zanovello

Supervisor: Ilaria Marigo, PhD

PhD student: Kevin Leone

TABLE OF CONTENTS

SUMMARY

The metastatic process is the main cause of cancer-associated death. Nonetheless, its underlying pathophysiological and molecular mechanisms are still poorly understood. The dissemination of malignant cells from the primary tumor to distant organs is a multistep process that requires detachment of cancer cells from the site of origin, remodelling of the extracellular matrix (ECM), migration into blood or lymph vessels, seeding to an ectopic tissue and proliferation. In recent years, tumor-infiltrating immune cells have been demonstrated to be critical determinants for ECM remodelling and metastatic progression. In particular, tumor-associated macrophages (TAMs) are able to suppress $CD8^+$ T-cell infiltration and anti-tumor immunity in primary tumors and can promote angiogenesis and metastasis formation. Although the number of studies in support of the pro-metastatic role of TAMs is rapidly increasing, the molecular mechanisms through which these cells act are not completely elucidated.

A gene-profiling analysis performed in our group on tumor-infiltrating myeloid cells from different murine tumors showed a significant upregulation of the gene *Dab2* (disabled 2, mitogen-responsive phosphoprotein). Dab2 codifies for an adaptor protein that is involved in the clathrin-mediated endocytosis (CME) of specific plasma membrane receptors, in particular integrins. Once internalized, integrins can be recycled back to other sites of the membrane where they are needed to function as ECM-binding receptors and ECM stiffness sensors.

In the present work, we prove that the expression of the protein DAB2 in TAMs is associated with an increased number of lung metastases in murine tumor models. We analyzed the possible role of DAB2 in the context of the tissue remodelling process that takes place during tumor progression and metastatization. Our data show that DAB2 is upregulated during *in vitro* M- or GM-CSF–induced macrophage differentiation, although it is not essential for this process. Interestingly, in tissue slices from murine tumors and metastatic lungs, DAB2-expressing TAMs were localized along the invasion frontline between the tumor and the surrounding healthy tissues, where they might have a specific function in facilitating cancer cell invasiveness. We demonstrate that DAB2 participates in CME-dependent recycling of α1, α5, α6 and β1 integrins. By mediating integrin turnover, DAB2 allowed the internalization of integrin-bound ECM fragments, thus promoting *in vitro* ECM remodelling and tumor cell invasion through the substrate.

A gene set enrichment analysis allowed us to correlate the expression of DAB2 in macrophages with the transcription regulator YAP (Yes-Associated Protein), that is emerging as a central modulator of cellular mechanotransduction pathways. By means of gene silencing, substrate stiffness

modulation and immunofluorescence we validated the existence of a YAP-mediated DAB2 regulation.
Finally, analyses on clinical data and samples from breast cancer patients indicated that DAB2 and YAP were coexpressed in macrophages at the tumor invasion frontline. Remarkably, the presence of $DAB2^{+}$ TAMs in biopsies correlated with a poor prognosis in terms of lymph node metastases, tumor vascularization, cancer cell proliferation and disease-free survival, thus representing a new, potential prognostic marker for breast cancer patients.

The results achieved with this work allow us to propose a novel role for DAB2 in the macrophage-assisted, mechanotransduction-driven metastatic process. We believe that the expression of the *Dab2* gene is regulated by the ECM stiffness, through a mechanism in which the mechano-sensing properties of integrins and the subsequent intervention of YAP might play a major role. In this way, the high ECM rigidity of the tumor could stimulate the YAP-mediated upregulation of DAB2 in TAMs, which in turn degrade the ECM.

INTRODUCTION

CANCER AND ITS MICROENVIRONMENT

The hallmarks of cancer

Tumorigenesis is a pathological process in which genetic alterations lead to a progressive transformation of normal cells into malignant derivatives that abnormally proliferate inside the host[1].

Cancer is a multi-faced and heterogeneous disease. However, some characteristics have been shown to be common to all types of cancer and in the last sixteen years they have been described as 'the eight hallmarks of cancer' with the aim of simplifying a complex and still not well-understood biological phenomenon (Figure 1)[1-3].

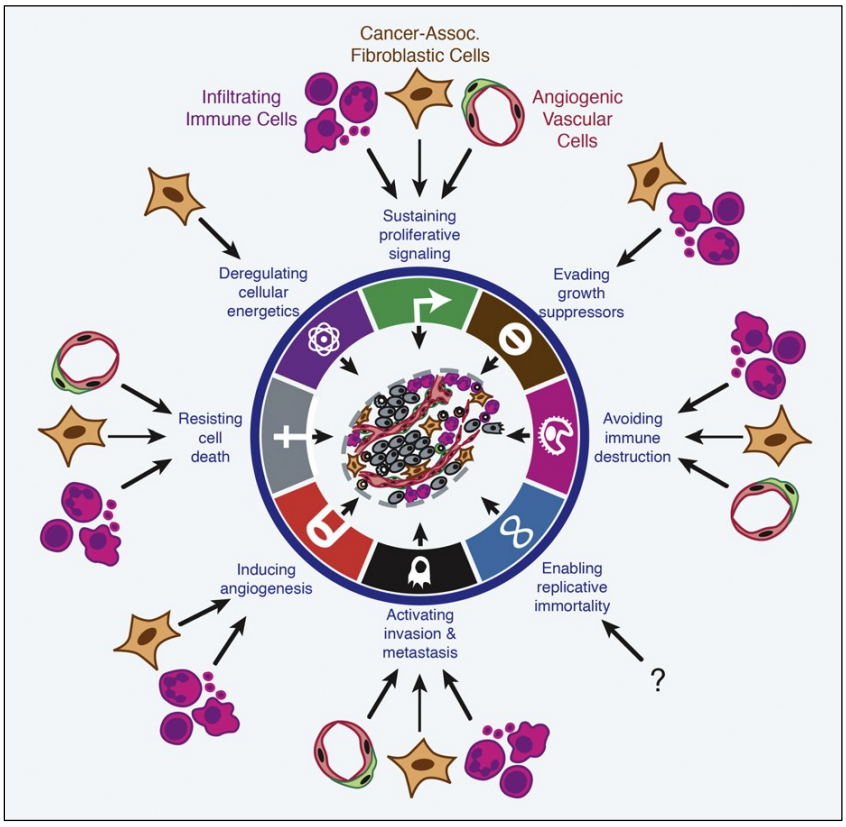

Figure 1 - The hallmarks of cancer and the contribution of stromal cells. *Among the eight largely accepted hallmarks of cancer, seven have been demonstrated to involve stromal cells from the tumor microenvironment. These cells include three groups: infiltrating immune cells, cancer-associated fibroblasts and angiogenic vascular cells, each having specific functions and pro- or anti-tumor contributions (reproduced from Hanahan and Coussens, 2012[3]).*

Four of these traits define cancer cells as able to sustain proliferative signalling, evade growth suppressors, resist cell death and enable replicative immortality. In this way aberrant cells can escape the homeostatic control and sustain indefinite, chronic proliferation leading to a loss of original tissue architecture and functionality. Moreover, neoplastic cells show a fifth metabolic alteration, since they deregulate cellular energetics and produce energy mainly through aerobic glycolysis. This biochemical pathway is thought to sustain high-rate anabolism and proliferation by providing the glycolytic intermediates necessary for amino acid and nucleoside biosynthesis[4].

A sixth hallmark of cancer is angiogenesis, consisting in the formation of new blood vessels in the tumor mass. On one hand, the circulation supplies cells with oxygen and nutrients, thus favouring their aerobic metabolism and further proliferation. On the other hand, angiogenesis ensures cells a way to enter the bloodstream and move elsewhere inside the host. This leads to another key characteristic of cancer: invasion of surrounding tissues and metastatization to distant organs.

Finally, the eighth hallmark is the ability of cancer cells to avoid recognition and destruction by the host immune system[5]. As discussed later, this is achieved by both selection of less immunogenic tumor cell clones and promotion of an immunosuppressive microenvironment able to hamper an efficient immune response against the neoplastic lesion.

It is worth to remember also an emerging feature of tumors, the presence of cancer stem cells (CSCs), a rare and chemotherapy-resistant subpopulation of undifferentiated cells defined by the ability to sustain their own self-renewal and, at the same time, to generate more differentiated cells, which constitute the great bulk of the tumor mass. CSCs are believed to arise from genetic mutations that disrupt the proliferative and differentiative programs of normal stem cells[6-8].

The metastatic spreading

During tumor progression, aberrant cells can acquire invasive capabilities and spread throughout the body, usually debilitating and even killing their host. This process, called 'metastatization', is responsible for the 90% of cancer-associated deaths[9]. Nonetheless, its underlying pathophysiological and molecular mechanisms are still poorly understood.

Dissemination of malignant cells from the primary tumor to distant organs is a multistep process (Figure 2). First of all, cancer cells assume an invasive phenotype and detach from the site of origin (A in Figure 2). After remodelling of basal membranes and extracellular matrix (ECM), cells migrate into blood or lymph vessels (intravasation) becoming anchorage-inde-

pendent CTCs (circulating tumor cells, B-C). Then, CTCs exit from the circulation (extravasation) and colonize the ectopic tissue (D). In this phase, it is fundamental that tumor cells survive to the immune system, either as a single cell or as a small cluster (E). If not eliminated, cells adapt to the new microenvironment and proliferate to generate a secondary tumor mass (F)[10].

Understanding the mechanisms of this physical translocation would be important for both prevention in patients with early cancer lesions and therapy in patients with already-established metastases[10].

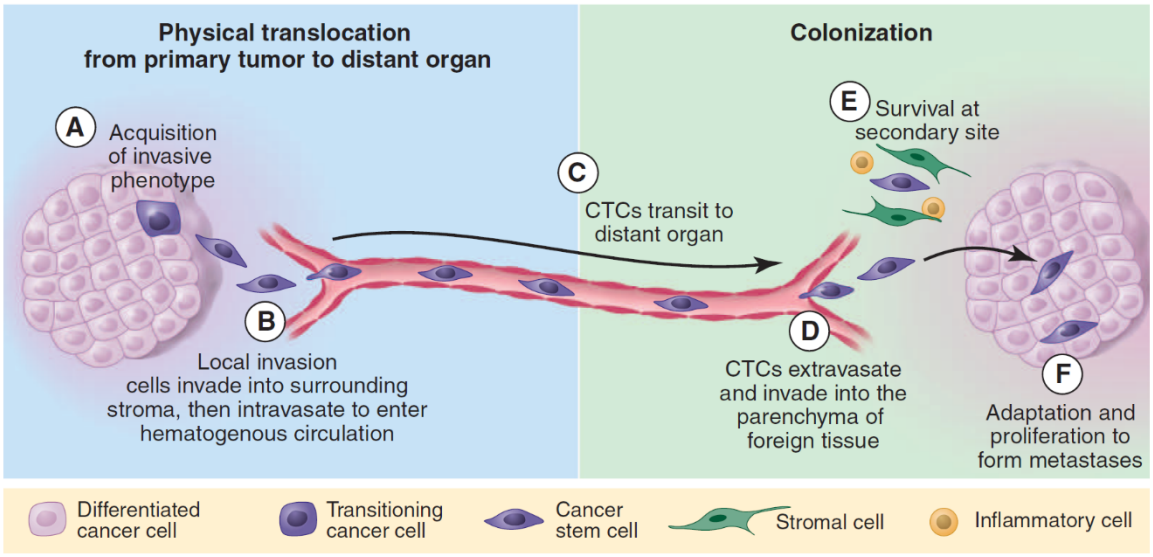

Figure 2 - The metastatic process. *Metastasis formation can be divided into two main phases: physical translocation of cancer cells from the primary tumor to a distant site (A-C) and colonization of that site (D-F). CTC: circulating tumor cell (reproduced from Chaffer et al., 2011[9]).*

Cellular components of the tumor microenvironment

For decades the attention of researchers focused only on neoplastic cells and their alterations in comparison to normal cells. Great efforts have been made to identify genetic/epigenetic mutations and dominant oncogenes or tumor suppressor genes and to understand the causes of tumor cell genomic instability. Several oncogenic factors and signalling pathways contributing to the transformation into cancer cells have been discovered, many of which have emerged as interesting potential therapeutic targets[3].

However, it became increasingly clear that tumors are complex, multi-component organ-like structures in which malignant cells co-exist with a repertoire of other cell populations found in the tumor-associated stroma and involved in intricate reciprocal interactions (Figure 1). Both resident and recruited stromal cells play key roles that can determine the final outcome in

terms of tumor progression and spreading. Some populations have an anti-tumor effect, while others can be corrupted by cancer cells to support their growth and invasiveness.

The stromal cells that are involved in this process belong to three subsets: angiogenic vascular cells, cancer-associated fibroblastic cells and infiltrating immune cells[3].
The angiogenic vascular cells are endothelial cells forming the tumor-associated vasculature. These cells can also be activated to construct new blood vessels (angiogenesis) or, in some cases, lymphatic vessels at the periphery of tumors (lymphangiogenesis)[11,12]. As already outlined, vessels are indispensable to continuously supply tumor cells with nutrients and oxygen and allow them to invade tissues and form metastases. Angiogenic vascular cells are supported by both pericytes and mesenchymal cells with finger-like projections that envelope blood vessels. These cells provide paracrine signals to the quiescent endothelium and collaborate with endothelial cells in synthesizing the vascular basement membrane that sustains the hydrostatic pressure within blood vessels[13]. The functioning of tumor pericytes (but not that of normal pericytes) is based on the platelet-derived growth factor (PDGF) signalling. Indeed, the pharmacological inhibition of its receptor on tumor pericytes compromises local vascular integrity and function[14].
The second stromal subset is represented by cancer-associated fibroblasts (CAFs), often the major constituent of the tumor stroma and able to favour tumor proliferation, angiogenesis, invasion and metastasis formation. CAFs can remodel the architecture of the stroma by degrading or synthesising components of the ECM and can recruit both endothelial cells and pericytes by releasing growth factors and chemokines[15-17].
The third stromal population consists in the infiltrating immune cells, that are leukocytes of both myeloid and lymphoid origins, already present in the tissue or recruited from the circulation due to the state of chronic inflammation established by the tumor[18]. As discussed later, these immune populations can be stimulated by the microenvironment to either suppress or favour tumor growth. In the second case, they can be reprogrammed by tumor-derived soluble factors (TDSFs) to create a tolerogenic environment or even sustain pro-tumor processes[18].

The relevance of each cell class varies with tumor type and organ, since they can behave differently in the presence of diverse microenvironments and underlying genetic alterations[2,3].
All the previously described hallmarks of cancer, with the exception of the gain of replicative immortality, have already been demonstrated to involve one or more of these subsets. For this reason, in the last years research efforts against cancer disease have focused on studying the single cell types that compose the tumor microenvironment and their pro- or anti-tumoral mechanisms of action.

Tumor-infiltrating inflammatory cells

One of the main challenges in immunology is to understand how the immune system acts in cancer development and progression. Tumors are infiltrated by leukocytes, although to various degrees[19]. These infiltrations are similar to those that arise in normal inflamed tissues, suggesting that an inflammatory reaction usually occurs in tumors. Historically, this was interpreted as an attempt of the immune system to eradicate the tumor.

The anti-tumor response is mainly mediated by $CD8^+$ cytotoxic T lymphocytes (CTLs), $CD4^+$ Th_1 (T helper) cells and natural killer (NK) cells, which have a central role in preventing tumor development[19,20]. Accordingly, in many tumor types, infiltration of these populations in the neoplastic lesion correlates with augmented disease-free and overall survival of patients, absent/reduced metastases and reduced relapse after therapy[19].

However, aberrant cells are often able to bypass the immune surveillance in order to uncontrollably proliferate and invade other tissues. The 'immunoediting' hypothesis was formulated to explain this. It describes tumor development as a three-phase process: 1) in the 'elimination' phase, arising cancer cells are subjected to the immune surveillance; 2) during the 'equilibrium', that can last even for decades, a balance is established between the elimination of immunogenic cancer cells and the survival of mutated less-immunogenic clones, which arise as a consequence of the selective pressure induced by the immune system (immunoediting); 3) in the 'escape' phase, some less immunogenic cancer cells can eventually become fully competent in evading the host defences and the tumor begins to progress[5].

Tumor cells can become less immunogenic by expressing less aberrant molecules or downregulating the antigen-presenting machinery[21,22]. However, another escape-promoting factor is that tumor-associated inflammation is generally not able to promote an efficient cell-mediated immune response[23]. Indeed, a plentiful literature in the last years has highlighted the presence of tumor-infiltrating immune cells able to actively suppress the immune surveillance and favour both tumor progression and metastatic spreading[5,24,25].

For this reason, the presence of specific immunosuppressive cell subsets in the tumor mass is considered a predictor of poor prognosis in oncological patients[19] and is also responsible for the poor efficacy of anti-cancer immunotherapies[26].

Among the immunosuppressive populations that accumulate in the tumor, the cells of myeloid origin play an important role[25]. Tumor progression can induce a blockade in the myeloid differentiation program that leads to the accumulation of immature myeloid cells. These cells can be recruited in the tumor mass attracted by the mounting inflammation state and, once infiltrated, can be reprogrammed by TDSFs, molecules that are able to promote tumor growth and invasion of surrounding healthy tissues[18]. Under the sustained influence of TDSFs, reprogrammed myeloid cells can promote a powerful immunosuppressive activity against $CD8^+$

CTLs[18,25]. Their immunomodulatory mechanisms comprise: the inhibition of the anti-tumor Th_1 immune response through the release of anti-inflammatory cytokines like transforming growth factor-β (TGF-β), interleukin (IL)-4/6/10/13, macrophage colony-stimulating factor (M-CSF or CSF-1) and vascular-endothelial growth factor (VEGF); the block of maturation and activation of antigen presenting cells (APCs) that in this way cannot prime T lymphocytes; the inactivation or elimination of previously activated T lymphocytes[25].
Moreover, immune suppressive cells can also migrate into secondary lymphoid organs and induce immune tolerance to tumor antigens, further impairing the anti-tumor immune response[27,28].
Tumor-infiltrating myeloid cells include dendritic cells, granulocytes, myeloid-derived suppressor cells and tumor-associated macrophages.

Dendritic cells

Dendritic cells (DCs) are terminally differentiated myeloid cells that act as APCs by processing and presenting antigens to T cells. They differentiate in tissues from bone marrow progenitors and, at least in part, from monocytes and comprise two major subsets: conventional DCs and plasmacytoid DCs[29]. Conventional DCs uptake antigens in peripheral tissues but do not present them to T cells unless they are activated by pathogen-associated molecular patterns (PAMPs) or damage-associated molecular patterns (DAMPs), both recognized by the evolutionary conserved toll-like receptors (TLRs)[30]. The binding of these ligands to TLRs induces maturation of immature DCs, which translates into expression of the antigen-presenting machinery, co-stimulatory molecules and T cell-activating cytokines, as well as upregulation of chemokine receptors that drive migration of DCs to lymph nodes. Plasmacytoid DCs recognize viral nucleic acids and self DNA fragments through the TLR pathway and consequently secrete high amounts of interferon (IFN)-α to induce innate and adaptive immune responses. Furthermore, these DCs are known to elicit autoimmunity, if chronically activated, as well as immune tolerance, if they remain resting[29].

DCs in tumor-bearing hosts do not usually adequately stimulate immune responses. TDSFs induce abnormal myelopoiesis bringing to decreased production of mature DCs, accumulation of immature DCs inside the tumor, shift of DC precursors towards macrophage differentiation and increased production of immature myeloid cells[31]. Hypoxia and stimulation of DCs with adenosine in the tumor microenvironment impair their allostimulatory activity and cause them to drive the development of a Th_2 rather than an anti-tumor Th_1 immune response[32]. Other compounds inducing dysfunction of DCs are lactic acid, which is abundant in the tumor due to increased glycolytic catabolism, and lipids, which accumulate in DCs from tumor-bearing hosts and impair DC ability to process soluble antigens[33,34].

Tumor-infiltrating DCs can also actively suppress $CD8^+$ T cell responses because of the expression of the immune suppressive molecules arginase 1 (ARG1), IL-10, TGF-β and indoleamine 2,3-dioxygenase (IDO), which is also produced by suppressive plasmacytoid DCs[35,36]. IDO is an enzyme that limits T cell growth by consuming local L-tryptophan and enhances the activity of regulatory T lymphocytes (Tregs), a particular subset of $CD4^+$ T helper cells that inhibit T cells to sustain peripheral tolerance in tissues[37].

While immature tumor-infiltrating DCs are considered to be immunosuppressive and tolerogenic, mature and functionally competent DCs show immunostimulatory properties[38]. Accordingly, the infiltration of mature DCs in tumors correlates with a better outcome for patients[39]. Moreover, we recently demonstrated that a particular subset of DCs, the tumor necrosis factor (TNF)- and inducible nitric oxide synthase (iNOS)-producing DCs (Tip-DCs), are pivotal for increasing the efficacy of adoptive cell therapy (ACT) against the tumor. Following ACT, Tip-DCs accumulate within the tumor microenvironment where they cross-present tumor antigens and activate adoptively-transferred and endogenous $CD8^+$ T cells through a pathway requiring CD40-CD40L[40].

Granulocytes

Granulocytes are leukocytes characterized by cytoplasmic granules and multi-lobed nuclei. They comprise neutrophils, eosinophils and basophils that can be distinguished on the basis of a specific histologic staining. Neutrophils, the most abundant granulocytes, are $CD11b^+$ $Ly6G^+$ phagocytic cells that rapidly respond to infections by destroying engulfed pathogens[41]. The role of granulocytes in cancer is controversial, probably due to the presence of two opposite tumor-infiltrating subsets: N1 neutrophils, with an anti-tumor cytotoxic effect and able to release pro-inflammatory cytokines, and N2 neutrophils, expressing ARG1 and low levels of pro-inflammatory molecules and able to favour tumor growth as well as inhibit activation of $CD8^+$ cytotoxic lymphocytes[42].

For instance, neutrophils were showed to kill tumor cells by producing reactive oxygen species (ROS) and inhibit the formation of metastases in a model of murine mammary carcinoma[43]. On the contrary, in response to anti-VEGF therapy, the tumor can secrete granulocyte colony-stimulating factor (G-CSF) to induce neutrophil production in the bone marrow and recruitment to the tumor; once there, neutrophils compensate for the effect of the therapy favouring angiogenesis and secreting matrix metalloproteinase 9 (MMP9), which helps the release of VEGF from the ECM[41,44]. Moreover, G-CSF induces early migration of granulocytes in premetastatic lungs of tumor-bearing mice, where they can assist metastasis formation[45].

Myeloid-derived suppressor cells

Myeloid-derived suppressor cells (MDSCs) are highly immunosuppressive immature myeloid cells further divided in polymorphonuclear MDSCs (PMN-MDSCs) and monocytic MDSCs (M-MDSCs). Both these subsets have been described in cancer patients, although there are some differences in the hierarchy and the mechanisms of immune suppression between humans and mice[18,25]. Murine PMN-MDSCs are defined as $CD11b^+$ $Gr\text{-}1^{high}$ $Ly6C^{low}$ $Ly6G^+$ cells[46] and can be distinguished from granulocytes for their suppressive activity and for higher levels of CD115 and CD244 but lower levels of CXC chemokine receptor 1 (CXCR1) and 2 (CXCR2)[47]. Conversely, M-MDSCs are $CD11b^+$ $Gr\text{-}1^{int/low}$ $Ly6C^{high}$ $Ly6G^-$ cells and express varying levels of classic monocytic markers as CD115, F4/80 and CC-chemokine receptor 2 (CCR2)[47-49]. M-MDSCs are distinguishable from circulating, inflammatory monocytes because the former are highly immunosuppressive (even higher than PMN-MDSCs) and can co-express the enzymes iNOS and ARG1[48]. In both PMN- and M-MDSCs, the synergy between these two enzymes results in the production of nitric oxide (NO), ROS and reactive nitrogen species (RNS), which impairs $CD8^+$ T cell responsiveness (by desensitizing the TCR), proliferation (by interfering with IL-2 receptor signalling) and ability to infiltrate the tumor mass and kill cancer cells (by nitrating CC-chemokine ligand 2, CCL2)[27,50,51]. However, also ARG1 alone is immunosuppressive since it depletes local L-arginine, an essential nutrient for lymphocytes, and converts naïve $CD4^+$ T helper cells into Tregs[50,52]. Similarly to ARG1, its homolog ARG2 has been recently found to be expressed in both neuroblastoma and acute myeloid leukemia tumor cells and to suppress T-cell proliferation and activity as well as to inhibit myeloid cell differentiation and activation[53,54].

The identification of human MDSCs is problematical, since there is not a homolog of the murine marker Gr-1. Moreover, there is often no correlation between phenotype and immune suppressive activity[46]. Human MDSCs have been divided into M-MDSCs, defined as $CD14^+$ $HLADR^{low/neg}$ cells, PMN-MDSCs, defined as $CD11b^+$ $CD33^+$ $CD66b^+$ $CD115^+$ $ARG1^+$ cells with a granulocyte morphology, and immature myeloid cells (iMCs), that are Lin^- $CD33^+$ $CD11b^+$ cells. All the subsets correlate with a poor prognosis in oncological patients[46].

Like Tregs, MDSCs may represent a control system to avoid excessive and dangerous immune responses. In support of this theory, it seems that the immunosuppressive activity of MDSCs requires IFN-γ to be activated and that IFN-γ mainly derives from activated $CD8^+$ CTLs and Th_1 cells[18,25,48].

Tumor-infiltrating MDSCs inhibit nearby T cells without the need for cellular contact, resulting in antigen-unspecific suppression[48,55]. On the contrary, MDSCs that migrate to secondary lymphoid organs (lymph nodes and spleen) exert their immunosuppressive activity against $CD8^+$ CTLs in an antigen-specific manner.

Apart from immunosuppression, the MDSCs support tumor progression in other ways. Indeed, it has been shown that populations of immature myeloid cells are able to release MMP2 and MMP9 for ECM degradation, differentiate into endothelial-like cells and promote angiogenesis, prepare the pre-metastatic niche for tumor cell arrival and induce epithelial to mesenchymal transition (EMT)-associated signalling pathways such as those dependent on TGF-β, epidermal growth factor (EGF) or hepatocyte growth factor (HGF)[56,57].

Tumor-associated macrophages

Macrophages are terminally differentiated and highly heterogeneous myeloid cells that act as specialized phagocytes. In adults, peripheral tissue macrophages derive from the differentiation of circulating inflammatory monocytes and M-MDSCs as well as from the self-renewal of resident macrophages[58,59]. The resident macrophages are found in almost all peripheral tissues of the body and have been demonstrated to originate from primitive macrophages of the yolk sac or monocytes of the fetal liver, thus precluding the possibility to be derived from circulating monocytes[60-62].

The main functions of macrophages are to eliminate pathogens, apoptotic cells and cellular debris generated in conditions of tissue remodelling, such as during embryogenesis, chronic inflammation, wound healing, fibrosis and cancer[63].

Phenotypical identification of murine macrophages can be achieved by evaluating the expression of the specific surface markers CD11b, F4/80 and CD115/CSF1-R (colony-stimulating factor 1 receptor) as well as the lack of the granulocytic marker Ly6G. Human macrophages, instead, are characterized by the expression of CD68, CD163, CD16, CD115 and CD312[64].

Macrophages can polarize into two opposite phenotypes, depending on specific local stimuli like TLR ligands and cytokines. The ‘M1’ or ‘classically activated’ macrophages are induced by microbial products and IFN-γ. They upregulate iNOS and ROS-generating enzymes to produce reactive nitrogen and oxygen intermediates and efficiently kill engulfed bacteria and intracellular pathogens. A drawback of this mechanism is that it can cause tissue-damaging reactions[65]. As opposed to DCs, macrophages are not professional APCs, but with the M1 polarization they become efficient APCs: they upregulate the major histocompatibility complex class II (MHC-II), the co-stimulatory molecule CD86 and the pro-inflammatory cytokine IL-12. Hence, M1 macrophages can present antigens to $CD4^+$ Th cells and drive a Th_1-oriented adaptive response[66].

The other is the ‘M2’ or ‘alternatively activated’ phenotype, which is induced on macrophages by IL-4 and IL-13 produced by Th_2 cells during helminth infection and allergy. M2 macrophages are not APCs, produce low levels of IL-12 and high levels of the anti-inflammatory cytokine IL-10, thus precluding them from induction of Th_1 cells. Conversely, they produce

Th_2- and Treg-attracting chemokines (e.g. CCL17, CCL22 and CCL24)[66]. M2 macrophages upregulate ARG1 and consequently produce polyamines, which sustain wound healing-associated vascularization and fibrosis, and deplete local L-arginine, suppressing $CD8^+$ CTL responses, as mentioned above[50]. Moreover, M2 macrophages are also involved in preserving tissue homeostasis by remodelling the ECM[67].

Mosser and Edwards proposed that M2 macrophages should be further divided in 'wound-healing macrophages' and 'regulatory macrophages'[63]. Wound-healing macrophages are induced by IL-4 and IL-13 and contribute both to the clearance of parasitic infections and tissue repair. By expressing ARG1, these macrophages furnish polyamines and L-proline, which are fundamental for the production of the ECM and nourishment of proliferating cells[50]. Thus, the immunosuppressive activity associated to ARG1 seems an additional way to promote wound healing.

Instead, the regulatory macrophages are induced by anti-inflammatory stimuli as IL-10 and glucocorticoids[63]. As opposed to the M1 pro-inflammatory subset, regulatory macrophages produce high levels of IL-10 and low levels of IL-12 when stimulated with LPS. Regulatory macrophages can present antigens to T cells and secrete TGF-β, causing the activation of antigen-specific $CD4^+$ Tregs[68].

Thus, M1 macrophages represent the pro-inflammatory subset, while the M2 macrophages the anti-inflammatory subset. Actually, complete M1 and M2 polarizations are considered as extreme conditions of a full spectrum of polarizations with multiple overlapping functions that macrophages can assume *in vivo*. Therefore, the M1/M2 classification represents only a simplification to distinguish between the many functions that macrophages can potentially exploit within tissues[69].

In physiological conditions, macrophages are versatile cells with a great variety of functions. They can also participate in cancer. In infiltrates from advanced neoplasias, tumor-associated macrophages (TAMs) have a very heterogeneous phenotype, showing a mix of both M1 and M2 characteristics[58,67]. M1 macrophages that infiltrate the tumor mass are able to engulf and destroy neoplastic cells and to sustain Th_1-type anti-tumor immune responses, while anti-inflammatory M2 and M2-like macrophages have been shown to favour tumor progression[25]. Although the existing heterogeneity, TAMs are generally considered to be mainly M2-like macrophages with tumor-promoting properties[70]. It was observed that during lung or mammary carcinoma progression the amount of M1-like macrophages decreased while that of M2-like macrophages augmented[59]. In another study, an initial accumulation within the tumor of M1 macrophages, recruited by the inflammatory process and induced by IFN-γ–producing NK cells and T lymphocytes, turns into a progressive M2 accumulation, likely due to the onset

of a regulatory, pro-tumoral immunity and a TAM-mediated depletion of that IFN-γ–producing populations[71].

In murine tumors a further level of complexity is given by the fact that TAMs may also express MHC-II and CD11c, which are also typical DC markers. Thus, *in vivo* it becomes difficult to identify extreme, theoretical myeloid subpopulations due to the presence of complex tissue-derived signals that generate intermediate, dynamic phenotypes and an overlap of surface markers[58,64,67].

Beyond the phenotypic classification, it is by now accepted that TAMs create a suitable microenvironment where cancer cells can escape the immune defences, proliferate and assume invasive capabilities. For this reason, the presence of TAMs in tumor infiltrates of patients correlates with a poor prognosis[64,72,73].

The tumor-promoting functions of TAMs

Different pro-tumoral functions have been described for TAMs, including suppression of anti-tumor immunity and promotion of cancer cell growth, angiogenesis and metastasis (Figure 3)[64,74].

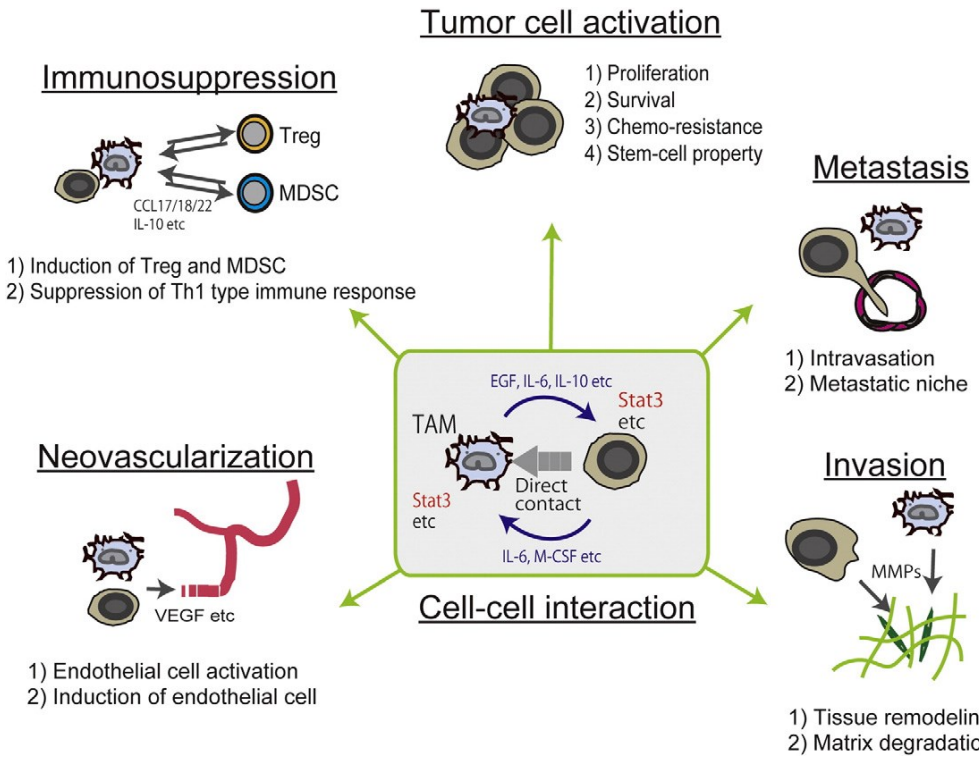

Figure 3 - The pro-tumoral functions of TAMs. *Macrophages in the tumor microenvironment can sustain cancer progression by inducing tumor cell activation and invasion, neovascularization, immunosuppression and metastasis (reproduced from Komohara et al., 2016[74]).*

TAMs favour the generation of an immunosuppressive tumor microenvironment

TAMs are not efficient APCs and, when isolated from tumors or stimulated *in vitro* with microbial products, release high levels of IL-10 and low/null levels of IL-12[75]. Consequently, TAMs are not able to activate NK and Th_1 cells and to induce an anti-tumor response; by contrast, they lead to the development of Th_2 cells, which in turn maintain an M2-like phenotype of TAMs by secreting IL-4[76]. In addition, IL-10 and TGF-β secreted by TAMs can induce $CD4^+$ T cell differentiation in Tregs that contribute to immune suppression in the tumor microenvironment[77,78]. TAM-released chemokines like CCL5, CCL20 and CCL22 attract Tregs in the tumor mass[79-82]. In turn, Tregs, together with Th_2 cells, promote macrophage M2 polarization. This is achieved through the release of IL-4, IL-10 and IL-13[83], which increase the expression of the mannose receptor CD206 and the scavenger receptor CD163 on macrophages and inhibit macrophage responsiveness to the M1-polarizing LPS stimulus. Also tumor cells induce the M2 phenotype by secreting TNF-α, which is able to upregulate types I and II scavenger receptors on macrophages[84]. Thus, TAMs favour the generation of an immunosuppressive microenvironment inside the tumor mass by recruiting and activating regulatory cell populations; in turn, these cells sustain TAM accumulation and immune-modulatory properties in a positive loop.

Moreover, TAMs can directly suppress $CD8^+$ lymphocyte proliferation and activity by upregulating ARG1, releasing immunosuppressive molecules like TGF-β, NO and prostaglandin E2 (PGE2), and expressing under hypoxic conditions PD-L1 (programmed death-ligand 1), that interacts with the inhibitory receptor PD-1 on activated T cells[40,85-88].

TAMs favour tumor activation

Macrophages can induce both *in vitro* and *in vivo* tumor cell activation and proliferation. This is achieved by stimulation of the EGF receptor (EGFR) and the signal transducer and activator of transcription 3 (STAT3) in cancer cells, respectively induced by TAM-derived heparin-binding EGF-like growth factor (HB-EGF) and oncostatin M, IL-6 or IL-10[89].

Besides proliferation, in different tumor types STAT3 induces also stem cell properties resulting in tumor cell survival and resistance to therapy[90-93]. Notably, an M2-like population of perivascular TAMs induced by the CXCL12 chemokine was recently retained responsible for revascularization and relapse after chemotherapy[94].

Another transcription factor, NF-kB, is involved in activation of stemness and therapeutic resistance in neoplastic cells upon stimulation with TAM-released TNF-α or other cytokines[95,96].

The same pro-tumor effects seem to be obtained also following physical interaction between macrophages and tumor cells, with involvement of membrane M-CSF, intracellular adhesion molecule-1 (ICAM-1) and ephrin[92].

TAMs favour angiogenesis inside the tumor

VEGF released by TAMs is directly responsible for promotion of angiogenesis[97,98]. Other indirect ways used by TAMs to induce angiogenesis have been described. For example, they release the WNT family ligand WNT7B and stimulate VEGF secretion from endothelial cells[99]. Moreover, Tie2-expressing macrophages (TEMs), a subpopulation of TAMs, are able to differentiate in perivascular macrophages and, since they express the receptor for angiopoietin 2 (ANG2), interact with $ANG2^+$ endothelial cells to induce the angiogenic process[100,101].

TAMs favour tumor invasion

Another pro-tumoral function of macrophages consists in the proteolytic disruption of cell-cell and cell-ECM interactions, in the latter case leading to degradation and remodelling of the ECM[70]. TAMs express high levels of several membrane-anchored and secreted proteases, which target cell-adhesion molecules (such as E-cadherin) or stromal proteins (such as collagens)[102]. Examples of these enzymes are cysteine cathepsins (like B ad S)[103], serine proteases (like the plasminogen activator)[104] and matrix metalloproteinases (like MMP2 and MMP9)[105]. In many tumor models, protease-mediated loss of ECM integrity allows tumor cells to escape beyond the basement membrane, facilitating both invasion of surrounding healthy tissues and formation of metastases in distant organs[106-108].

TAMs favour tumor metastasis

Finally, TAMs can directly stimulate the migration of tumor cells by secreting paracrine factors, such as EGF. EGF-activated tumor cells can in turn release CSF-1 to promote the motility of TAMs[109]. Accordingly, inhibition of CSF-1 signalling in mice reduces the number of CTCs and tumor metastases[110]. Also SPARC (secreted protein acidic and rich in cysteine) can be released by macrophages and can favour cancer cell migration by aiding their interaction with the ECM[111]. Furthermore, perivascular TAMs may promote the synthesis of fibrillar collagen I, an ECM protein that anchors blood vessels and enhances cell motility of ten times if compared to surrounding stroma[112]. When these TAMs release chemoattractant signals, tumor cells easily migrate toward blood vessels and, subsequently, intravasate[110].

The role of macrophages at the metastatic site

The previously considered TAM-mediated mechanisms facilitate the invasiveness of neoplastic cells and their entry into the circulatory system. However, the metastatic process requires not only the release of cells from the primary site, but also their extravasation and

colonization of the target tissue. Myeloid cells and, in particular, macrophages are known to play a central role also in these steps of tumor spreading[64].

It has not been fully elucidated how tumor cells are aided to exit the circulatory stream, survive and proliferate in the ectopic tissue. In humans, this process has a low rate of success, considering that a tumor can release thousands of CTCs every day and that only a few of them are able to generate a metastasis[64]. This inefficiency derives in part from the intervention of the host immune defences that, for example, comprise the population of circulating $Ly6C^-$ 'patrolling monocytes', able to remove tumor cells from the vasculature[113].

$CD11b^+$ myeloid cells are known to accumulate in metastatic organs before tumor cells are detected[114]. Among all the myeloid populations that accumulate in the pro-metastatic site, it is likely that macrophages have a key role in tumor spreading[64]. It has been shown that systemically-released TDSFs can summon myeloid cells at distant sites defined as 'pre-metastatic niches', where they can prepare the local microenvironment to facilitate extravasation and colonization by CTCs[24]. Examples of such TDSFs are the ECM protein versican produced by the Lewis lung carcinoma[115] or VEGFA, TNF and TGF-β, which induce the release of the inflammatory mediators S100A8 and S100A9 in the lungs with subsequent recruitment of myeloid cells[116]. Recently, it has been demonstrated that also tumour-derived exosomes prepare the pre-metastatic niche and even determine metastatic organotropism, since they are internalized by organ-specific cells in an integrin-dependent manner[117]. Other pro-metastatic TDSFs are the procoagulants released by the primary tumor, like the platelet tissue factor. These molecules induce the formation of clots inside lung vessels (step 1 in Figure 4), which have been shown to hold the CTCs and induce the expression of the adhesion molecules VCAM-1 and VAP-1 on the vascular endothelium[118,119]. CTCs release CCL2 to attract circulating monocytes and myeloid progenitors, which consequently anchor to the endothelium and extravasate (2 in Figure 4)[120]. CCL2-recruited inflammatory monocytes and myeloid progenitors from the circulation can be induced by cancer cell-released CSF-1 to differentiate into macrophages, that have been defined by Pollard and colleagues as metastasis-associated macrophages (MAMs) (3 in Figure 4)[24,121].

In accordance with this, when inflammatory monocytes are injected in tumor-bearing animals by means of ACT, they preferentially accumulate in metastatic lungs in a CCL2-dependet manner and differentiate into MAMs[120]. CCL2 fosters the accumulation of a macrophage subset also in the metastatic liver[122]. Moreover, TAMs and other infiltrating myeloid cells secrete VEGF or mediate protease-dependent release of matrix-bound VEGF[78,123]. The VEGF-induced vasodilatation in the pre-metastatic niche is essential for a further, prominent accumulation of MAMs, that are then maintained by CSF-1 signalling, as occurs for TAMs in the primary tumor[110,120,121]. It has been reported that in the lungs of polyomavirus middle T-antigen

(PyMT) mice (a spontaneous model of breast cancer) MAMs are CD11b^{+}, F4/80^{+}, VEGFR1^{+}, CXCR3^{+}, CCR2^{+} but Gr1^{-} and CD11c^{low}, thus showing a different phenotype from that of lung CD11c^{+} resident macrophages[121,124].

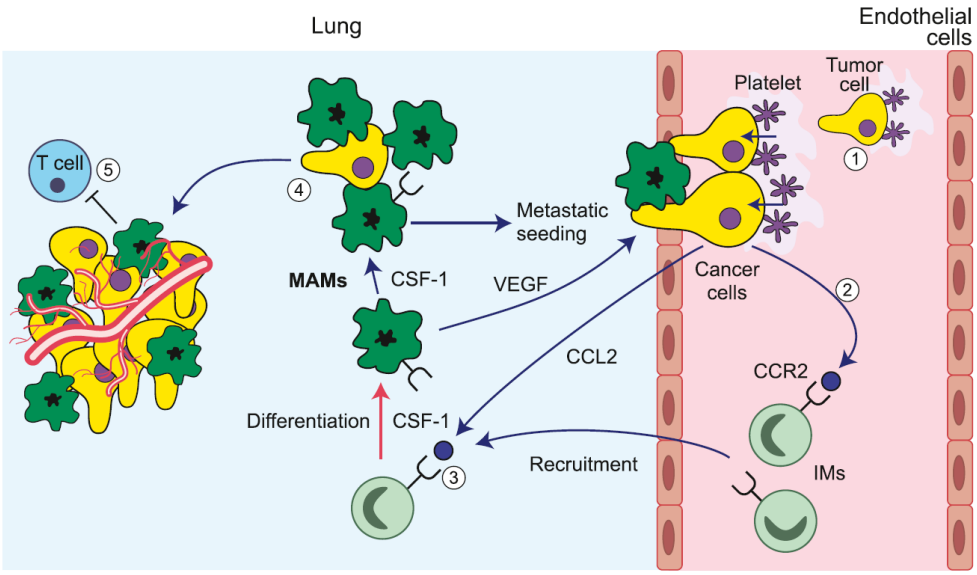

Figure 4 - Promotion of the metastatic process by macrophages. *The formation of microclots allows the arrest of cancer cells in the blood vessels of the target organ (1). Circulating monocytes are attracted by cancer cell-derived CCL2 and extravasate (2). Once in the target tissue, monocytes are induced by CSF-1 to differentiate into MAMs, that increase vascular permeability by releasing VEGF (3). MAMs, under CSF-1 stimulation, mediate tumor cell survival, angiogenesis and immune suppression (4-5). MAM: metastasis-associated macrophage; IM: inflammatory monocyte (reproduced from Noy and Pollard, 2014[78]).*

In the presence of tumor cells, MAMs acquire pro-metastatic functions. First of all, they directly contact tumor cells and support their exit from blood vessels (4 in Figure 4). Indeed, elimination of MAMs reduces the number of extravasating cells and, even after metastases are established, loss of macrophages inhibits further metastatic growth, suggesting that MAMs are necessary also for cancer cell survival and proliferation[121]. This can be achieved through engagement of VCAM1 on tumour cells and triggering of the Akt signalling pathway[125].

As described for TAMs in the primary tumor, also MAMs release matrix metalloproteinases to promote tumor cell invasion and favour immune suppression in the metastatic site (5 in Figure 4)[78]. Furthermore, it has been demonstrated that Tie2^{+} macrophages enhance angiogenesis and tumor growth also in metastatic sites, as above-mentioned for the primary tumor[100].

Although interesting results have been recently obtained in this field, a great effort has still to be done to characterize MAMs and their cancer cell-supporting interventions.

Macrophages as therapeutic targets

Understanding the functions of TAMs and MAMs and the underlying signalling pathways might be useful to identify possible therapeutic targets with the aim of reducing, or even blocking, their pro-tumoral and pro-metastatic mechanisms of action. For example, an approach of this kind has been recently applied to successfully hamper macrophage CSF-1 signalling pathway[78]. Mutation of the CSF-1 gene in PyMT mice inhibited tumor progression and metastasis[126], while inhibition of the pathway in different mouse models through the use of an anti-CSF-1R blocking antibody or a small-molecule inhibitor resulted in reduction of tumor burden and increase of survival[127,128]. In other works, treatment with an anti-CSF1 neutralizing antibody or an inhibitor of the CSF1R signalling cascade enhanced the efficacy of chemotherapy, mice survival and $CD8^+$ T cell response, but also reduced tumor-initiating cells, tumor growth, metastasis and angiogenesis[72,129]. It has been proposed that inhibition of CSF-1R leads to the repolarization of TAMs to an anti-tumoral GM-CSF–regulated state, rather than eliminating TAMs[130]. An anti-CSF-1R blocking antibody has been recently used in pre-clinical and early-phase clinical trials to treat diffuse-type giant-cell tumors overexpressing CSF1; remarkably, the therapy resulted in increase of lymphocyte infiltration and significant clinical benefits[131]. We recently demonstrated that blocking CSF-1R signalling before ACT reduced the accumulation of TAMs and their suppressive activity without altering Tip-DC generation from precursors and increasing their accumulation at the tumor site; this resulted in an increased efficacy of the ACT therapy[40].

Thus, the discovery of new promising strategies to fight cancer and potentiate the therapeutic approaches requires the comprehension of specific mechanisms of action used by myeloid cells and, in particular, TAMs to promote tumor progression and the metastatic process. With this goal our group conducted an experiment by using Affimetrix high-density gene expression arrays on $CD11b^+$ tumor-infiltrating myeloid cells from different tumors and on splenic $CD11b^+$ myeloid cells purified from healthy mice (baseline control). Gene chip analyses were performed comparing the transcriptome in our samples matched with the relative genetic backgrounds. The obtained results showed that the gene *Dab2* (disabled 2, mitogen-responsive phosphoprotein) was one of the most upregulated genes in myeloid cells from tumors as compared to healthy spleen. Relative fold-change results for this gene in different tumor models are shown in Table 1.

Tumor model	Tumor classification	Genetic background	Relative fold-change
4T1	Mammary carcinoma	BALB/c	63.83
C26GM	Colon carcinoma	BALB/c	53.82
MCA203	Fibrosarcoma	C57BL/6	50.22
EL4	Thymoma	C57BL/6	33.02

Table 1 *- Relative fold-changes of Dab2 gene expression in tumor-infiltrating CD11b⁺ myeloid cells isolated from different tumor models.*

To confirm these data, we performed Western blot analyses to evaluate DAB2 protein expression on CD11b⁺ cells purified from tumors and spleens of animals that had been injected with the same cell lines of the gene chip analyses. Healthy spleens were used as negative control. As shown in Figure 5, the two isoforms of DAB2 (p96 and p67) were expressed in intratumoral myeloid cells, but not in splenic myeloid cells from both healthy and tumor-bearing mice. DAB2 was detected in all the tumor models, although we noticed a tumor-specific expression level. Thus, we confirmed the results of the gene chip analyses and concluded that induction of DAB2 expression in myeloid cells is a general feature of the tumor microenvironment, regardless of both the histologic origin of the tumor and the genetic background of the animal. This prompted us to investigate DAB2 function in tumor-infiltrating myeloid cells.

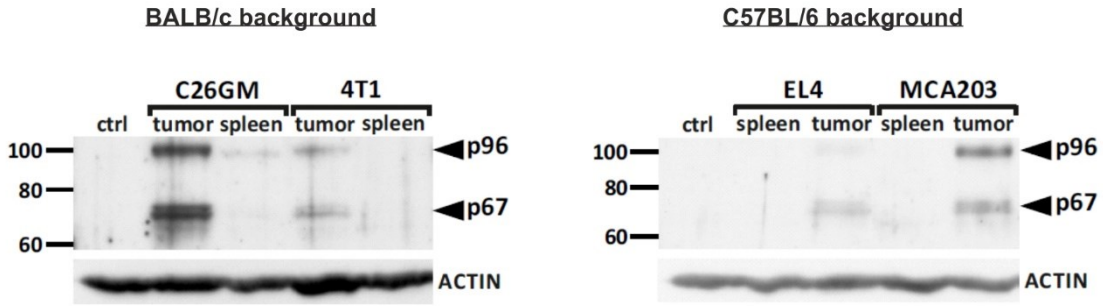

Figure 5 - Expression of the protein DAB2 in CD11b⁺ myeloid cells. *Western blot analyses for the expression of DAB2 isoforms (p96 and p67) in CD11b⁺ cells isolated from spleens and tumors of mice injected with different cell lines in both C57BL/6 and BALB/c backgrounds. Splenic CD11b⁺ cells from healthy mice with the two genetic backgrounds were used as negative controls (ctrl).*

DISABLED HOMOLOG 2 AND THE CLATHRIN-MEDIATED ENDOCYTOSIS OF INTEGRINS

The molecular structure of Disabled homolog 2

DAB2 is a protein that acts as a molecular adaptor in the clathrin-mediated endocytosis of specific transmembrane receptors and in signal transduction pathways[132].

The human transcript of *DAB2* (initially called *DOC2*) was identified by Liang and Pardee[133] and the murine orthologous protein was discovered by Xu and colleagues in the BAC1.2F5 macrophage cell line[134]. The gene was sequenced from both the human genome, where it is on the chromosome 5, and the murine genome, where it is on the chromosome 15[135,136]. The name of the protein derives from its homology with the *Disabled* (*Dab*) gene product previously identified in *Drosophila melanogaster*, where it interacts with the Abl kinase during neuronal development[137-139].

DAB2 is a phosphoprotein containing an N-terminal PTB (phosphotyrosine-binding) domain that binds membrane proteins with an NPXY motif in their cytoplasmic tails, a central clathrin- and adaptor protein-binding domain with a high degree of similarity with the *Drosophila* protein, and a proline/serine-rich C-terminal domain with binding sites for SH3-domains and myosin VI (Figure 6)[134,140,141]. Alternative splicing generates two isoforms of DAB2 with a molecular weight of 96 and 67 kDa and for this reason named p96 and p67, respectively. Over the past years, the majority of works describing the role of DAB2 in endocytosis were conducted on the p96 isoform and, for this reason, little is known about the functions of the p67 isoform. p96 was shown to be phosphorylated in BAC1.2F5 macrophages stimulated with the growth factor M-CSF, a cytokine that is required *in vivo* and *in vitro* for the differentiation, proliferation and survival of the mononuclear phagocyte lineage[134].

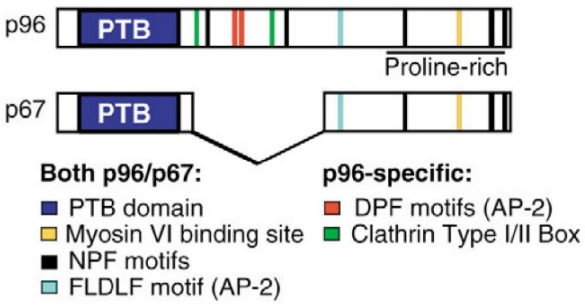

Figure 6 *- Schematic representation of the two isoforms of DAB2, p96 and p67 (reproduced from Maurer et al., 2005[142]).*

The aminoacidic sequence NPXY, recognized by the PTB domain of DAB2, has been found in the intracellular domains of several membrane receptors, like the low-density lipoprotein receptors (LDLRs), megalin, integrins and E-cadherin[132,143,144].

Once bound the receptor that must be internalized, DAB2 allows the formation of clathrin assemblies beneath the plasma membrane. This process requires the anchoring of DAB2 to phospholipids and the recruitment of clathrin. The interaction between DAB2 and phospholipids is mediated by an evolutionarily conserved poly-lysine stretch, that is adjacent to the PTB domain and recognizes phosphoinositides with a negative charge. In this way DAB2 is initially recruited at the inner leaflet of the plasma membrane. The Ser24 residue, near the poly-lysine sequence, can be phosphorylated to positively or negatively regulate DAB2 binding to phospholipids, depending on the cellular context[145-148]. The interaction with clathrin is mediated by an aminoacidic sequence in the central region of DAB2, that is present in p96 but not in p67 (Figure 6)[147]. This sequence is also suitable to bind other endocytic proteins like AP2[143]. Intracellular transport of clathrin-coated vesicles requires myosin VI, whose cargo-binding domain interacts with the C-terminus of DAB2[149]. Therefore, DAB2 acts as a linker between myosin VI and clathrin, allowing the transfer of clathrin-coated vesicles away from the plasma membrane into the cell along actin filaments[150].
In the next sections the cellular endocytic pathways and the known functions of DAB2 are reviewed.

Mechanisms of endocytosis

Endocytosis is the conserved mechanism used by eukaryotic cells to internalize plasma membrane proteins and lipids, extracellular fluids, molecules, exosomes and pathogens. By controlling this process, cells are able to uptake nutrients, transduce signals and respond to microenvironmental stimuli, recycle membrane components, present antigens, carry out neurotransmission at synapses, and migrate[151,152]. Thanks to the use of electron microscopy and the advent of reflection fluorescence microscopy, many types of endocytosis have been described (Figure 7), differing for the nature of the cargo to be internalized, the size of vesicles, the involved molecular machinery, and the type of regulation[152]. The distinct pathways sort cargoes into various endosomal, membranous compartments with distinct internal and surface composition to induce different intracellular events. When the cargo arrives in early/sorting endosomes, it can be sent back to the surface through recycling endosomes or targeted to more mature compartments known as late endosomes or multivesicular bodies (MVBs), that can fuse with lysosomes for degradation of the internalized material (Figure 7)[151,152].

The endocytic routes have been classified in clathrin-dependent and -independent. The clathrin-independent pathways are the main mechanisms of endocytic internalization used by cells[154]. The most common is that based on the budding of caveolae (for ‘little caves’), which

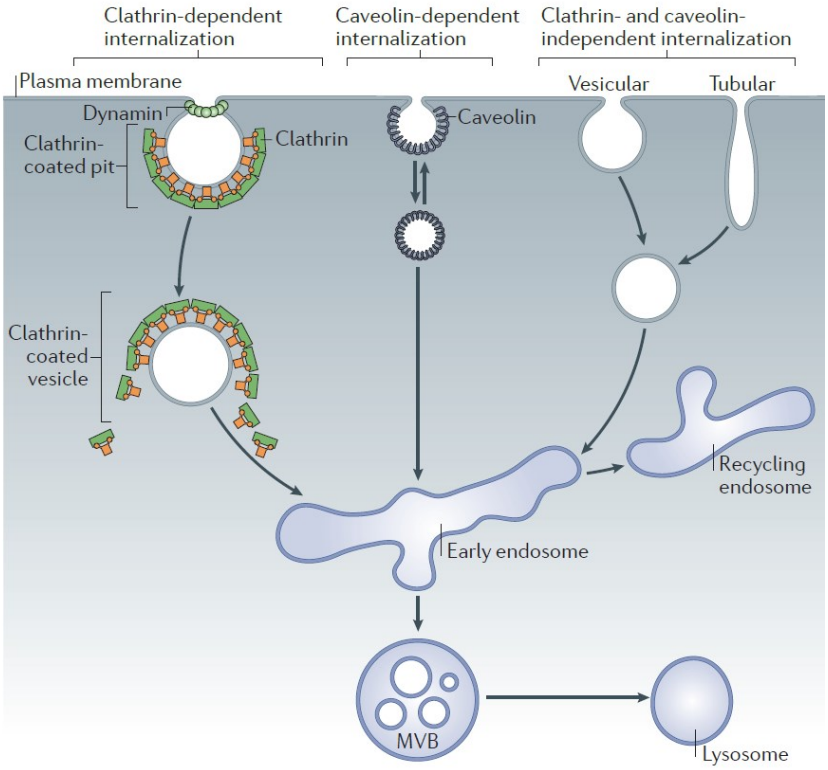

Figure 7 - Clathrin-dependent and -independent endocytic pathways. *Endocytosis can be mediated by clathrin or not. Clathrin-independent internalization includes caveolae-mediated endocytosis as well as other vesicular pathways; also tubular pathways have been described. In all cases, uptaken cargo is trafficked into endosomes, where it is sorted either back to the surface of the cell or into other compartments for degradation. MVBs: multivesicular bodies (reproduced from McMahon and Boucrot, 2011[153]).*

are bulb-shaped invaginations of the plasma membrane with a diameter of about 50-100 nm[155]. These structures are detectable in cell types like fibroblasts, endothelial cells, smooth muscle cells, myoblasts and adipocytes, and permit the internalization of plasma membrane glycosphingolipids, glycosylphosphatidylinositol (GPI)-anchored proteins, extracellular ligands (e.g. albumin and folic acid), bacterial toxins (e.g. tetanus and cholera) or viruses (e.g. Polyoma or SV40)[155,156]. Caveolae are enriched in structural sterols and the transmembrane protein caveolin-1 (Cav1), that is necessary for their budding in association with other accessory proteins like dynamin[155]. Caveolae are involved in several cellular processes, such as transcytosis, signal transduction, pathogen invasion, membrane lipid homeostasis and mechanotransduction aimed at protecting the cell from mechanical stress[157].

Another central clathrin-independent endocytic pathway is phagocytosis, that occurs in specialized cell types, such as DCs, neutrophils and macrophages (professional phagocytes), or occasionally in other cell types like endothelial cells (facultative phagocytes). This process

depends on membrane invaginations that are larger than caveolae and form around opsonized and particulate materials often greater than 0.5 μm, such as nutrients, pathogens and necrotic or apoptotic cells to be destroyed[152].

These particles bind to cell surface receptors and are internalized through a mechanism involving actin polymerization and rearrangements of the cytoskeleton[158]. The selective fusion of phagosomes with primary lysosomes leads to the degradation of the cargo, accompanied by extensive membrane turnover mediated by recycling of endosomes between the cell compartments[158].

Clathrin-independent internalization can also take place through fluid-phase macropinocytosis, in which extensive regions of the plasma membrane (0.5-5 μm) form ruffles around a region of extracellular fluid and, finally, close up determining the uptake of the whole material[152]. This endocytic route is regulated by several proteins, including Ras and Rho small GTPases, ADP-ribosylation factor (ARF6), and dynamin, that is implicated in the formation of actin structures for the intracellular trafficking of macropinosomes[151].

Other clathrin-independent endocytic mechanisms employ circular dorsal ruffles, flotillin-associated invaginations or whole cell engulfment; the latter is known as entosis and takes place when a cell detaches from the ECM and must be eliminated[152]. In mammalian cells it has been reported also the presence of an endocytic route into tubular, rather than vesicular, compartments, known as CLIC/GEEC-type endocytosis *(CL*athrin-*I*ndependent *C*arriers and *G*PI-*E*nriched *E*ndocytic *C*ompartments). This pathway is activated through small G proteins, in particular Cdc42, and allows internalization of bacterial exotoxins, GPI-linked proteins and extracellular fluids[159].

Clathrin-mediated endocytosis

Clathrin-mediated endocytosis (CME) is the most studied endocytic route, although it is not the most occurring inside cells. It is also known as receptor-mediated endocytosis, because it is used by cells to package and internalize a great variety of transmembrane receptors and associated ligands into 50-100 nm membrane vesicles[125,153]. Internalization of receptors can be induced by binding of the ligand, as in the case of EGFR, or can be constitutive, as in the case of the transferrin receptor[160].

Many adaptor and accessory intracellular proteins intervene in the CME process either acting directly, for example by promoting the membrane bending or by acting as scaffold molecules, or indirectly by recruiting other proteins[153].

CME consists of five steps: nucleation, cargo selection, coat assembly, scission and uncoating (Figure 8). The endocytic process begins with the inward bending of the plasma membrane in the region to be internalized. Adaptor and accessory proteins assemble in a nucleation module to deform the membrane and induce polimerization of soluble clathrin[161,162]. Then, the Adaptor Protein-2 (AP2) is recruited to the nucleation module and binds at the same time the membrane, the target receptor, cargo-specific adaptor proteins and clathrin (Figure 8). The adaptors are putatively involved in both binding/selection of the cargo proteins and bending of the membrane[153].

Once cargo is selected, recruited soluble clathrin polimerizes into a curved lattice beneath the inner face of the cell membrane[153]. This coating structure guides the deformation of the membrane to form a clathrin-coated pit (CCP) and stabilizes its curvature. Clathrin and adaptor proteins force a further bending of the CCP until the upper edges are close enough to allow the binding of the scission protein dynamin, a GTPase that promote the fission of the clathrin-coated vesicle (CCV) and its release into the cytoplasm[163-165]. After scission, CCVs lose their clathrin coating aided by the ATPase HSC70 (heat shock cognate 70) and other proteins (Figure 8)[153].

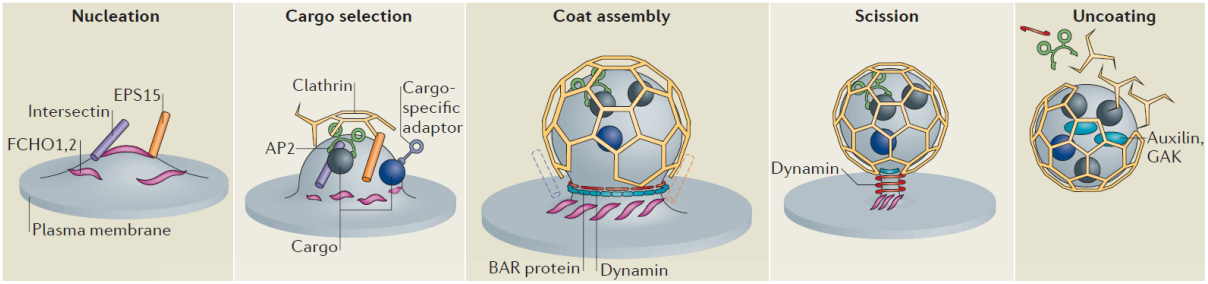

Figure 8 - The 5 steps of clathrin-mediated endocytosis. *The process begins with the nucleation of the first endocytic proteins on PIP_2 phospholipids to initiate clathrin-coated pit formation. AP2 is recruited together with cargo-selection proteins. Then, clathrin adds to the nucleation module and polymerizes to form a coating that is able to further bend the membrane pit. Upon dynamin intervention, the forming vesicle is released from the membrane into the cytoplasm (scission). Finally, the clathrin-coated vesicle loses its coating and the cargo can be trafficked to the endosomal compartment of destination. The actin machinery can participate in the last phases to promote membrane invagination and scission as well as cargo delivery (reproduced from McMahon and Boucrot, 2011[153]).*

Actin participates in the late phases of CME, although in some cell types the protein was reported not to join the process[166,167]. Actin polymerization may be useful to produce further force for membrane bending in the case of large cargoes, such as bacteria, or when the membrane is particularly rigid, as in yeast, or submitted to high tension, such as in adherent

cells[153,168,169]. Moreover, actin filaments are required for CCV trafficking inside the cell. Myosins are actin-bound motor proteins that interact with the budding CCV to pull it away from the membrane and move it toward the destination compartment[169]. An example is myosin VI, a minus-end-directed motor protein that can be recruited by DAB2[149].
Finally, the CCVs fuse with early/sorting endosomes to deliver their cargoes. As already seen in Figure 7, internalized receptors can be recycled back to the plasma membrane for a sustained ligand binding and transduction of the signal, or can be destroyed in lysosomes for normal protein turnover or termination of the signalling; alternatively, receptor-bound ligands inside endosomes can begin a signal amplification pathway inside the cell[153].

The endocytosis of different receptors can depend on the intervention of different adaptor and accessory proteins, that in part are well conserved from yeast to mammalian cells[170]. For this reason, CME has not a precise molecular mechanism but it rather represents a flexible array of similar pathways all based on the use of the clathrin protein[152].
Examples of alternative, cargo-specific adaptor and accessory proteins are β-arrestins and Dishevelled for G protein-coupled receptors (GPCRs)[171,172], ARH for LDLRs[173], Numb for Notch receptors[174], HRB for SNARE proteins[175], stonin for synaptotagmin[176] and DAB2 for LDLRs, megalin, integrins and E-cadherin[132,143,144]. All these proteins also interact with AP2. Moreover, they can be widely expressed in the organism or be tissue-specific: for instance, DAB2 is found in many tissues, while ARH only in hepatocytes and stonin in neurons[153].
Thus, in the same cells various adaptors and accessory proteins can have overlapping and redundant functions. A consequence of this is that in some cell types CME mediates the uptake of only one kind of receptor per vesicle, while in others, like at synapses, it mediates the uptake of multiple cargoes per vesicle, even more than 20. This is achieved thanks to the differential affinity that receptors have for specific adaptor proteins and that results in their clustering and sorting into distinct vesicles and in the following fusion with distinct endosomal compartments[152].
The presence of accessory proteins with redundant functions guarantees the robustness of the system, since endocytosis of a specific receptor is not compromised in the absence of the highest-affinity adaptor protein but can proceed anyway with other (maybe lower-affinity) adaptors[152].

The physiological functions of DAB2

DAB2 is widely distributed among body tissues and is highly expressed in many epithelial cell types, contrarily to its *Drosophila* orthologue DAB and its paralogue DAB1 that are expressed only in neural tissues. Most of DAB2 functions derive from its role as an endocytic adaptor

and are involved in various physiological processes as well as during embryonic development[177].

The protein participates in spatial organization of epithelial cells in tissues by controlling their positioning and their exigency for basement membrane attachment[178]. This is probably due to DAB2 ability in polarizing cell membranes by trafficking surface receptors like integrins and E-cadherin[177]. Consequently, downregulation of DAB2 determines a disorganized and basement membrane-independent growth of cells, as it occurs in ovarian and breast carcinomas[179]. It is noteworthy that DAB2 is expressed in the visceral endoderm of mice embryos, where it mediates the internalization of megalin, cubilin, cholesterol and E-cadherin[142,177,180]. Before the formation of placenta, transport across the visceral endoderm is the only way the developing embryo can assimilate maternal proteins and lipids. In this phase DAB2 is essential for polarizing the distribution of cell surface proteins. A consequence is that Dab2 KO embryos are not able to develop and die prior to gastrulation, due to loss of nutrients and endodermal cell organization[149,177,178].

Furthermore, DAB2 has been demonstrated to have a role also in kidney functioning. Conditionally mutant Dab2 KO mice showed defects in the formation of clathrin-coated pits in kidney proximal tubule cells and in the transport of the megalin lipoprotein receptor. Consequently, KO mice had excessive levels of plasma proteins in the urine[149].

DAB2 is also expressed in platelets and has been implicated in homeostasis and in the positive control of clotting responses by interacting with G protein-mediated thrombin signalling[181].

DAB2 as tumor suppressor

Besides its endocytosis-related pleiotropic functions, DAB2 is considered to be a tumor suppressor and has long been described as a predictor of poor prognosis and metastasis[182,183]. Indeed, DAB2 expression is often lost or downregulated in many cancer types, in comparison to the correspondent normal cells of origin. DAB2 depletion has been observed in tumors of the ovary[184,185], colon[186], breast[179,187-189], prostate[190], oesophagus[191], bladder[192], head and neck[182], nasopharynx[193], and in some of these cases in the associated metastases. Forced re-expression of *Dab2* suppressed cell growth and tumorigenicity of cancer cell lines[179,184,194,195]. However, DAB2 negatively regulates cell growth and survival not only in cancer. For example, it has been demonstrated that, during pregnancy and lactation in mice, mammary epithelial cells proliferate and their DAB2 level is low; on the contrary, during mammary gland evolution, mammary epithelial cells are in part eliminated and DAB2 level is

high[188]. Similarly, in castrated rats the degenerating prostate gland upregulates *Dab2* expression[194].

The tumor suppressor and growth inhibitory role of DAB2 derives from its participation as signal transducer in many cellular processes. By linking surface receptors to downstream effector molecules, the protein controls essential signalling cascades that determine cell growth, differentiation and migration, such as the Ras/MAPK, the TGF-β and the Wnt pathways[180]. The Ras/MAPK pathway is activated by mitogens like EGF and results in the transcriptional regulation of several genes, a prominent fraction of which is involved in cell cycle progression[195]. In physiological conditions, DAB2 negatively regulates this pathway by inhibiting ERK and c-Fos activation[195,196]. In cancer, DAB2 is downregulated, often by the oncogene *Ras* itself[197], and cells can proliferate without control[195].

DAB2 is also an essential component in the signalling pathway of TGF-β, a cytokine that acts as a tumor suppressor in normal epithelial cells by inhibiting cell proliferation and migration. In particular, DAB2 participates in the signal transmission from the TGF-β receptors to the transcriptional activators belonging to the Smad family[182,198,199]. DAB2 depletion in cancer cells leads not only to the loss of the TGF-β tumor suppressor function, but even to a promotion of TGF-β–aided cell motility, EMT and tumor growth[182,199]. It has been also demonstrated that tumor-associated increased Ras/MAPK signalling can sustain an autocrine TGF-β signalling loop, further promoting EMT and tumor cell invasive properties[189]. Moreover, DAB2 loss caused a reduction in TGF-β receptor internalization via CME; the consequent accumulation of TGF-β in extracellular space induced the conversion of naive $CD4^+$ T cells to pro-tumor Tregs[200].

Finally, the Wnt pathway plays a pivotal role in modulating cellular proliferation and differentiation, as well as tissue organization and embryonic development. It initially requires caveolin-dependent internalization of low-density lipoprotein receptor-related protein 6 (LRP6). DAB2 acts as a negative regulator of the Wnt signalling in several ways, but in particular by engaging LRP6 in CME so that it is not available for caveolin-mediated endocytosis[201]. Cancer cells can suppress this DAB2-mediated inhibitory activity and can divide in an uncontrolled manner[201].

In addition to the literature showing a role for *Dab2* as a tumor suppressor, others suggest a *Dab2* pro-tumoral role. Recently, a signature of genes comprising *Dab2* resulted to be expressed by a small subpopulation of breast cancer cells, defined ‘trailblazer’, and associated to increased invasive properties. Trailblazer cells were able to initiate tumor invasion by creating channels into the ECM and to guide the follower breast cancer cells from the bulk of the tumor. This genetic signature correlated with a poor prognosis in breast cancer patients[202].

Moreover, DAB2 was required also for migration and invasion of prostate cancer cells[203]. In another work, DAB2-expressing cancer cells were showed to release TGF-β, that in turn induced endothelial cell migration and angiogenesis[204].
Definitely, the significance of a pro-tumor activation of the *Dab2* gene needs to be clarified.

DAB2 in myeloid cell populations

While the great majority of published works on DAB2 have been conducted on tumor cells and fibroblasts, there are only a few reports about DAB2 functions in myeloid cells. Rosenbauer and colleagues demonstrated that DAB2 is expressed in bone marrow-derived macrophages and is necessary for both cellular adhesion and spreading on the ECM components laminin and collagen IV[145]. Moreover, in the same cells the *Dab2* promoter is recognized by the transcription factors IRF8 and PU.1 and the former was found to be involved in the downregulation of the gene upon IFN-γ stimulation[145].
A recent work on macrophages has shown that DAB2 expression induced their M2 polarization. Indeed, the protein was upregulated in M2 macrophages, but downregulated in M1. Interestingly, myeloid lineage-specific Dab2 KO mice both treated with LPS or fed with high-fat chow had an increased pro-inflammatory gene signature and M1 macrophage polarization as compared to control mice. The authors demonstrated that DAB2 binds TNF receptor-associated factor 6 (TRAF6) and reduces the activation of the pro-inflammatory transcription factor NF-κB[205]. A role for DAB2 has also been described in DCs, where it acts as a negative regulator of immunogenicity. The protein was significantly induced during the GM-CSF–driven differentiation of both murine and human DCs and required the activation of STAT5 and hnRNPE1 as well as the expression of Foxp3. Remarkably, DAB2 was associated with a reduced IL-12 and IL-6 expression, antigen uptake, migration, T cell stimulation and therapeutic efficacy when DCs were used in vaccines. Contrarily, DAB2-depleted DCs showed an increment in all these abilities[206].
These studies seem to delineate an anti-inflammatory role for DAB2, but further work has to be done to elucidate its function and regulation in myeloid subpopulations.

DAB2 and integrin recycling

Among the transmembrane receptors that are recycled in a DAB2-mediated manner, integrins are particularly important since they mediate the interactions between the cell and the surrounding microenvironment, including contact with the ECM and other cells[207].

Integrins are surface proteins able to interact with collagen, fibronectin and other ECM components. They consist of 24 different heterodimers yielded by the combination of 18 α and 8 β subunits, each specific for one or more ligands[208]. Integrins regulate a large number of cellular biological functions, acting as bidirectional signal transducers. On one hand, they can begin 'outside-in' signalling by recruiting cellular mediators and inducing cellular responses like proliferation or migration; on the other hand, they can receive 'inside-out' signals affecting the affinity for their extracellular ligands[144]. For example, cell adhesion and migration on the substrate need the generation of plasma membrane clusters of active integrins known as 'focal adhesions'. These contact regions anchor the cell cytoskeleton to the substrate and generate the necessary tension to make the cell move forward. Conversely, unbound (inactive) integrins diffuse freely in the phospholipidic bilayer[208].

DAB2 internalizes inactive integrins freely diffusing or localized in focal adhesions that are no more useful for the cell. In this way, DAB2 maintains an internal pool of integrins that can be either degraded for normal integrin turnover or recycled back to the plasma membrane in order to assemble new focal adhesions for anchorage or migration[209,210]. The position of these new contact sites with the ECM depends on the cell type and on the biological context: for example, in some cases cell motility requires assembly of focal adhesions at the front of the cell (leading edge-driven movement), while in others at the cell rear (rear-steering movement)[208]. Thus, the CME-dependent vesicular trafficking that occurs inside the cell has the important function to allocate integrins in specific regions of the plasma membrane where they can carry out their functions. The resultant 'molecular polarization' of the cell confers to DAB2 a key role in many processes, such as epithelial cell spatial organization, cellular adhesion to the ECM, cell migration and spreading[208].

Up to date, DAB2 involvement in integrin endocytosis has been studied almost exclusively in fibroblasts and tumor cell lines. The protein has been mainly associated with the integrin dimer α1β1, that binds collagens, and with the dimers α4β1 and α5β1, that both interact with fibronectin[147,209-213]. Although to a less extent, other integrins are internalized through a DAB2-mediated mechanism, for example integrins α2β1 and α3β1 in HeLa cells[210,214] or αIIbβ3 in megakaryocytes and platelets[146].

In addition to these studies, it has been recently demonstrated that β3 integrins are recycled via DAB2-dependent CME[215]. Interestingly, ligand-bound β3 integrins can sense force generation from the substrate and, consequently, induce different cellular responses. When cells are seeded on glass (high traction force), β3 integrins form focal adhesions and induce both the actomyosin network to assemble and DAB2 to remain free in the cytosol; on the contrary, when cells are seeded on a lipid membrane (low traction force), focal adhesions do not form

and DAB2 is recruited to membrane clusters of inactive β3 integrins in order to mediate their endocytosis[215].

Integrins and Yes-associated protein in mechanotransduction

As reported about the β3 subunit, integrins are known for their ability in sensing substrate stiffness and inducing force-dependent 'outside-in' signalling pathways, that are gathered with the word 'mechanotransduction'[216]. The conversion of mechanical forces into biochemical signals is a key process in virtually all tissues for development, physiology and also pathology. For example, bone development and remodelling are guided by gravity and mechanical forces from locomotion, formation of blood and lymph vessels is induced by fluid shear stress, lung growth and physiology are controlled by breathing-derived tissue stretching, tissue function and tumor progression are determined by ECM stiffness[216]. Integrins are involved in all these processes and in many others.

From a cellular point of view, the ability of integrins to act as sensors for ECM stiffness can affect cellular proliferation, survival, cytoskeletal rearrangement, migration and differentiation[217,218]. According to the literature, the integrin dimers with a reported role in mechanotransduction are α5β1 (verified in chondrocytes, endothelial cells and fibroblasts), α1β1 (endothelial cells) and α4β1 (vascular smooth muscle cells)[219-223]. Of note, these were also the dimers mainly recycled through DAB2-mediated endocytosis.

The force sensing ability is based on the strengthening of the ligand-integrin-cytoskeleton interactions[216]. This is achieved in at least three ways: 1. integrins assume high affinity conformations to stably bind the ligand[224]; 2. bound integrins under tension induce the unbound, low affinity integrins to change conformation[225,226]; 3. cytoskeletal and accessory proteins, such as talin, vinculin, Rho GTPases and zyxin, are recruited to directly or indirectly strengthen the integrin-actin connection[227].

In addition to force sensing, cells can also sense ECM stiffness and mechanical properties. Cells initially exert force on the substratum, probably at sites of focal adhesions and by means of periodic contractions of the cytoskeleton. These contractions seem to derive from cyclic conformational changes of low-affinity integrins that turn into high-affinity integrins, in a mechanism requiring FAK, paxillin and vinculin[228,229]. Then, myosin modulates the traction force it generates proportionally to that coming from the substrate. So, a soft ECM induces low traction by myosin determining reduced number and affinity of focal adhesions, actin stress fibers and force across the ECM-integrin-cytoskeleton axis[230]. A rigid ECM leads to the opposite response.

It has been demonstrated that myosin contractility on rigid substrates induces nuclear translocation of the two transcriptional regulators YAP (Yes-associated protein) and TAZ (transcriptional coactivator with PDZ-binding motif). Once in the nucleus, YAP and TAZ interact with transcription factors, in particular the TEAD family members, and activate the expression of growth- and differentiation-related genes[231-233]. On the contrary, on soft matrices, YAP and TAZ remain in the cytoplasm.

In recent years, the pivotal role of YAP/TAZ in mechanotransduction has been recognized. Remarkably, they are largely expressed in human malignancies and their activation seems to sustain stiffness-dependent tumor initiation and progression[234].

The pro-tumor functions of YAP/TAZ

YAP and TAZ are enhancer-binding transcriptional coactivators that belong to the mammalian Hippo pathway. Once bound to DNA, they promote enhancer acetylation and transcription elongation[234].

In normal tissues YAP/TAZ seem to be dispensable for homeostasis, but intervene as mechanotransducers in organ development and tissue repair. That is, in response to specific mechanical stimuli from the microenvironment, they induce changes in cell growth, polarity, shape and cytoskeletal organization, finally determining organ size and architecture[232,235]. Although YAP/TAZ are usually inactive in healthy, adult organs, their sustained activation has been observed in many tumors, such as mammary, lung, pancreatic, gastric and colorectal[234]. Indeed, in transformed cells they foster excessive proliferation (even when contact inhibition of proliferation should block it), survival and motility in response to mechanical inputs from the ECM[232]. The genes they activate are involved in DNA synthesis and repair, S-phase entry and mitosis. Moreover, YAP/TAZ could induce c-Myc and other proto-oncogenic transcription factors[236].

YAP/TAZ in cancer cells have been also associated with increased resistance to anoikis and apoptosis, preventing both the intrinsic and the extrinsic pathways[237,238], as well as increased autophagy rate aimed at rescue cells from senescence[239]. Interestingly, these transcription regulators are expressed in CSC subpopulations and promote CSC characteristics in cancer cells, such as the abilities to generate undifferentiated precursors, initiate tumor growth, survive chemotherapy and form metastases[240,241].

Another pro-tumor mechanism of action carried out by YAP/TAZ in cancer cells consists in their capacity to reprogram the tumor microenvironment: for example, they induce epithelial cells to release angiogenic factors like amphiregulin (AREG) or recruit myeloid suppressor populations[232,242].

Also CAFs have been demonstrated to express YAP/TAZ in a pathway that foster the deposition of extracellular matrix by CAFs themselves in order to increase ECM stiffness and sustain expression of YAP/TAZ in a self-reinforcing loop[17]. The matrix rigidity can activate the two proteins also in nearby cancer cells to induce the above-mentioned pro-tumor functions. Taken together, all these findings on YAP and TAZ activities can explain why their expression in human and murine cancers correlates with malignant clinicopathological characteristics, such as high histological grade, cancer stemness, metastasis, chemoresistance, relapse and general poor outcome[234,236].

AIM OF THE STUDY

The metastatic process consists in an ordered series of events in which tumor cells detach from the primary site, enter into the circulatory system and reach the target organs in order to colonize them[10]. Despite the high frequency and mortality associated to this pathological process, the cellular and molecular mechanisms that drive it remain still undisclosed[9]. However, it is clear that during the metastatic process, likewise to the previous phases of tumor initiation and progression, cancer cells receive assistance from myeloid cells infiltrating the tumor microenvironment, such as TAMs[24,107].
The pro-metastatic role of TAMs is supported by an increasing number of publications[78]. In particular, TAMs are acknowledged as critical determinants for metastatic progression associated to ECM remodelling[78,106,107], but the precise molecular pathways through which these cells are activated and operate are poorly known.

As reported in the introduction, our group performed preliminary studies with the goal of identifying new molecular pathways involved in tumor progression. Gene chip data showed that the *Dab2* gene was upregulated in tumor-infiltrating myeloid $CD11b^+$ cells in comparison to $CD11b^+$ cells from healthy spleens, suggesting a function for the DAB2 protein in tumor progression.
DAB2 is a protein that acts as a molecular adaptor in the clathrin-mediated endocytosis of specific transmembrane receptors, like integrins, and in signal transduction pathways[132]. The protein participates in various physiological processes such as embryonic development, kidney functioning, spatial organization of epithelial cells, cell adhesion and migration as well as inhibition of cellular proliferation[177]. Considering the many and essential functions it exerts, DAB2 appeared to be a good candidate molecule involved in the pro-tumoral activity of myeloid cells. Indeed, the detailed definition of specific mechanisms of action used by myeloid cells to sustain cancer cells might permit to potentiate the therapeutic approaches currently used to fight cancer and metastatic spreading.

In the present work, we aimed at defining whether DAB2 expressed by myeloid cells was really involved in tumor progression and in events that lead to the formation of metastases.
To this end, we used Dab2 KO mice, a transgenic model where the deletion of the gene was limited to the hematopoietic lineage and where we investigated tumor growth and metastasis

formation. The identification of specific DAB2^{+} myeloid subsets within the tumor microenvironment and their localization was one of the first goals of this work. Successively, we investigated the mechanism of action of DAB2 and how this protein is activated and regulated. Considering that DAB2 participates in clathrin-mediated endocytosis[132], we evaluated its possible involvement in the endocytosis-dependent remodelling of the tumoral ECM carried out by myeloid cells. Finally, we evaluated whether a pro-tumoral role of DAB2 expressed by myeloid cells might be found in patients with breast cancer, with the aim of employing DAB2 as a novel prognostic marker of disease. This work was carried out in the framework of a project supported by Associazione Italiana Ricerca contro il Cancro (A.I.R.C.).

MATERIALS AND METHODS

Cell culture

E0771 is a breast cancer cell line derived from C57BL/6 mice. MN-MCA, a C57BL/6 primary cell line of fibrosarcoma that spontaneously forms metastases in lungs, was a gift from Antonio Sica (Istituto Humanitas, Milan, Italy)[75]. Cancer cell lines were cultured in RPMI 1640 (Euroclone) supplemented with 10% heat-inactivated FBS (Gibco), 2mM L-glutamine, 10 mM HEPES (for E0771) or 1 mM sodium pyruvate (for MN-MCA), 150 U/ml streptomycin and 200 U/ml penicillin (all purchased from Lonza).

Murine RAW 264.7 macrophages and human HeLa cells (cervix carcinoma) were cultured in DMEM supplemented with 10% heat-inactivated FBS, 2mM L-glutamine, 10 mM HEPES, 150 U/ml streptomycin, 200 U/ml penicillin and, only for RAW 264.7, 20 μM β-mercaptoethanol.

Cells were seeded at desired concentrations on normal or low-adhesion plastic plates or, for immunofluorescence stainings, on 13 or 24 mm coverslips (VWR).

Gene-silencing in RAW 264.7 and HeLa

For production of *Dab2*-silenced RAW 264.7 cells, a 3rd generation packaging system was used, comprising three plasmids of packaging (a gift from Prof. L. Naldini, Università Vita-Salute San Raffaele, Milan, Italy) and one plasmid in which both a scramble or *Dab2*-specific shRNA and the Orange reporter were inserted. The four plasmids were co-transfected into 293T packaging cells by using calcium-phosphate co-precipitation. After 48 hours of culture, the lentiviral vector-containing supernatants were recovered, centrifuged (1500 g, 10 min), filtered and concentrated by ultracentrifugation (76,000 g, 2 hours). RAW 264.7 cells were seeded in 24-well plates with the infection mix, consisting of culture medium supplemented with Polybrene (1:1000, Sigma-Aldrich) and lentivirus (MOI 10 or 30) for a total volume of 500 μl/well. Plates were centrifuged (2000 rpm, 4h, RT) and then incubated until confluence was reached. Successfully transfected Orange^{+} cells were isolated through clonal selection from the whole culture and tested for DAB2 downregulation by WB.

For YAP-silencing in HeLa, $4 \cdot 10^4$ cells were seeded in 24-well plates. After 20 hours, cells were transfected with 5 pmol of *YAP*-specific or scramble siRNA (10 mM final) and 1.5 μl of Lipofectamine RNAiMAX Transfection Reagent (ThermoFisher Scientific) in 500 μl of medium/well. Medium was changed after 24 hours; cells were harvested after 48 hours for WB analysis.

Animal studies

Eight-week-old C57BL/6 WT mice (here and after simply called WT mice) were purchased from Charles River Laboratories. *Tie2cre*$^{+/+}$ and *Dab2*$^{flox/flox}$ mice were a gift from P. J. Murray (Department of Immunology, St. Jude Children's Research Hospital, Memphis, Tennessee) and were crossbreeded. In the text, the resulting *Dab2*$^{flox/flox}$*;Tie2cre*$^{+/-}$ mice are named Dab2 KO mice.

All animal experiments were approved by our local animal ethics committee at the University of Padova and were executed in accordance to Italian law as well as EU directives and guidelines. Mice were monitored daily and euthanized when displaying excessive discomfort. All mice were maintained under specific pathogen-free conditions in the Istituto Oncologico Veneto animal facility.

For *in vivo* experiments of tumor growth and metastasis induction, cells were injected orthotopically (o.t.) in mice, E0771 into the fat pad of the 4th (inguinal) mammary gland[243] and MN-MCA into the left quadriceps of mice (intra-muscle, i.m.)[75], both at the dose of $1 \cdot 10^5$ cells/mouse. Tumor growth was monitored every 2 days using a digital caliper. In the case of E0771-injected mice, tumors were resected when they reached dimensions of about 12x12 mm and mice were left to restart tumor progression. All mice were euthanized when tumors had an area of approximately 150 mm^2.

Wound healing experiments were performed as previously reported[244]. Harmless wounds were created on the dorsal skin of animals and daily photographed and measured up to 9 days to assess the healing process. Initial wound areas were always comparable. For every measurement, wound area was subtracted to the initial wound area to calculate the extension of healed area; finally, healed areas were expressed as percentages relative to the initial wound areas.

Generation of bone marrow-derived macrophages

Tibiae and femurs of C57BL/6 and Dab2 KO mice were removed by using sterile techniques and bone marrow (BM) cells were flushed with culture medium. Red blood cells were lysed with a hypotonic solution containing 8.3% NH_4Cl, 1% $KHCO_3$ and 0.5 M EDTA. After filtration, $1 \cdot 10^6$ cells were plated in 90 mm Petri dishes (Falcon) with 10 ml of RPMI 1640 medium (Euroclone) supplemented with 10% standardized heat-inactivated FBS (Superior, Bio-Chrom), 2 mM L-glutamine, 1 mM sodium pyruvate, 150 U/ml streptomycin, 200 U/ml penicillin (all from Lonza), 20 μM β-mercaptoethanol and 100 ng/ml recombinant murine GM-CSF or M-CSF (Miltenyi Biotec). The cultures were maintained at 37°C in 5% CO_2-humidified atmosphere for 7 days. On day 3 of culture, 5 ml of fresh cytokine-supplemented complete

medium were added. Differentiated BM-derived macrophages from both the non-adherent and adherent fractions were recovered by rinsing the dishes with PBS + 2 mM EDTA.
To evaluate the number of macrophages during *in vitro* M-CSF–induced differentiation of BM precursors, every two days cells were harvested, stained with Trypan Blue (Sigma-Aldrich) and counted. Final values were obtained multiplying the number of counted cells for the percentage of macrophages, as assessed by flow cytometry.

Endocytosis assays

In vitro uptake experiments were performed on differentiated WT or Dab2 KO BM-derived macrophages to evaluate the endocytosis of ECM proteins. Previously reported protocols were adapted for these analyses[245-247]. Rat collagen type I (cat. 354236), mouse collagen type IV (cat. 354233) and growth factor-reduced Matrigel (cat. 354230) were purchased from Corning Inc., while bovine fibronectin from ThermoFisher Scientific (cat. 33010-018). Proteins were labelled by using the FluoReporter FITC Protein Labeling Kit (ThermoFisher Scientific) in accordance with the manufacturer's instructions. At day 7 of culture, $0.5 \cdot 10^6$ macrophages were seeded in 24-well plates. After 24 hours, they were starved at 4°C for 30 minutes in complete medium without FBS to synchronize cell cycle and increase the endocytic ability. Then, the labelled proteins were diluted in complete medium without FBS and supplemented with M-CSF 100 ng/ml; the final concentration for each protein had been previously determined in order to have a detectable, non-saturating fluorimetric signal (50 µg/ml for collagen I, 25 µg/ml for collagen IV, 40 µg/ml for fibronectin). Proteins were added on cells for 2 hours at 4°C to permit binding to cell membranes. Then, macrophages were incubated at 37°C for 3, 16 or 20 hours. Not treated macrophages were always used as basal background control; in addition, cells treated with proteins but not incubated (0-hour control) were used to assess the signal of non-internalized, surface-bound proteins. At the end of culture, cells were detached with 0.25% trypsin (Gibco), washed in PBS to remove free ECM proteins, resuspended in PBS + 0.04% Trypan Blue (Sigma-Aldrich) to quench the FITC fluorophore on non-endocytosed proteins and fixed in PBS + 3.7% formaldehyde (Sigma-Aldrich) for 10 minutes. Finally, samples were analysed with an LSR II flow cytometer (BD Biosciences) and uptake of ECM proteins was expressed as the percentage of $FITC^+$ cells normalized on the 0-hour control.

Phagocytosis assays

To evaluate phagocytosis, differentiated WT and Dab2 KO BM-derived macrophages were starved and synchronized in medium without FBS for 30 minutes at 4°C. Then, cells were

seeded in 96-well plates (10^5 cells/well) and left to adhere for 1 hour at 37°C. After the incubation, culture medium was substituted with medium supplemented with pHrodo Green *Staphylococcus aureus* BioParticles (ThermoFisher Scientific), which are soluble particles designed to be uptaken through phagocytosis and becoming fluorescent only in acidic conditions, such as inside phagolysosomes. The manufacturer's instructions were followed. In short, bacteria were left for different periods of time (30-120 minutes). Cells without pHrodo and pHrodo without cells were used as controls to check background signals; all controls and experimental conditions were tested in triplicate. For each time point, the fluorescence emitted at 485 nm and the non-specific fluorescence at 535 nm were measured by means of a VICTOR X4 plate reader (PerkinElmer). The 485 nm signal from samples was corrected by subtracting the 535 nm signal and that of the control with particles alone.

Invasion assays

In vitro invasion assays were performed adapting a previously reported protocol[248]. Briefly, $5{\cdot}10^5$ WT or Dab2 KO BM-derived macrophages were mixed with Matrigel (Corning Inc.) to a final concentration of 2.2 mg/ml. Alternatively, $1{\cdot}10^5$ RAW 264.7 cells treated with the *Dab2*-specific or scramble shRNAs were embedded. The mixture was added on Transwells with 8 µm pores (Falcon) and let jellify in a 24-well plate to a thick, 3-dimensional matrix for 1 hour at 37°C. Then, culture medium supplemented with M-CSF 100 ng/ml was added both in the underneath well and on top of the Matrigel.

Cells were left in culture for 3 days to remodel the matrix and finally killed with puromycin 5 µg/ml for 48 hours. Transwells were washed three times with RPMI (at least 30 minutes per wash). E0771 cells were seeded on top of the Matrigel in culture medium + 2% FBS, while medium + 20% FBS was added in the well as chemoattractant for tumor cells. After 24 hours, Transwells were cleared of Matrigel with swabs, rinsed in PBS, fixed in methanol for 2 minutes, rinsed again in water and stained with crystal violet for 10 minutes. Dye in excess was washed away and cells that entered the Transwell porous membrane were imaged with a 2.5x objective on a Leica DMIL LED inverted optical microscope equipped with a Leica EC3 CCD camera. Images were acquired by using the LAS EZ software (Leica). Invasion by E0771 was quantitatively evaluated by dissolving crystal violet with a solution containing ethanol (final 50%) and acetic acid (final 0.1%). Absorbance at 595 nm was measured with a VICTOR X4 plate reader (PerkinElmer) and shown as membrane invasion.

***In vitro* migration assays**

Migratory ability of WT and Dab2 KO BM-derived macrophages was assessed as previously described[249]. BM-macrophages from WT or Dab2 KO mice were recovered at day 7 of culture

and seeded on 35 mm Petri dishes. A scratch was applied directly on the monolayer by means of a sterile pipette tip. The ability of cells to move and fill in the gap was evaluated by optical microscopy after 24 and 48 hours.

Cell shape measurements

Differentiated BM-derived macrophages were cultured at sub-confluence for 24 hours on 24-well plates. Pictures were taken by using a 10x objective on a Leica DMIL LED inverted optical microscope equipped with a Leica EC3 CCD camera. Images were acquired by using the LAS EZ software (Leica) and cell shape was calculated as ratio between the major and the minor axes of cells (aspect ratio) by means of the ImageJ software (NIH).

Culture on hydrogels

Acrylamide hydrogels were prepared into 24-well plates according to Tse et al., 2010[250]. Acrylamide and bis-acrylamide amounts were calculated to obtain an elastic modulus equal to 0.1 or 1 kPa. 10^5 HeLa cells were seeded on hydrogel-coated or uncoated plates and cultured for 24 hours. Cells were recovered with trypsin 0.25% (Sigma-Aldrich) and WB analysis for DAB2 was performed.

Lung metastasis detection and quantification

In already euthanized mice, lungs were flushed from blood by injecting 5-10 ml of PBS solution into the right ventricle after removal of the left kidney. In this way circulating tumor cells were eliminated from lungs.

Organs were then harvested and fixed in PBS + 10% formaldehyde. To optimize the detection of microscopic metastases and ensure systematic uniform and random sampling, lungs were cut transversally into 2 mm-thick parallel slabs with a random position of the first cut in the first 2 mm of the lung, resulting in 5-8 slabs per lung. The slabs were then embedded and sections were stained with hematoxylin and eosin (Bio-Optica). The number of lung micrometastases was blindly evaluated by two pathologists with a Leica DMRD optical microscope.

Breast cancer patients

For histological evaluations, primary tumor samples from 5 breast ductal carcinoma patients were collected at the University Hospital of Padova in collaboration with Dr. M. Fassan (Pathology Department, University of Padova). Breast samples from healthy reduction mammoplasty donors were used as a control for this analysis.

For prognosis and survival correlation analyses, data and samples from a preliminary series of 32 patients affected by pure invasive lobular carcinoma (ILC), surgically treated at the University Hospital of Verona, were collected in collaboration with Dr. L. Carbognin and Dr. E. Bria (Department of Medicine, University Hospital of Verona, Italy).
All the studies on biopsies from patients were approved by the local ethics committees. Informed consent was obtained from all subjects at the collection time. A database for individual data and information was appropriately fulfilled.

Organ cryoconservation and tissue sectioning

Tumors and flushed lungs were explanted and immediately fixed in PBS + 3.7% formaldehyde for 3 hours at 4°C. After fixation, organs were progressively dehydrated in PBS + 20% sucrose for 48 hours and, subsequently, in PBS + 30% sucrose for other 48 hours. Then, organs were included in cryostat embedding medium (Killik, Bio-Optica), frozen on liquid nitrogen vapours and stored at -80°C. Frozen organs were cut with a Leica CM 1950 cryostat in 7 µm-thick slices, which were stored at -20°C until staining for immunofluorescence (IF) or immunohistochemistry (IHC).

Immunofluorescence (IF)

For IF on cell lines or tissue sections, respectively coverslips and slides were rehydrated in PBS for 10 minutes, fixed in PBS + 3.7% formaldehyde for 5 minutes at room temperature (RT) and washed once in PBS and twice in PBS + 0.1% Tween20 (Sigma-Aldrich) for 5 minutes. Cell were permeabilized with PBS + 0.1% Triton X-100 (Sigma-Aldrich) for 10 minutes and then washed. Unspecific binding sites were blocked for 1.5 hours with either PBS + 10% FBS or PBS + 15% FBS + 3% BSA + 0.25% gelatin for more intense backgrounds to be reduced. Primary antibodies were incubated over-night at 4°C in PBS + 10% FBS. After 3 washes of 5 minutes in PBS + 0.01% Tween20, conjugated secondary antibodies were added and kept for 2 hours at RT. After 2 washes in PBS + 0.01% Tween20 and one in PBS, nuclei were stained with DAPI (Invitrogen) for 10 minutes at RT.
To visualize YAP on tissue sections, some variations were introduced (adapted from Morsut et al., 2010[251]): permeabilization was done in PBS + 0.3% Triton X-100; blocking, antibody and wash solutions were supplemented with a 0.1% of Triton X-100 to enhance intra-cellular staining.
Coverslips and slides were mounted by using Fluorescent Mounting Medium (DAKO) and analysed with a Leica TCS SP5 confocal microscope. Images were acquired and processed with the Leica LAS AF software.

Immunohistochemistry (IHC) and histological evaluations

For IHC on tissue sections from murine organs, slices were fixed as in IF and endogenous peroxidases were inactivated with PBS + 0.3% FBS + 0.3% H_2O_2 for 10 minutes. Permeabilization, blocking and incubation with primary antibodies were performed as in IF. The subsequent steps were performed following Elite ABC Kit (Vectastain) protocol. Briefly, slices were incubated with the provided anti-rabbit biotinylated secondary antibody for 30 minutes, washed, incubated with the avidin-HRP (horse radish peroxidase) reagent for other 30 minutes, washed and stained with the DAB chromogen (Sigma-Aldrich) until colour developed. Nuclei were stained with Mayer's hematoxylin (Sigma-Aldrich) for 2 minutes and dehydrated in increasing concentrations of ethanol. Finally, slices were mounted with the Eukitt mounting medium (Bio-Optica) and observed with a Leica DMIL LED inverted optical microscope equipped with a Leica EC3 CCD camera.

For histological evaluations on tissue sections from patients, a different protocol was used. Paraffin was removed from slices with one incubation in xylene for 30 minutes, two in ethanol 100% for 20 minutes, two in ethanol 95% for 20 minutes, one in ethanol 80% for 5 minutes. Antigens were unmasked by heating slices at sub-boiling temperature in 10 mM citrate buffer (pH 6) for 30 minutes; for CD68 staining, a second step of unmasking was performed by incubating samples with proteinase K (Sigma-Aldrich) for 10 minutes at RT. The profiling for DAB2, YAP and CD68 was automatically performed on a Bond TM Polymer Refine Detection System (Leica). Then, sections were lightly counter stained with hematoxylin. Appropriate positive controls (normal placenta) were run concurrently for all the applied antisera. For each tissue region of interest (intratumoral, normal peritumoral, invasive frontlines, healthy breast), $DAB2^+$ or YAP^+ cells with a macrophage-like morphology were counted in a 40x high power field (HPF) from 5 patients and the mean number per HPF was calculated.

For prognosis and survival correlation analyses in patients, an average number of $DAB2^+$ cells into the peritumoral and intratumoral infiltrates was obtained by analyzing 10 HPFs (40x). Positive endothelial and neoplastic cells were not retained for scoring.

Preparation of cell suspensions from organs

Spleens, lungs and tumors were collected from sacrificed mice and processed as previously described[252]. Spleens were only mechanically disaggregated and filtered on cell strainers (Falcon). Tumors and lungs were cut in small pieces with scissors, enzymatically digested with a solution containing collagenase IV (1 mg/ml), hyaluronidase (0.1 mg/ml) and DNase (4.5 mg/ml) (all from Sigma) and incubated at 37°C for 1 hour or more if necessary. Every 15 minutes tumors were mechanically disaggregated by means of a 2 ml needle-less syringe. Then, cells were collected and washed in complete medium to remove the residual digestive

solution. In all cases, cell suspensions were centrifuged and red blood cells were lysed as for BMs. Finally, cells were washed and counted for immunomagnetic sorting, FACS analysis or Western blot.

Cytofluorimetric stainings

0.5-2·10^6 cells, included those immunomagnetically sorted, were washed in cold PBS and incubated with a purified anti-FcγR antibody (2.4G2 clone) for 10 minutes at 4°C to minimize unspecific antibody binding. A mix with the antibodies of interest was directly added and kept for 20 minutes at 4°C in the dark. Then, samples were washed and resuspended in PBS for cytofluorimetric analysis. To evaluate cell viability, cells were stained with Aqua LIVE/DEAD dye (ThermoFisher Scientific), added in the antibody mix.

For integrin evaluation, cells were detached with a mild PBS + 2 mM EDTA treatment instead of the more aggressive trypsin to avoid damage of surface proteins. Samples were immediately put and always kept on ice to block receptor recycling into the cells and, after a wash at 4°C, were fixed with PBS + 3.7% formaldehyde[210,213]. The MFI (mean fluorescence intensity) of integrins was used to calculate the fold change relative to WT BM-derived macrophages or RAW 264.7 cells.

Samples were acquired with an LSR II flow cytometer (BD Biosciences) and analysed with the FlowJo software (Tree Star, Inc.).

Immunomagnetic sorting and fluorescence-activated cell sorting (FACS)

After organ disaggregation, cells were resuspended in sorting buffer (PBS + 0.5% BSA + 2 mM EDTA) supplemented with an anti-CD11b (MN-MCA) or anti-CD45 (PyMT) antibody conjugated with magnetic microbeads (Miltenyi Biotec) in accordance to the producer's instructions. After the labelling step, cell suspensions were washed and loaded on LS Separation Columns (Miltenyi Biotec) and $CD11b^+$ or $CD45^+$ cells were enriched by immunomagnetic sorting. Then, isolated cells were stained for markers of interest, resuspended in FACS buffer (PBS supplemented with 0.5 mM EDTA, 3% FBS, 150 U/ml streptomycin, 200 U/ml penicillin) and sorted with a FACS Aria (BD Biosciences). Sorted populations were analysed by Western blot or, after attachment on coverslips, by IF.

In MN-MCA tumors, TAMs were defined as $CD11b^+$ $F4/80^+$ $Ly6C^-$ $Ly6G^-$ (ref.[40]). In lungs from MN-MCA–tumor-bearing mice, resident macrophages were identified as $CD11b^{low}$ $CD11c^{high}$, while MAMs in the same way of MN-MCA TAMs[121]. In PyMT tumors, TAMs were defined as $CD11b^{low}$ MHC-II^{high} $Ly6C^-$ and MTMs as $CD11b^{high}$ MHC-II^{high} $Ly6C^-$ (ref.[58]).

Ex vivo T cell suppression assays

OT-I/CD45.1 splenocytes derived from the spleen of OT-I mice were labelled with carboxyfluorescein succinimidyl ester (CFSE Cell Trace Kit, Invitrogen) according to manufacturer's instructions. A mixed leucocyte-peptide culture (MLPC) was prepared by adding γ-irradiated C57BL/6 splenocytes to the OT-I/CD45.1 CFSE-labelled splenocytes in order to obtain a final concentration of the latter equal to 1%. The MPLC culture was plated in flat-bottom 96-well plates ($6 \cdot 10^5$ cells/well) and 1 µg/ml H-2 Kb-restricted OVA peptide (OVA257-264, SIINFEKL, from JPT Peptide Technologies) was added to the culture to stimulate OVA-specific OT-I $CD8^+$ T lymphocytes. $CD11b^+$ cells immunomagnetically sorted from MN-MCA tumors at 21 days after tumor cell injection were added at degreasing percentages with respect to the MLPC culture (24%, 12%, 6% and 3%). Also controls without MDSCs (fully activated lymphocytes) and without OVA (resting lymphocytes) were considered. Cultures were maintained at 37°C in RPMI supplemented with 10% FBS (Superior, Biochrom), 2 mM L-glutamine, 1 mM sodium pyruvate, 150 U/ml streptomycin, 200 U/ml penicillin, 20 µM β-mercaptoethanol. After 3 days, cells were harvested, washed in PBS, stained for CD45.1 and CD8, and CFSE dilution upon T cell proliferation was assessed with a FACSCalibur flow cytometer (BD Biosciences). CFSE distribution within the $CD8^+$ $CD45.1^+$ population was evaluated relatively to resting lymphocytes. The percentage of suppression exerted by tumor-infiltrating $CD11b^+$ cells was calculated with the formula *[1-(% divided cells in sample/% divided cells in activated control)]·100*, as previously described[253].

Western blot (WB)

Cells were collected and rinsed twice in PBS, then immediately pelleted and frozen in liquid nitrogen. Once thawed, samples were dissolved in Laemmli Buffer and denatured for 10 min at 100°C. Proteins were loaded according to Bradford quantification, electrophoretically separated on an 8% SDS-PAGE gel and transferred onto PVDF membranes (Immobilon P membranes Millipore).

PBS + 5% non-fat dry milk (Santa Cruz Biotechnology) was used to block unspecific sites for 1 hour at RT. Membranes were incubated overnight at 4°C with primary antibodies in PBS + 5% non-fat dry milk, then washed in PBS + Tween 0.05% (Sigma-Aldrich). HRP-conjugated secondary antibodies were incubated for 1 hour at RT in PBS + 5% non-fat dry milk. After washes in PBS + Tween 0.05%, protein levels were revealed on High Performance Chemiluminescence film (GE Healthcare) after 5 minutes of incubation with SuperSignal WestPico Chemiluminescent substrate (ThermoFisher Scientific). For signal quantification, the software ImageJ (NIH) was employed.

Antibodies

The following conjugated antibodies were used for flow cytometry/FACS: rat anti-CD11b PE-Cy7 (1:500), rat anti-Ly6G APC-Cy7 (1:200), rat anti-Ly6C eFluor 450 (1:250), rat anti-I-A/I-E PerCP-Cy5.5 (1:250), mouse anti-CD45.1 PE (1:250), rat anti-CD8a PerCP-Cy5.5 (1:250), rat anti-CD49e Alexa Fluor 647 (1:25), Armenian hamster anti-CD49e PE (1:25), rat anti-CD49f PerCP-eFluor 710 (1:25), hamster anti-CD29 PerCP-eFluor 710 (1:20) (all from eBioscience), Armenian hamster anti-CD11c PE (1:250), Armenian hamster anti-CD29 PE (1:250, both Biolegend), hamster anti-CD49a PE or PerCP-Cy5.5 (1:25, BD Biosciences), rat anti-F4/80 FITC (1:125, AbD Serotec). Alternatively, rat anti-F4/80 biotin (1:125, BIO-RAD) followed by streptavidin-APC (1:1000, Becton Dickinson Co.) were used.

The following primary antibodies were used for IF: rabbit anti-DAB2 H-110 (1:100), goat anti-DAB2 D-19 (1:100 or 1:200), mouse anti-YAP 63.7 (1:100 or 1:200), rabbit anti-YAP H-125 (1:50 or 1:100) (all from Santa Cruz Biotechnology), rat anti-F4/80, Cl:A3-1 (1:400, AbD Serotec), mouse anti-CD68, KP1 (1:100, Abcam). The secondary conjugated antibodies were purchased from Jackson ImmunoResearch: anti-rabbit RRX or Alexa Fluor 488, anti-rat Alexa Fluor 647, anti-mouse Alexa Fluor 488, anti-goat Alexa Fluor 488 or DyLight 405 (1:200). Anti-mouse DyLight 649 was purchased from Abcam (1:200). The following antibodies were used for WB: rabbit anti-DAB2 H-110, mouse anti-YAP 63.7 (1:1000, both Santa Cruz Biotechnology), polyclonal rabbit anti-actin residues 20-33 (1:200, Sigma-Aldrich) and anti-GAPDH 65C (1:200, Millipore); secondary HRP-conjugated anti-rabbit and anti-mouse antibodies (1:10,000, GE Healthcare).

Bioinformatic analysis

A Gene Set Enrichment Analysis (GSEA) was performed in collaboration with Professor Bicciato's group (Department of Life Sciences, University of Modena and Reggio Emilia, Italy) to correlate the *Dab2* gene expression in macrophage datasets with hundreds of already described tumor-associated pathways. Only predicted correlations with a False Discovery Rate (FDR) ≤ 0.05 were considered to be significant.

Statistical analyses

Student's t-test was performed on parametric groups. Values were considered significant at $p \leq 0.05$ and are indicated as $*p \leq 0.05$, $**p \leq 0.01$ and $***p \leq 0.001$. Values are reported as mean ± standard error (s.e.) or standard deviation (s.d.). All analyses were performed by using SigmaPlot (Systat Software Inc).

Statistical analyses for studies with human samples

Descriptive statistics was adopted. Follow-up was analyzed and reported according to Shuster, 1991[254]. DAB2 expression data were obtained from the IHC stainings on patient biopsies. The receiver operating characteristic (ROC) analysis was applied to the DAB2 continuous score to dichotomize the obtained values according to DFS. To correlate DAB2 expression with clinicopathological data, Pearson's chi-squared test or Fisher's exact test were used, depending on sample size. The presence of lymph node metastases, tumor cell proliferation (Ki-67 expression) and vascular invasion (V.I.) inside the primary tumor were considered as characteristics of interest. Disease-free survival (DFS) curves were elaborated by using the Kaplan-Meier method and significance was calculated with the Log-Rank test. p-values were considered significant when ≤ 0.05. The SPSS 18.0, R 2.6.1 and MedCalc 14.2.1 statistical programs were used for all analyses.

RESULTS

Myeloid cells expressing DAB2 support the metastatic process

The data previously obtained by our group demonstrated that the induction of DAB2 in myeloid cells was tumor-related suggesting a peculiar function of the protein in the tumor microenvironment. To establish the consequences of DAB2 deficiency in intratumoral myeloid cells, we generated a conditional knockout mouse strain based on the Cre/Lox deletion system. The *Dab2$^{flox/flox}$;Tie2Cre$^{+/-}$* (Dab2 KO) mice express the CRE recombinase under the control of the *Tie2* gene promoter, allowing a specific deletion of the LoxP-flanked (floxed) *Dab2* gene in the hematopoietic precursors[255].

We initially examined the role of DAB2 in tumor progression and metastatic spreading. This multistep process begins from the primary tumor and it is known that myeloid cells, in particular macrophages, have a central role in assisting all its steps[64]. WT or Dab2 KO mice were orthotopically injected with MN-MCA (fibrosarcoma)[75] or E0771 (breast carcinoma) cells[243], respectively in the quadriceps and in the mammary fat pad. Both cell lines are known to spontaneously form metastases in the lungs. Interestingly, we observed that Dab2 KO mice showed a significant reduction in the number of lung micrometastases in comparison to WT mice in both tumor models (Figure 9A). Nevertheless, we did not find any difference in primary tumor growth (Figure 9B).

These results prompted us to investigate the effects of DAB2 depletion on myeloid cells in the metastatic process. It is well established that an immunosuppressive microenvironment in the primary tumor fosters tumor cell invasion and metastatization in other organs[107]. Hence, the observed reduction in the number of metastases could be explained supposing that DAB2 depletion in myeloid cells could alter their immunosuppressive functions in the tumor microenvironment. To test this initial hypothesis, we purified myeloid cells from either WT or KO mice by using anti-CD11b microbeads and immunomagnetic sorting. Then, we co-cultured CD11b$^+$ cells with CFSE-labelled OVA-specific CD8$^+$ T cells in a mixed lymphocytes-peptide culture (MLPC). After three days, the proliferation of CD8$^+$ T cells was evaluated by FACS analysis. We found that Dab2 KO CD11b$^+$ cells were not impaired in their immunosuppressive activity as compared to WT CD11b$^+$ cells (Figure 9C).

Moreover, analysis of the myeloid infiltrate in MN-MCA tumors at 21 days from tumor cell injection showed that the absence of DAB2 in KO mice did not affect the accumulation of myeloid subpopulations. Indeed, the percentages of granulocytes (Ly6G$^+$ Ly6C^{low}), monocytes (Ly6G$^-$ Ly6C^{high}) and TAMs (Ly6G$^-$ Ly6C$^{low/-}$ F4/80$^+$) were comparable between WT and

KO mice (Figure 9D). Likewise, also in the lungs of MN-MCA tumor-bearing WT and Dab2 KO mice we found similar percentages of granulocytes ($Ly6G^+$ $Ly6C^{low}$), monocytes ($Ly6G^-$ $Ly6C^{high}$), resident macrophages ($CD11c^+$ $CD11b^{low}$) and MAMs ($Ly6G^-$ $Ly6C^{low/-}$ $F4/80^+$) (Figure 9E).

These data showed that DAB2 had an effect on the metastatic process but that this effect was not due to a defect in myeloid cell accumulation or due to their immunosuppressive abilities inside the primary tumor. For this reason, the primary tumor growth was very similar in WT and Dab2 KO mice.

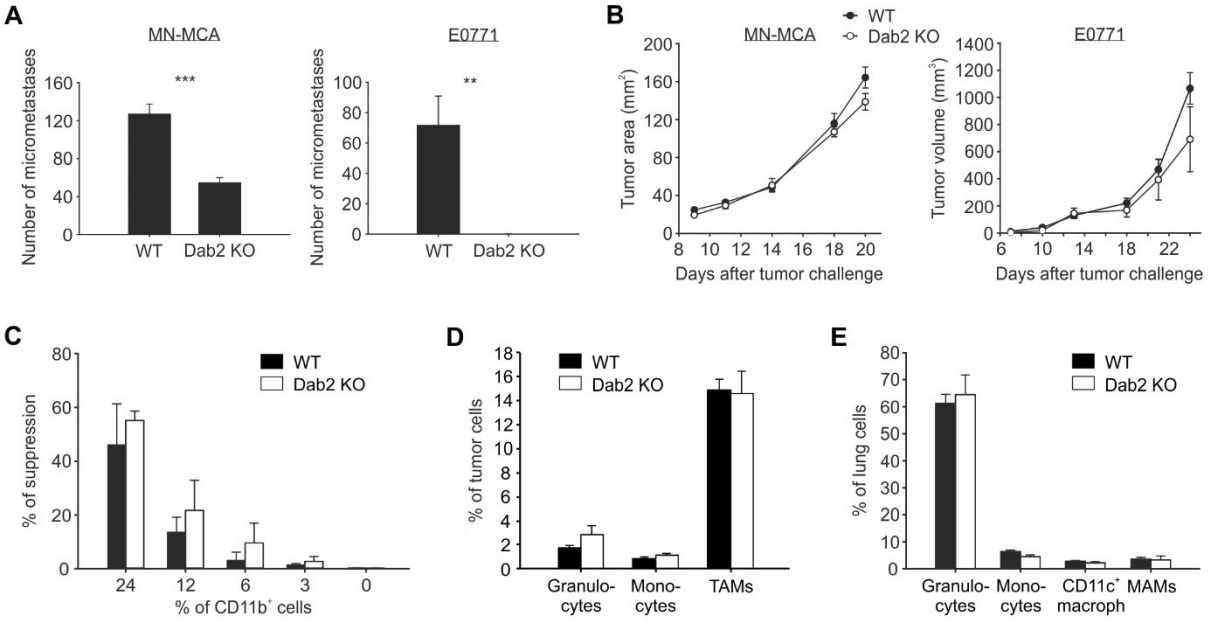

Figure 9 - Myeloid cells expressing DAB2 support the metastatic process. *(**A, B**) WT or Dab2 KO mice (lacking the protein in the hematopoietic lineage) were orthotopically injected with MN-MCA (fibrosarcoma) or E0771 (breast carcinoma) cells. Tumor growth was monitored and mice were sacrificed when tumor area reached 150 mm^2. (**A**) The number of micrometastases in the lungs was quantified. (**B**) Tumor area for MN-MCA and tumor volume for E0771 are reported. (**A, B**) n = 18 mice/group pooled from 3 independent experiments. (**C-E**) WT or Dab2 KO mice were injected with MN-MCA tumor cells. After 21 days mice were euthanized and tumor masses or lungs were collected. (**C**) The immunosuppressive ability of tumor-infiltrating MDSCs was evaluated. $CD45.1^+$ OT-I splenocytes were labelled with CFSE and cultured in the presence of the SIINFEKL ovalbumin (OVA) peptide to induce antigen-specific activation of $CD8^+$ T cells. $CD11b^+$ myeloid cells isolated from MN-MCA tumors were added at different ratios to the splenocyte cultures. CFSE dilution upon T cell proliferation was measured by flow cytometry after 3 days of culture and the percentage of suppression was calculated. (**D, E**) The percentages of different myeloid subpopulations within tumors (**D**) and lungs (**E**) are reported. (**C-E**) n = 3 mice/group, representative of 3 independent experiments. (**A, C-E**) Error bars are mean ± s.e.; *p ≤ 0.05, **p ≤ 0.01 and ***p ≤ 0.001 by Student's t-test.*

DAB2 is mainly expressed by TAMs

To further investigate the role of DAB2 in promoting the metastatic process, we decided to identify the specific DAB2-expressing myeloid subpopulation. Thus, myeloid subsets were

FACS-sorted from tumors and lungs of MN-MCA–injected mice or from the primary tumors of PyMT mice. PyMT transgenic mice represent a more physiological model since they spontaneously develop metastatic breast carcinoma. The gating strategies used to sort the subsets of interest are shown in Figure 10A,B.

Then, we evaluated protein expression in WB by using a specific anti-DAB2 antibody on FACS-sorted populations. As shown in Figure 10C, in MN-MCA primary tumors, p96 and p67 isoforms were intensely expressed by TAMs, while they were expressed at low levels in monocytes and were not detected in granulocytes. In metastatic lungs from the same animals, p96 and p67 were expressed in metastasis-associated macrophages (MAMs) but not in the other myeloid subsets.

We then analysed DAB2 expression in primary tumors from PyMT transgenic mice. DAB2 isoforms were expressed in sorted TAMs, but at irrelevant levels in resident mammary tissue macrophages (MTMs) (Figure 10D).

Furthermore, upregulation of the DAB2 protein in myeloid cells was specific for the tumor microenvironment, because DAB2 was not detectable in BM or splenic myeloid precursors from WT mice (Figure 10E,F at time 0). Therefore, we tried to identify the factors that were required to upregulate the protein within the tumor. We speculated that the same stimuli which initiate the macrophage differentiation were also responsible for the expression of DAB2. M-CSF and GM-CSF are two cytokines which are abundantly secreted in the tumor microenvironment[31] and both are known to drive the differentiation and proliferation of monocytes and macrophages[256,257]. Thus, when we stimulated BM precursors with M-CSF or GM-CSF to induce *in vitro* differentiation toward, respectively, macrophage or granulocyte/macrophage phenotypes, p96 and p67 were increasingly expressed during the culture (Figure 10E). Similarly, when $CD11b^+$ myeloid cells were immunomagnetically sorted from spleens and stimulated for 24 hours with M-, G- or GM-CSF, the differentiation into macrophages, but not granulocytes, led to the expression of both DAB2 isoforms (Figure 10F). In accordance with these results, DAB2 had been initially identified in a macrophage cell line, where it was phosphorylated in response to the growth factor M-CSF[134].

Since DAB2 was expressed upon stimulation of WT BM cells with M- or GM-CSF, we tried to understand if the protein could have a role in the differentiation process of BM precursors into macrophages. To verify this, we stimulated WT or Dab2 KO BM cells with M-CSF and every two days counted cells after vitality staining. The number of macrophages in culture was calculated by multiplying the count for the percentage of macrophages, as assessed by flow cytometry. As shown in Figure 10G, there was no observable defect in BM-derived macrophage differentiation and proliferation, thus suggesting that DAB2 is not involved in these processes.

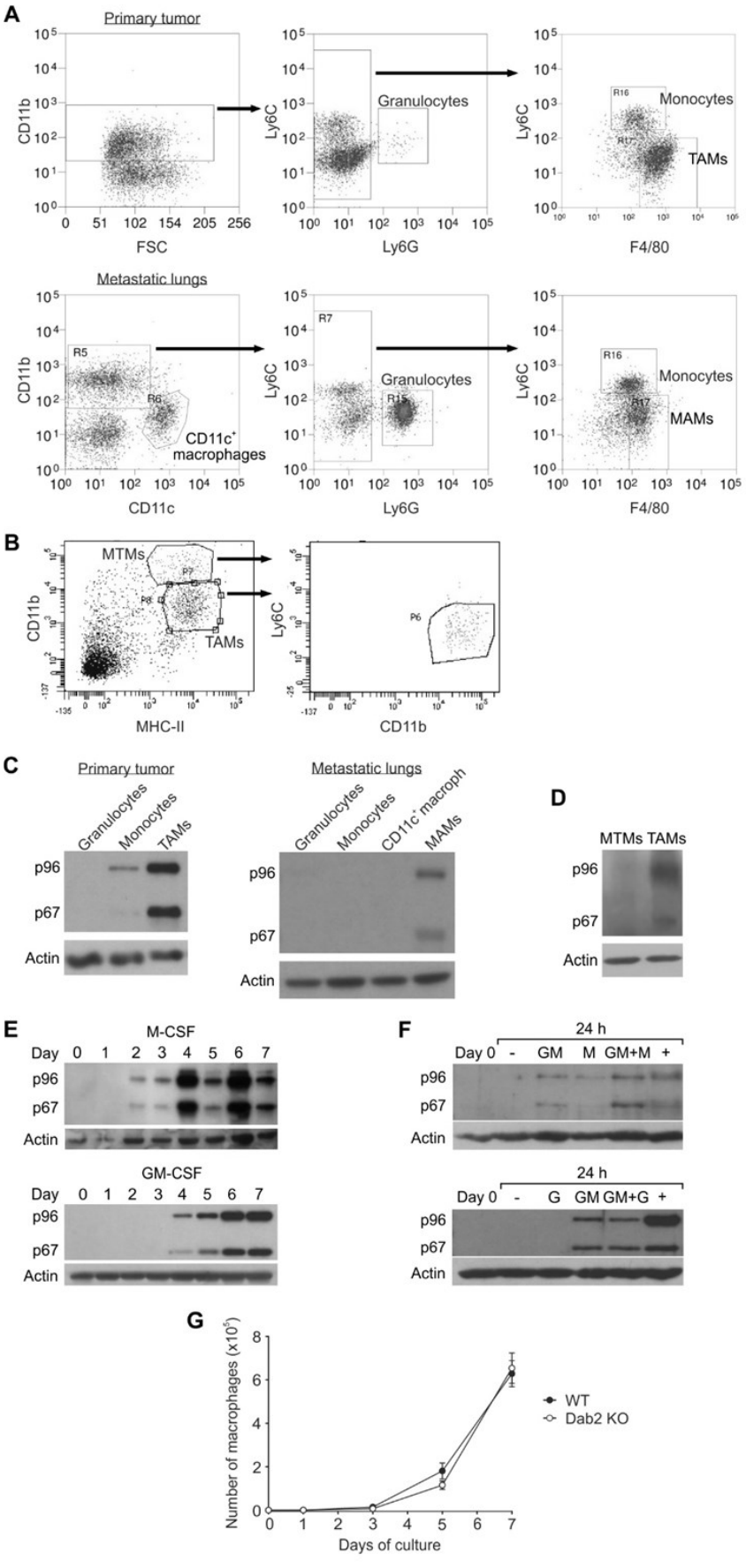
A
Primary tumor
CD11b
FSC
Ly6C
Ly6G
Granulocytes
Monocytes
TAMs
F4/80
Metastatic lungs
CD11c
CD11c+ macrophages
MAMs
B
MTMs
TAMs
MHC-II
CD11b
C
Primary tumor
Metastatic lungs
Granulocytes
Monocytes
TAMs
CD11c+ macroph
MAMs
p96
p67
Actin
D
MTMs TAMs
E
M-CSF
GM-CSF
Day 0 1 2 3 4 5 6 7
F
24 h
Day 0 - GM M GM+M +
Day 0 - G GM GM+G +
G
Number of macrophages (x10^5)
Days of culture
WT
Dab2 KO

Figure 10 - DAB2 is expressed by TAMs and during in vitro macrophage differentiation. *(**A, B**) Gating strategies for FACS isolation of myeloid subsets from tumors and lungs of MN-MCA–injected mice (**A**) or from the primary tumors of PyMT mice (**B**). Different myeloid populations were purified: granulocytes, monocytes, CD11c$^+$ resident macrophages, TAMs, MAMs and MTMs (tumor-associated, metastasis-associated and mammary tissue macrophages, respectively). (**C, D**) WB analyses to evaluate the expression of DAB2 isoforms (p96 and p67) on FACS-sorted myeloid subsets infiltrating primary tumors or lungs from MN-MCA–tumor bearing mice (**C**) or primary tumors from PyMT mice (**D**). Actin was used as loading control. (**E**) BM (bone marrow) precursors from WT mice were induced to differentiate with M-CSF or GM-CSF for 7 days. During the whole culture, cells were daily collected to assess DAB2 expression by WB. (**F**) CD11b$^+$ myeloid cells were immunomagnetically sorted from WT spleens and stimulated for 24 hours with M-, G-, GM-CSF or a combination of them. We used CD11b$^+$ unstimulated cells as negative control (indicated with –) and intratumoral CD11b$^+$ cells as positive control (indicated with +). A WB analysis was performed to evaluate the expression of DAB2 isoforms. Actin was used as loading control. (**C-F**) Results are representative of n = 3 independent experiments. (**G**) BM precursors from either WT or Dab2 KO mice were differentiated in vitro with M-CSF. The number of macrophages obtained every two days of culture is reported. Values were calculated by multiplying the count of retrieved cells by the percentage of macrophages, as assessed by flow cytometry. Error bars are mean ± s.e.; n = 3 independent experiments, each obtained using a pool of 3 mice.*

DAB2-expressing TAMs localize along the tumor border

The observation that DAB2 was mainly expressed by macrophages prompted us to further define the localization of DAB2$^+$ cells in tissue slices from primary tumors and metastatic lungs (Figure 11A-C). IHC analysis on tumor masses isolated from MN-MCA–injected mice showed that DAB2$^+$ cells were mainly localized in peri-lesional areas, at the invasive frontline between the tumor and the surrounding healthy muscle (Figure 11A). In particular, as indicated by double IF stainings (Figure 11A), DAB2 was expressed in stromal F4/80$^+$ TAMs (in violet) around muscle fibers partially or not-yet reached by invading tumor cells. By quantifying in IF the fraction of DAB2$^+$ F4/80$^+$ cells, we observed that in internal areas of the tumor there was no DAB2 expression and that the percentage of DAB2$^+$ TAMs increased progressively moving toward external areas, up to a maximum of almost 70% at the invasion frontline. In PyMT tumors the localization of DAB2$^+$ TAMs was similar, being more concentrated in the stroma around healthy or not completely transformed acini in external areas of the tumor mass as well as along the border with the surrounding healthy breast (Figure 11B).

Moreover, looking to the expression of DAB2 in the metastatic site by using IHC and IF, we could observe DAB2$^+$ macrophages among lung MAMs from MN-MCA tumor-bearing animals (Figure 11C). These cells were localized inside metastases in increasing numbers from the centre to the borders, likewise to the primary tumor. Only few DAB2-expressing macrophages were present in healthy areas of metastatic lungs. In order to understand the extent of DAB2$^+$ macrophage accumulation in tumors and metastatic lungs, we checked tissues from healthy

mice for DAB2 expression. We found few DAB2-expressing resident macrophages in the breast (as seen in PyMT MTMs, Figure 10D), lungs and quadriceps, since a part of the cells was single positive. However, the number of DAB2^{+} macrophages increased during tumor establishment and assumed a peculiar localization.

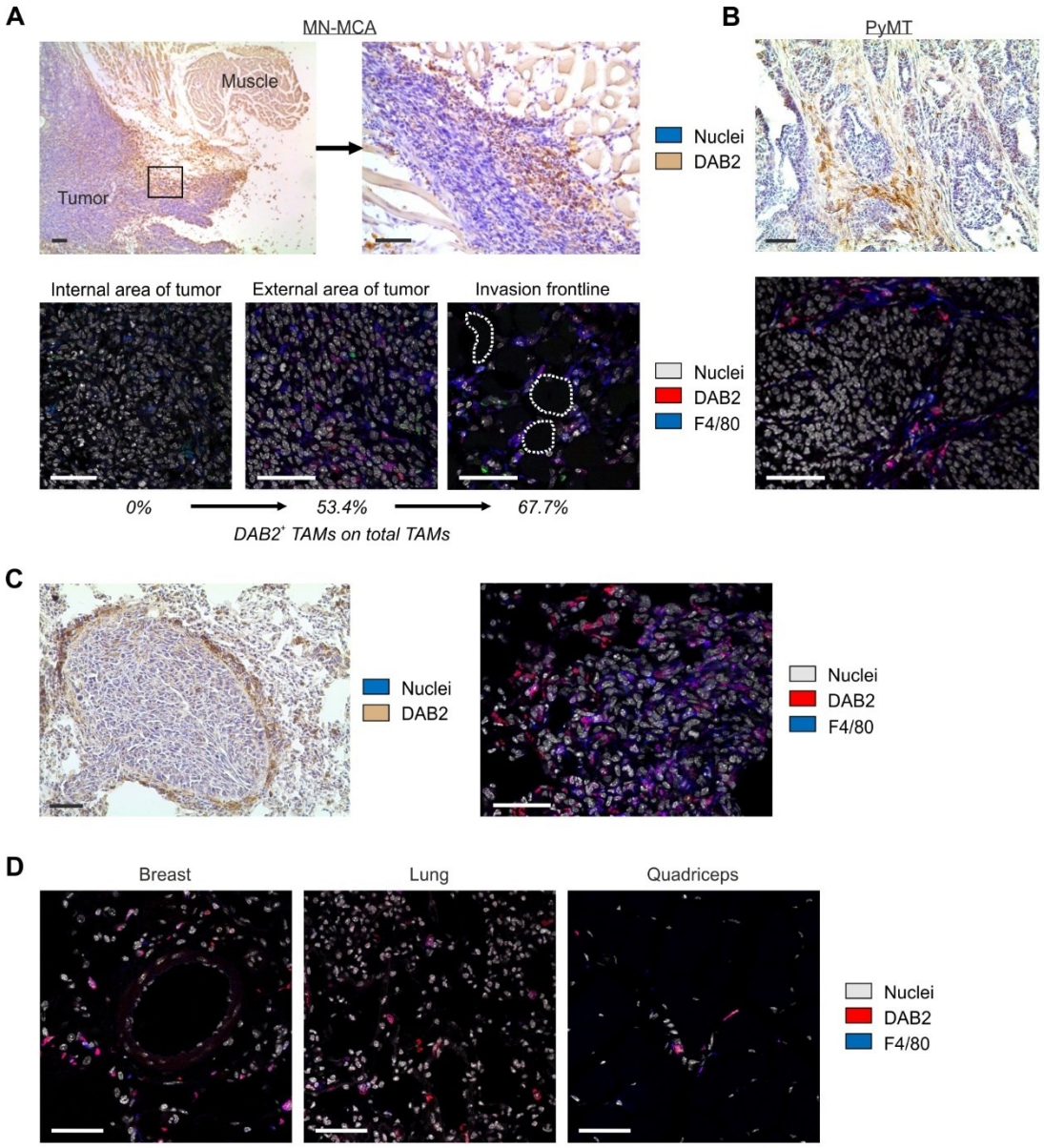

Figure 11 - DAB2-expressing TAMs localize along the tumor border. *(**A**) MN-MCA tumor cells were injected in WT mice. Slices of tumor masses were analyzed by IHC and IF. At the top of the panel a representative IHC image for a DAB2 specific staining is reported (left) with an image of a detail along the tumor border (right). At the bottom, IF images from different areas of the tumor are reported, showing specific stainings for DAB2 and the macrophage marker F4/80. DAB2 staining localizes mainly in macrophages along the tumor border, close to healthy muscle fibers (dashed lines in IF). An exemplificative quantification of DAB2^{+} TAMs on total TAMs, relative to the shown images, is reported. Scale bars, 50 µm. (**B**) PyMT mice bearing large tumor masses were euthanized to perform IHC and IF analyses. At the top, a representative IHC staining for DAB2 is reported. DAB2 mainly*

*localizes in external areas of the tumor, around healthy or not completely transformed acini. At the bottom, the IF image shows the co-localization of DAB2 and the F4/80 marker in a similar area. Scale bars, 50 µm. (**C**) Lungs from MN-MCA tumor-bearing animals were stained for DAB2 in IHC (left); a representative metastasis is shown. An exemplificative IF image of the metastasis border is also reported (right), with a specific staining for DAB2 and F4/80. DAB2$^+$ MAMs were localized mainly on the border of metastases. Scale bars, 50 µm. (**D**) Different tissues from healthy mice were checked for DAB2 expression in IF. Scale bars, 50 µm.*

DAB2 regulates macrophage morphology but not motility

After having determined the particular spatial distribution of DAB2-expressing TAMs and MAMs in the tumor and metastatic site, we tried to identify in these cells other effects derived from the expression of the protein. We noticed that BM-derived macrophages from WT mice had a more elongated shape if compared to that from Dab2 KO mice (Figure 12A). The ImageJ software was used to quantify the shape of cells in terms of aspect ratio, that is defined as the ratio between the major and the minor axes of a cell. An aspect ratio equal to 1 corresponds to a perfect circle and greater values correspond to longer objects. It resulted that WT macrophages had a significantly higher aspect ratio than Dab2 KO macrophages (Figure 12A).

This observation is in line with previous works from Rosenbauer et al. on macrophages and from Chetrit et al. on fibroblasts, HeLa and epithelial cells, where DAB2 was shown to mediate cell spreading on the substrate by trafficking β1 integrins near focal adhesions and mediating the assembly of actin fibers[145,147].

Since the renewal of focal adhesions and cell migration are associated mechanisms, we next tried to understand if the different spreading abilities could entail a different motility of WT and Dab2 KO macrophages. BM-derived macrophages were seeded and a scratch was applied directly on the monolayer with a sterile pipette tip. The cell ability to move and fill again the scratch was evaluated after 24 and 48 hours. As shown in Figure 12B, WT and Dab2 KO macrophages closed the gap with comparable speeds.

Hence, DAB2 seems not to control macrophage migratory ability. This is in accordance with the work from Westcott et al., where it is shown that siRNA-mediated silencing of *Dab2* in SUM159 breast cancer cells did not affect their motility in a monolayer culture[202].

Considering that WT and Dab2 KO mice have a similar percentage of tumor infiltrating TAMs (Figure 9D) and that DAB2 seems not to be involved during *in vitro* macrophage differentiation (Figure 10G), it is plausible to think that also *in vivo* DAB2 expression does not give an advantage in terms of macrophage motility. Nonetheless, this speculation needs to be further validated and experiments to confirm the absence of a DAB2 involvement in macrophage migratory ability are ongoing.

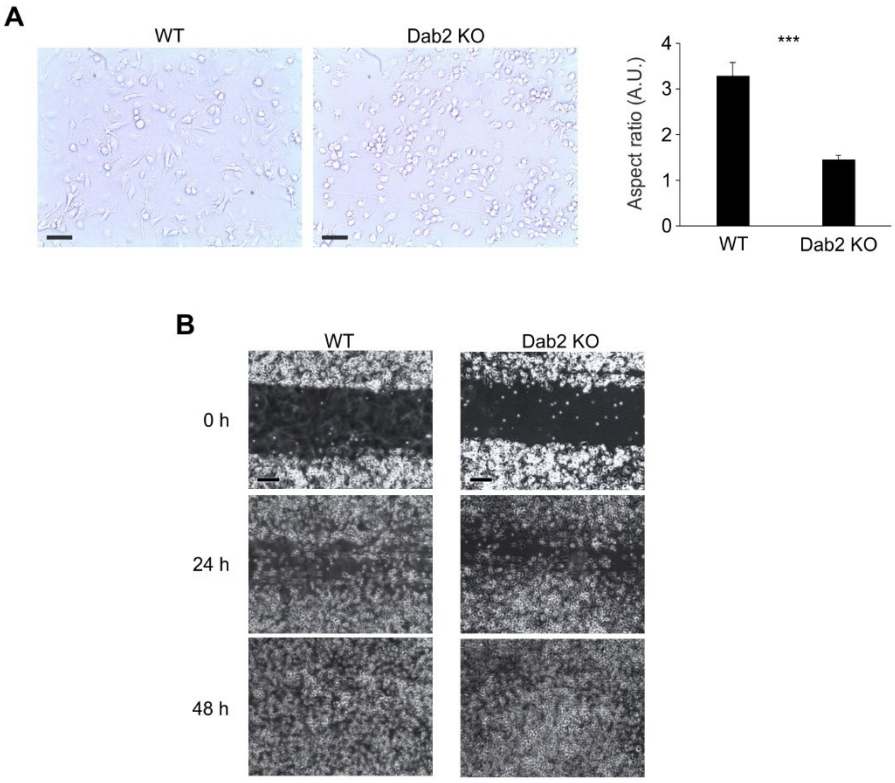

Figure 12 - DAB2 regulates macrophage morphology but not motility. *(**A**) BM-derived macrophages from WT and Dab2 KO mice were obtained after 7 days of culture in the presence of M-CSF. Cells were detached and seeded on 24-well plates for 24 hours. Optical micrographs of cultured cells are shown (left). Scale bars, 100 µm. Cell shape was quantified as aspect ratio (right), that is calculated as the ratio between the major and the minor axes of the cell, where 1 corresponds to a perfect circle and greater values to longer cells. Error bars are mean ± s.e.; n = 3 independent experiments; ***p ≤ 0.001 by Student's t-test. A.U.: arbitrary units. (**B**) BM-derived macrophages from WT or Dab2 KO mice were recovered at day 7 and cultured on 35 mm Petri dishes. A scratch was applied on the monolayer and the ability of cells to move and fill in the gap was evaluated by optical microscopy after 24 and 48 hours. Scale bars, 500 µm.*

YAP regulates DAB2 expression in TAMs

In order to identify the specific mechanism of DAB2 activation, we performed a gene set enrichment analysis (GSEA) to correlate *Dab2* expression in macrophages with known tumor-associated molecular pathways. Among the resulting matches (Table 2), the correlation between DAB2 and the signature related to YAP (Yes-Associated Protein) appeared particularly interesting.

YAP is a mechanotransduction-related transcription regulator found to be hyper-activated in transformed cells, where it regulates proliferation, survival and motility in response to mechanical inputs from the ECM[232]. In accordance with the found correlation, the *Dab2* gene

had been already reported as a predicted target of YAP[233,236], suggesting a possible role for DAB2 in YAP-mediated mechanotransduction in TAMs. It is worth to note that, since these were *in silico* predictions, the association between DAB2 and YAP has never been experimentally validated up to date.

	GS follow link to MSigDB	GS DETAILS	SIZE	ES	NES	NOM p-val	FDR q-val	FWER p-val	RANK AT MAX	LEADING EDGE
1	CSF1R_PROLIFERATION	Details ...	14	0.80	2.40	0.000	0.000	0.000	2033	tags=71%, list=13%, signal=82%
2	REACTOME_SIGNALING_BY_WNT	Details ...	57	0.51	2.21	0.000	0.000	0.000	2778	tags=44%, list=18%, signal=53%
3	CORDENONSI_YAP_CONSERVED_SIGNATURE	Details ...	54	0.48	2.05	0.000	0.001	0.002	2017	tags=35%, list=13%, signal=40%
4	CSF1R_ADHESION	Details ...	17	0.59	1.91	0.000	0.004	0.013	3793	tags=59%, list=25%, signal=78%
5	CSF1R_DIFFERENTIATION	Details ...	16	0.56	1.78	0.010	0.019	0.070	2033	tags=50%, list=13%, signal=58%
6	AUTOPHAGY	Details ...	18	0.48	1.58	0.038	0.066	0.253	3810	tags=50%, list=25%, signal=67%
7	CSF1R_SURVIVAL	Details ...	15	0.48	1.50	0.060	0.095	0.400	4104	tags=67%, list=27%, signal=91%
8	ANGIOGENESIS	Details ...	45	0.32	1.35	0.087	0.211	0.731	2586	tags=29%, list=17%, signal=35%
9	KEGG_PATHWAYS_IN_CANCER	Details ...	310	0.23	1.33	0.014	0.209	0.765	2353	tags=22%, list=15%, signal=25%

Table 2 - In silico correlation between DAB2 expression in macrophages and tumor-related pathways. *The GSEA produced a list of tumor-related pathways possibly associated with Dab2 expression in macrophages. Only the first 5 results have an FDR (false discovery rate) ≤ 0.05 and are predicted to be significant.*

It has been demonstrated that YAP expression is modulated by the substrate stiffness: soft matrices induce its cytoplasmic retention, while stiff matrices cause its nuclear transfer and activation[233]. YAP is generally upregulated in tumor cells and CAFs, since the ECM stiffness in tumors is high[17,258].

To evaluate the hypothesis that DAB2 could be regulated through YAP, we performed preliminary *in vitro* experiments using HeLa cancer cells, in which both the p96 isoform (but not p67) and YAP are constitutively expressed, as shown in the confocal image reported in Figure 13A.

First, we checked if DAB2 expression was regulated by the substrate stiffness. HeLa cells were plated on wells coated with hydrogel of two different, tissue-mimicking elastic moduli (0.1 and 1 kPa) or on uncoated wells ($2.78 \cdot 10^9$ kPa, the stiffness of plastic, that is much more rigid than tissues)[258,259]. The expression of DAB2 was progressively upregulated while increasing the substrate stiffness (Figure 13B) and this modulation strongly suggested a regulation by the transcriptional factor YAP. To further confirm this hypothesis, we treated HeLa cells with a non-correlated (scramble) siRNA or two different *YAP*-specific siRNAs, either alone or in combination; then, we evaluated both YAP and p96 expression by WB (Figure 13C). Remarkably, in all cases depletion of YAP induced a significant downregulation of DAB2. Altogether, these results indicate that DAB2 expression is directly or indirectly regulated by YAP.

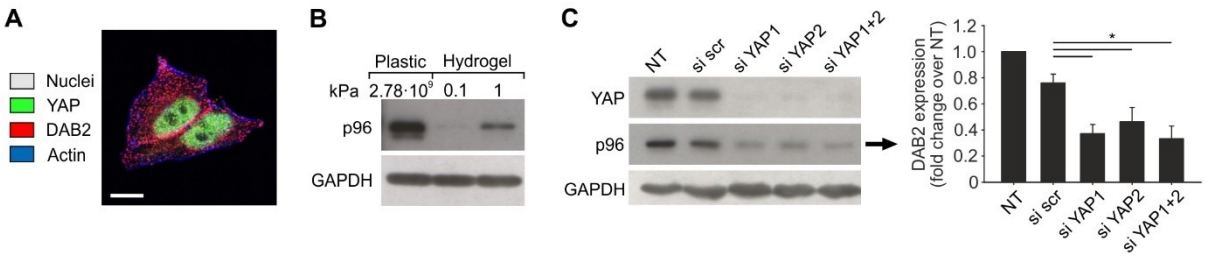

Figure 13 - The transcription regulator YAP modulates DAB2 expression in HeLa cells. *(**A**) HeLa cancer cells were stained in IF for the expression of DAB2, YAP and actin; nuclei were also stained. A representative image is reported to show the co-expression of DAB2 and YAP. Scale bar, 10 μm. (**B**) HeLa cells were seeded on wells coated with hydrogel of different elastic moduli (0.1 and 1 kPa) or on uncoated wells ($2.78 \cdot 10^9$ kPa). Cells were collected after 24 hours and the expression of the DAB2 isoform p96 was evaluated by WB. (**C**) The YAP gene was silenced in HeLa cells by using two different siRNAs, either alone or in combination. A WB analysis was performed to evaluate YAP and DAB2 (p96) expression in silenced cells and in their controls (left). The detected level of DAB2 was quantified (right). NT: not treated; si: siRNA; scr: scramble. Error bars are mean ± s.e.; *p ≤ 0.05 by Student's t-test. (**B, C**) GAPDH (glyceraldehyde-3-phosphate dehydrogenase) was used as loading control. Results are representative of n = 3 independent experiments.*

We next tried to understand if YAP was expressed in $DAB2^+$ tumor-infiltrating macrophages. By using WB, we confirmed the expression of YAP in $DAB2^+$ FACS-sorted TAMs from MN-MCA and PyMT tumors (Figure 14A). YAP was also present in $DAB2^-$ MTMs from PyMT tumors (Figure 14A), suggesting that YAP expression was independent from DAB2.

After having demonstrated a role for YAP in regulating DAB2 expression, we looked at the protein expression in tumors (Figure 14B,C). The IHC analysis of PyMT tumor slices showed the presence of stromal, periacinar, elongated cells that in most cases had a nuclear staining for YAP (in brown in Figure 14B), indicating the transcriptional regulator was active. We observed also that tumor cells inside transformed acini were YAP^+, as previously reported[17]. A double IF staining confirmed that these YAP^+ cells were also $F4/80^+$ macrophages (in violet in Figure 14C). Moreover, an IF triple staining of DAB2, YAP and F4/80 on a PyMT tumor showed their co-localization on the same cells in the stromal area at the border between the tumor mass (upper right) and an acinus in transformation (lower left) (Figure 14D). In accordance with previous observations, IF on TAMs sorted from MN-MCA tumors showed that YAP was co-expressed with DAB2 and that its localization was nuclear (Figure 14E).

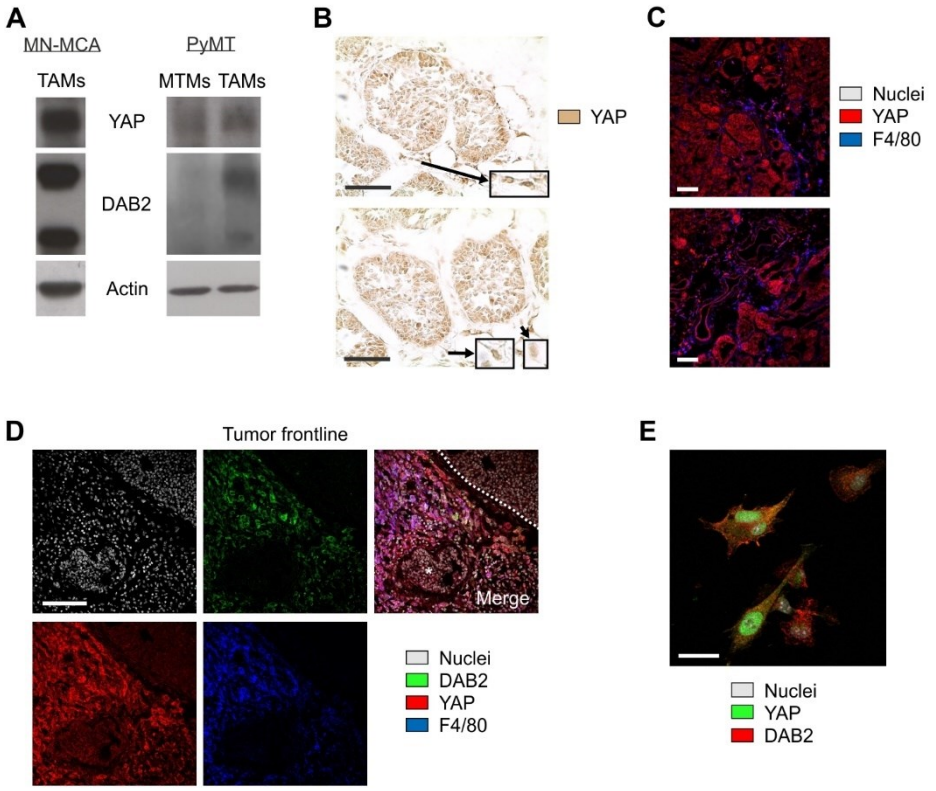

Figure 14 - YAP is expressed by DAB2⁺ TAMs. *(**A**) The expression of DAB2 and YAP was evaluated by WB analysis on FACS-sorted TAMs (tumor-associated macrophages) from MN-MCA–injected or PyMT mice, or on MTMs (mammary tissue macrophages) isolated from PyMT mice. Results are representative of n = 3 independent experiments. (**B, C**) PyMT tumor slices were analyzed for YAP expression. (**B**) Representative IHC images of the external areas of the tumor, where some acini are still normal or are only partially transformed. In the insets, magnifications of stromal cells with nuclear localization for YAP are shown. Scale bars, 50 μm. (**C**) Representative IF images of a specific staining for YAP and the macrophage marker F4/80 in an external area of the tumor. Scale bars, 100 μm. (**D**) PyMT tumor slices were analyzed for the expression of the proteins DAB2, YAP and F4/80. The reported images of an IF triple staining show that the proteins co-localize on the same cells in a stromal area at the border between the tumor mass (upper right, delimited by the dashed line) and an acinus in transformation (lower left, indicated with the asterisk). Scale bar, 100 μm. (**E**) TAMs were FACS-sorted from MN-MCA tumors and cultured on glass coverslips for one hour. Then, IF was performed on cells to evaluate expression and cellular localization of both YAP and DAB2 proteins. The staining is representative of n = 3 independent experiments. Scale bar, 25 μm.*

Silencing of the *Dab2* gene in RAW 264.7 cells

We decided to use the murine macrophage cell line RAW 264.7 to perform molecular and functional assays in addition to BM-derived macrophages. We also silenced the *Dab2* gene in order to study the role of the protein. WT RAW 264.7 cells were infected with lentiviral

vectors codifying a *Dab2*-specific or a scramble shRNA and the Orange reporter. Two different ratios of viral particles to infection targets (or MOI, multiplicity of infection) were used. After infection, Orange-expressing RAW 264.7 cells were isolated through clonal selection; a WB analysis finally allowed to verify DAB2 downregulation. As shown in Figure 15, the *Dab2*-specific shRNA could deplete DAB2 at both MOIs, while the scramble shRNA was ineffective. Cells with lower expression of the protein (corresponding to the infection at 30 MOI) were chosen to perform further *in vitro* experiments.

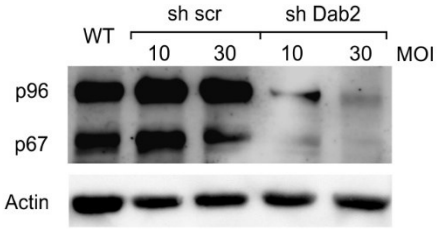

Figure 15 - Silencing of the Dab2 gene in RAW 264.7 macrophages. *WT RAW 264.7 macrophages were infected with lentiviral vectors previously produced in 293T cells and codifying a Dab2-specific or a scramble (scr) shRNA and the Orange reporter. Two different MOIs (multiplicity of infection) were used. Successfully infected Orange$^+$ RAW 264.7 cells were then sorted by FACS and tested for DAB2 depletion by WB. See materials and methods for details.*

DAB2 mediates integrin recycling and uptake of ECM components

As reported in the literature, the endocytic adaptor DAB2 is involved in the internalization and recycling of membrane integrins, a family of receptors that function as bidirectional signal transducers in many cellular processes. In particular, these proteins mediate the interactions between the cell and the surrounding microenvironment, including contact with ECM components[207]. Active, ligand-bound integrins assemble in focal adhesions, that are the contact sites of the cell with the substrate. When integrins are localized within inactive focal adhesions or are free to diffuse and not engaged by ligands, DAB2 allows their internalization by CME for a subsequent re-collocation or degradation[208,209]. We thought DAB2 absence could compromise this turnover, leading to an accumulation of integrins on the cell surface. Thus, we verified their expression on WT and Dab2 KO BM-derived macrophages. As expected, flow cytometry showed significant higher levels of α1, α5, α6 and β1 integrins on macrophages derived from Dab2 KO mice in comparison to that from WT mice (Figure 16A). These results were reproduced also by comparing RAW 264.7 cells silenced with the *Dab2*-specific or the scramble shRNAs (Figure 16A). Hence, we demonstrated that DAB2 mediates integrin recycling in macrophages.

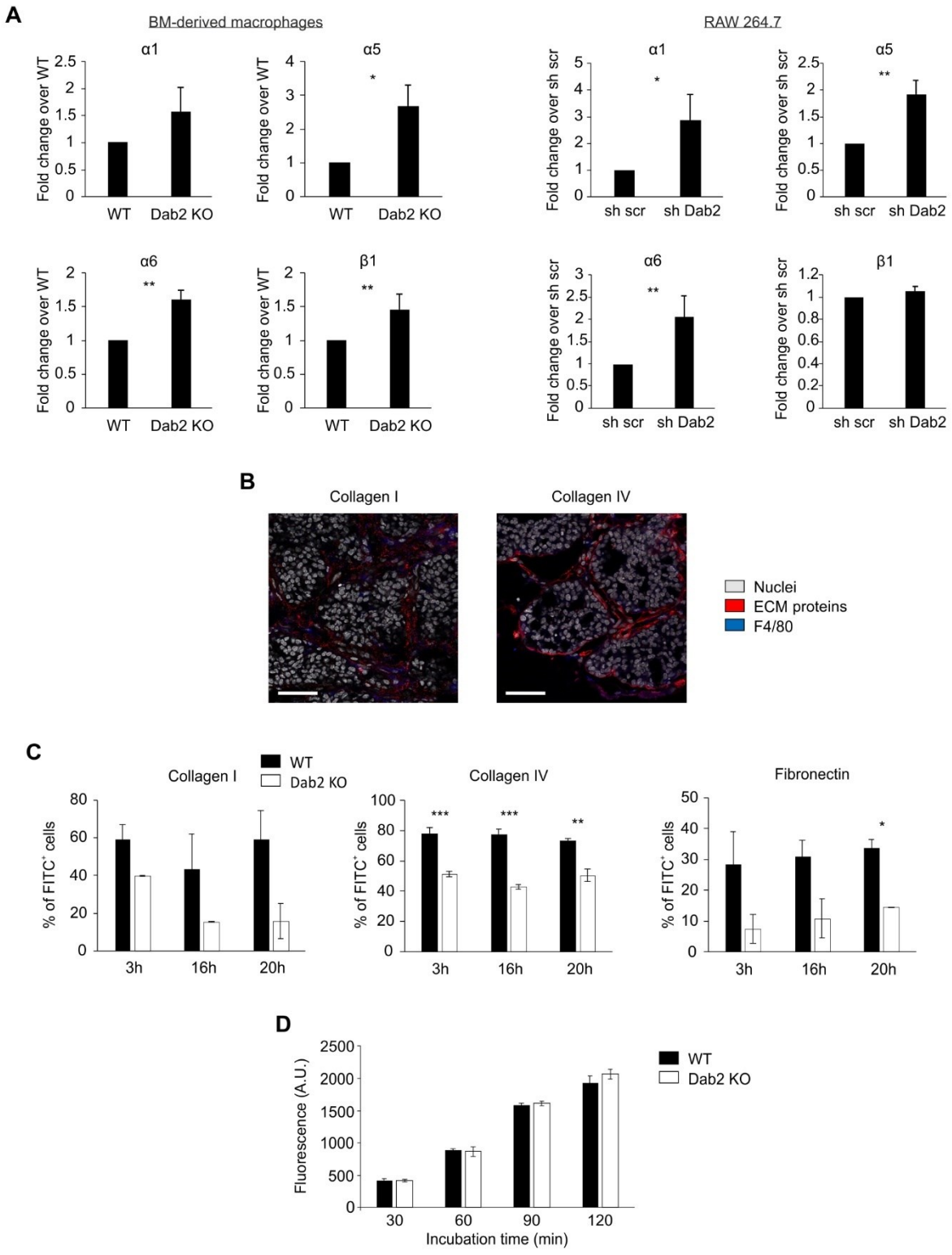

Figure 16 - DAB2 mediates integrin recycling and uptake of ECM components. *(**A**) BM-derived macrophages from WT or Dab2 KO mice were analysed by flow cytometry for the surface expression of α1, α5, α6 and β1 integrins, that is reported on the left of the panel. As shown on the right of the panel, integrin expression was also evaluated on silenced RAW 264.7 (sh DAB2) cells and on their control treated with the scramble shRNA (sh scr). The fold change of MFI (Mean Florescence Intensity) relative to controls (WT or sh scr) is reported for each integrin. n = 6 independent experiments. (**B**) The expression of type I and IV collagens was evaluated in the ECM*

*of spontaneous breast tumors from PyMT mice. Representative IF images showing specific stainings for the two proteins are reported. Scale bars, 50 µm. (**C**) BM-derived macrophages from WT and Dab2 KO mice were cultured for different time periods in the presence of soluble FITC-labelled ECM proteins. The endocytic ability was measured by flow cytometry. For each protein, n = 3 independent experiments. (**D**) BM-derived macrophages from WT and Dab2 KO mice were cultured in the presence of soluble S. aureus particles to induce phagocytosis. The particles are designed to become fluorescent only when phagocytosed. At different incubation time points, the fluorescence emitted by particles was measured with a photometer and expressed in A.U. (arbitrary units). n = 2 independent experiments. (**A, C, D**) Error bars are mean ± s.e.; *p ≤ 0.05, **p ≤ 0.01 and ***p ≤ 0.001 by Student's t-test.*

These results are in accordance with the data published by Teckchandani and colleagues where *DAB2* silencing in HeLa tumor cells resulted in an increase of integrin surface levels[210,213].

The integrins α1, α5 and α6 are all known to bind β1 integrin on the surface of cells and the resulting dimers are able to interact with specific ECM proteins: α1β1 binds collagens, α5β1 binds fibronectin and α6β1 binds laminin[260]. These proteins are among the most abundant components of the ECM and basement membranes in mammalian tissues and tumors[261].

PyMT tumors were analysed for the expression of different ECM proteins. As shown in the IF images of Figure 16B, type I and IV collagens were extensively expressed in the connective tissue around acini.

During the ECM remodelling process, ECM proteins are degraded following the release of tissue proteases. When integrins are recycled by the endocytic machinery, the fragments of ECM ligands bound to them are transported inside the cell[144,210]. Thus, we measured the ability of WT and Dab2 KO BM-derived macrophages to internalize ECM proteins or their fragments. Differentiated macrophages were cultured in the presence of soluble FITC-labelled ECM proteins and their internalization was evaluated by flow cytometry. At different time points, the uptake of type I and IV collagens and fibronectin was higher in WT as compared to KO macrophages (Figure 16C). Therefore, Dab2 KO macrophages showed an impaired endocytosis of ECM proteins.

To exclude the possibility that the observed difference of uptake could depend on phagocytosis, rather than on endocytosis, we performed an *in vitro* assay by culturing BM-derived macrophages in the presence of soluble *Staphylococcus aureus* particles (ThermoFisher Scientific), whose internalization requires phagocytosis and activates their fluorescence. As reported in Figure 16D, the photometer measurements showed no differences in particle uptake between WT and KO macrophages. This observation suggests that the difference in ECM protein internalization derived from a defect in endocytosis in the absence of DAB2, and not from an impairment of the phagocytic pathway.

DAB2 promotes the remodelling of the extracellular matrix

Cancer cells need continuous tissue remodelling for both local invasion and spreading to distant sites[3]. The obtained results demonstrate that DAB2 expressed by macrophages is able to control both recycling of surface integrins and internalization of ECM proteins.

To assess if DAB2 could mediate ECM remodelling by macrophages and favour invasiveness of tumor cells, we performed *in vitro* invasion assays. In these experiments Matrigel was used as a physiological matrix to set up organotypic cultures. According to the manufacturer, it derives from an ECM protein-rich mouse sarcoma and contains approximately a 60% of laminin and a 30% of collagen IV (Corning Inc.).

Transwells were coated with a 3-dimensional layer of Matrigel mixed with WT or KO BM-derived macrophages, which were left to remodel the matrix for 3 days. Macrophages were eliminated and E0771 tumor cells were added on top of the Matrigel for 24 hours. E0771 ability to invade the Transwell porous membrane through the Matrigel layer was measured. In accordance with the above-reported findings, tumor cells invaded significantly more in the case of WT macrophage-remodelled Matrigel (Figure 17A). Consistently, embedding in the Matrigel scramble shRNA-treated RAW 264.7 cells resulted in a much higher E0771 invasion ability in comparison to embedding the analogue *Dab2*-silenced cells (Figure 17A).

To demonstrate a DAB2-mediated ECM remodelling ability *in vivo*, we performed wound healing experiments on WT and Dab2 KO mice. Harmless wounds were created on the dorsal skin of animals and daily measured to assess the healing process, that is known to depend on tissue remodelling mechanisms[262]. As shown in Figure 17B, wounds were significantly faster healed on WT mice in comparison to KO mice, suggesting that DAB2 absence could partially hamper tissue remodelling.

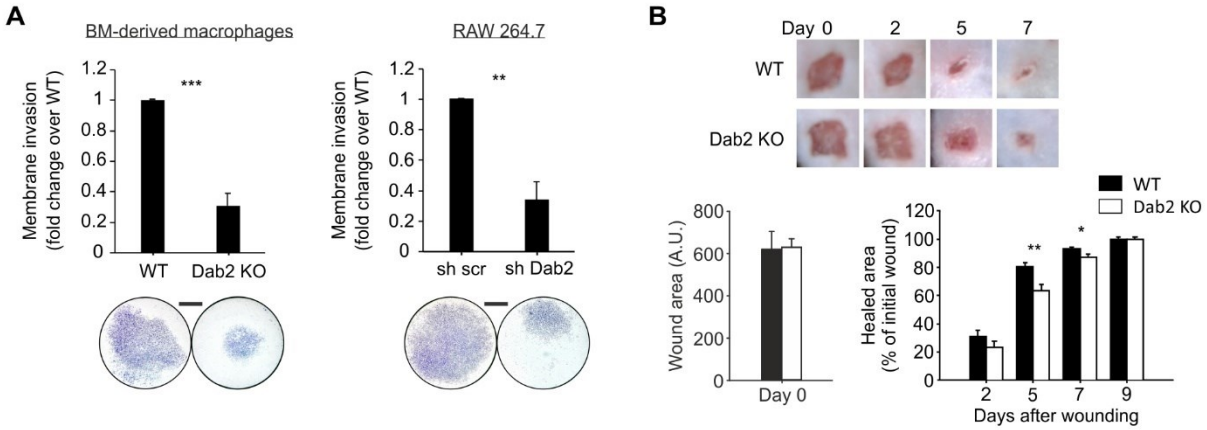

Figure 17 - DAB2 promotes the remodelling of the extracellular matrix. *(**A**) The macrophage ability to remodel the matrix was assessed by performing in vitro invasion assays. Transwells were coated with Matrigel mixed with macrophages maintained in culture for 3 days. BM-derived macrophages from WT or Dab2 KO mice (left) were tested; in alternative, silenced RAW 264.7 (sh DAB2) cells or their control treated with the scramble shRNA (sh*

*scr) were used (right). After the 3 days of culture, macrophages were killed with puromycin and, after extensive washes, E0771 tumor cells were added on top of the Matrigel. After 24 hours of incubation, Matrigel was discarded and Transwell membranes were stained with crystal violet. The invasion into the membrane was evaluated measuring the absorbance at 595 nm, that was reported as fold change relative to the controls. Representative micrographs of the stained Transwell membranes are also shown. For each graph, n = 3 independent experiments. Scale bars, 2 mm. (**B**) Harmless wounds were created on the dorsal skin of WT and Dab2 KO mice and daily measured to assess the healing process. Representative images of the wounds at different time points during the repair process are shown. The healed area was calculated as percentage of the initial wound area, that is reported in A.U. (arbitrary units). n = 20 mice per strain. (**A, B**) Error bars are mean ± s.e.; *p ≤ 0.05, **p ≤ 0.01 and ***p ≤ 0.001 by Student's t-test.*

In breast cancer patients DAB2 and YAP are expressed by macrophages at the tumor invasion frontline

To evaluate the clinical significance of the previous findings, we analysed by IHC the expression of DAB2 in different areas of primary tumors (internal, external/healthy and border) from 5 breast cancer patients. Healthy breast samples obtained from reduction mammoplasty donors were used as a control for this analysis.

A 40x HPF (high power field) was acquired from each tumor region of interest of each patient. The average number of $DAB2^+$ macrophage-appearing cells per region type was calculated and reported in Figure 18A. This number was significantly higher at invasive frontlines as compared to intratumoral areas, normal peritumoral tissue and healthy breast. Inside the tumor there were very few $DAB2^+$ cells. Importantly, the distribution of the protein was similar to that observed in our murine models, since it increased from inside the tumor moving toward the invasive frontline. In the examined tumor slices, we confirmed through a double staining that $DAB2^+$ cells were mainly $CD68^+$ macrophages (Figure 18B).

We performed an analogous quantification for YAP. YAP^+ cells with a macrophage morphology were mainly localized along tumor borders, while their number was negligible in internal areas (Figure 18C), similarly to the expression pattern of DAB2 in macrophages. In stromal regions also YAP was mainly expressed by $CD68^+$ cells (Figure 18D).

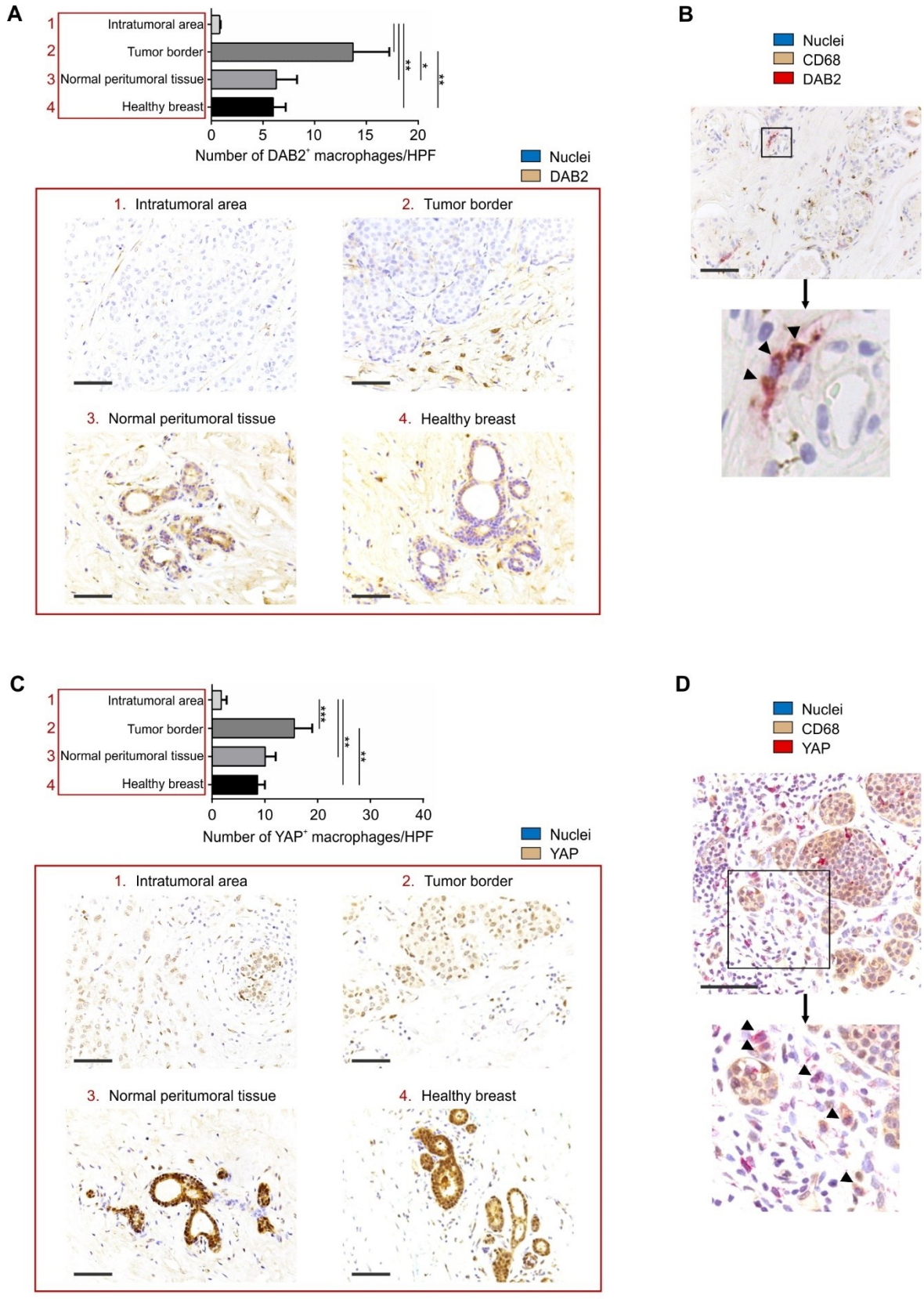

Figure 18 - In breast cancer patients DAB2 and YAP are expressed by macrophages at the tumor invasion frontline. *DAB2 and YAP expression were evaluated by IHC in slices of breast tumors from 5 patients. (**A**) The number of DAB2⁺ cells with a macrophage morphology was quantified in intratumoral areas, tumor borders, normal*

*peritumoral tissue and breast from healthy donors. The graph on the top of the panel represents the average numbers of counted cells from 5 high-power fields (HPFs), one from each patient. Representative images for different tumor areas and from healthy breast are reported at the bottom of the panel. (**B**) DAB2 and CD68 co-localization was evaluated to assess the presence and prominence of DAB2$^+$ CD68$^+$ macrophages inside the tumors. A representative IF image of the double staining and its magnification are reported. (**C**) Similarly, the number of YAP$^+$ cells with a macrophage morphology was quantified in the different tumor areas. The graph with the quantification and the representative images for different tumor areas are reported. (**D**) Also YAP and CD68 co-expression was evaluated in the regions of interest. A representative IF image and its magnification are reported. (**A-D**) Scale bars, 100 μm. (**A, C**) Error bars are mean ± s.d.; *p ≤ 0.05, **p ≤ 0.01 and ***p ≤ 0.001 by Student's t-test.*

The presence of DAB2$^+$ TAMs in breast cancer from patients correlates with a worse prognosis

Finally, we aimed to assess the value of DAB2 expression as a prognostic marker of disease. In the last years a growing interest has developed toward the potential prognostic value of immune tumor infiltrates in early breast cancer. Thus, we collected samples from 32 patients with pure early-stage invasive lobular carcinoma (ILC) and that had undergone surgery.

ILC comprises up to 15% of all invasive breast tumors and represents the second most common type of breast cancer after invasive ductal carcinoma[263]. Since the possible prognostic role of DAB2 expression in ILC-associated macrophages has not been established, we investigated the expression of DAB2 in selected samples and considered the possible associations with the clinicopathological characteristics of patients.

The median age of ILC patients was 56 years (range 36-80 years). The clinicopathological characteristics of patients are reported in Table 3. At a median follow-up of 92 months (range 13-297), median disease-free survival (DFS) was 44.9 months (95% confidence interval 36.6-53.1).

Clinicopathological characteristics	Subcategories	Number of patients (%)
Menopausal status	Premenopausal Postmenopausal	10 (31.2) 22 (68.8)
Performance status (ECOG)	0 1 2	28 (87.5) 3 (9.4) 1 (3.1)
Ki-67	≤ 4% > 4% Unknown	9 (28.1) 21 (65.6) 2 (6.3)
Grading	1 2 3 Unknown	4 (12.5) 7 (21.8) 6 (18.8) 15 (46.9)
Oestrogen receptor status	Positive Negative Unknown	27 (84.3) 2 (6.3) 3 (9.4)
Progesterone receptor status	Positive Negative Unknown	22 (68.8) 3 (9.4) 7 (21.8)
HER2 status	Positive Negative Unknown	15 (46.9) 3 (9.4) 14 (43.7)
T stage	1 2 3 4	11 (34.4) 18 (56.3) 2 (6.3) 1 (3.1)
Lymph-nodal status	Positive Negative	13 (40.6) 19 (59.4)
Vascular invasion	Present Absent Unknown	9 (28.1) 11 (34.4) 12 (37.5)
Multifocality	Present Absent	6 (18.8) 26 (81.2)

Table 3 *- Clinicopathological characteristics of considered breast cancer patients.*

By using IHC analysis on all selected cases, we evaluated the expression of DAB2 in peritumoral or intratumoral areas. DAB2 expression was assessed in terms of average number of

positive non-neoplastic and non-endothelial cells with a macrophage morphology in 10 high power fields (HPFs) (Figure 19A). The median value of DAB2 expression was 2.15 (range 0-11) and 2.55 (range 0-14) for the peritumoral and intratumoral infiltrates, respectively.

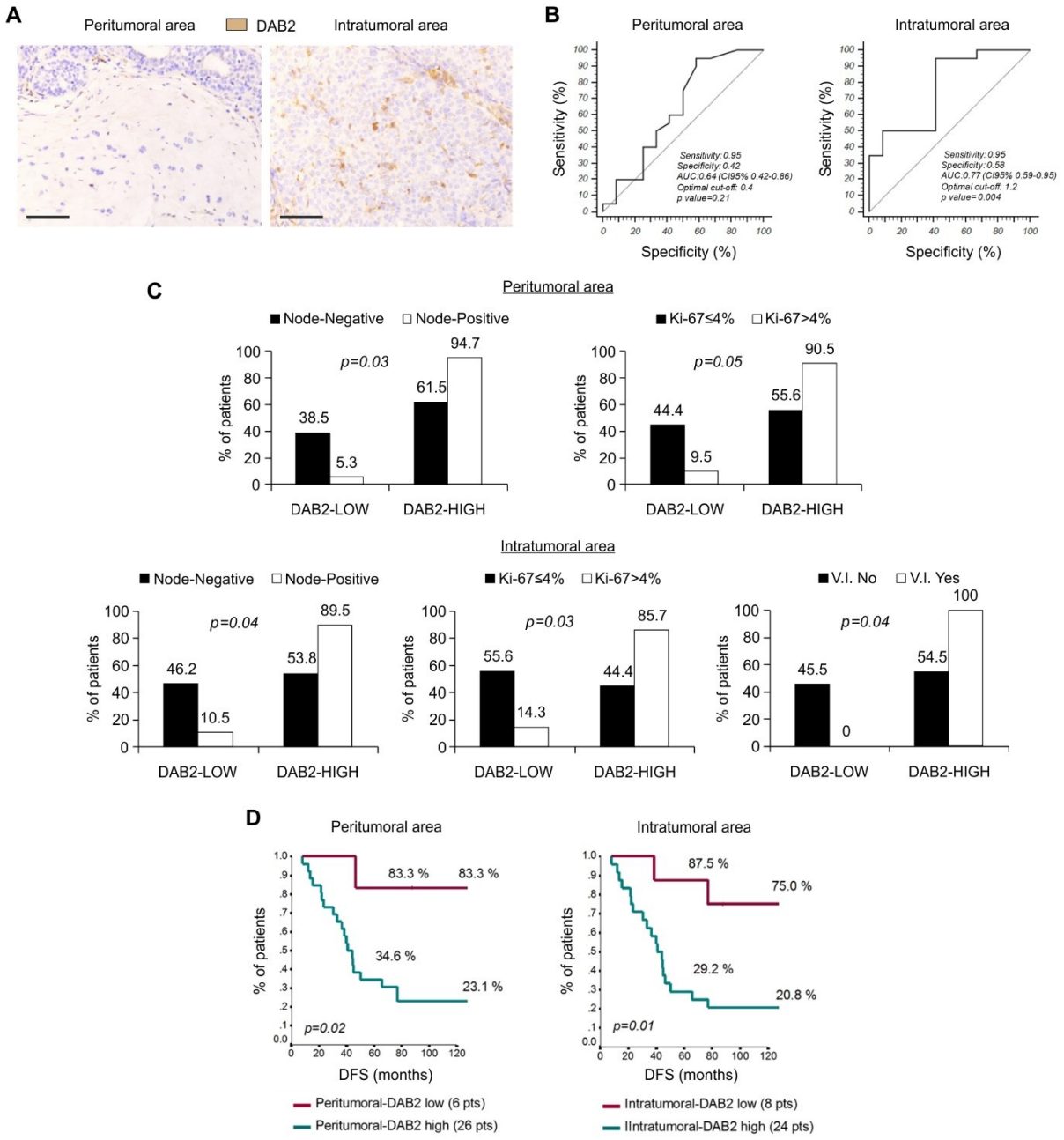

Figure 19 - The presence of DAB2⁺ TAMs in breast cancer from patients correlates with a worse prognosis. *To assess the value of DAB2 expression in TAMs as a prognostic marker, samples from 32 patients with pure early-stage invasive lobular carcinoma (ILC) and that had undergone surgery were collected. (**A**) The expression of DAB2 was evaluated by IHC in peritumoral and intratumoral areas. Scale bars, 100 µm. (**B**) ROC analysis-based identification of the optimal cut-offs of DAB2 expression in peritumoral and intratumoral infiltrates according to disease-free survival (DFS). The sensitivity (probability to detect true positives among the considered subjects)*

*and the specificity (probability to identify true negatives) are indicated. The AUC (area under the curve) is > 0.6 in both analyses, indicating that found cut-offs are enough accurate. The p-values for the ROC analyses are significant (< 0.5). (**C**) Preliminary associations between DAB2 expression in peritumoral or intratumoral infiltrates and the clinicopathological characteristics of patients. The analyses were performed by using Pearson's chi-squared test or Fisher's exact test, depending on sample size. The presence of lymph node metastases, tumor cell proliferation (Ki67 expression) and vascular invasion (V.I.) inside the primary tumor were considered as characteristics of interest. The p-values are < 0.5. (**D**) The correlations between either peritumoral or intratumoral DAB2 levels and DFS are reported. The analysis was performed by using the Kaplan-Meier method and the Log-Rank test. The p-values are < 0.5.*

We performed a receiver operating characteristic (ROC) analysis that has identified two different cut-offs of peritumoral and intratumoral DAB2 values able to discriminate the prognosis according to disease-free survival (DFS). The optimal cut-off was 0.4 (p = 0.21) for the peritumoral infiltrate and 1.2 (p = 0.004) for the intratumoral infiltrate (Figure 19B).
Figure 19C shows the associations between high (≥ 0.4) or low (< 0.4) peritumoral expression of DAB2 and different clinicopathological characteristics; it shows also the associations between high (≥ 1.2) or low (< 1.2) intratumoral expression of DAB2 and the characteristics of ILC patients.
Interestingly, it resulted that the majority of patients expressing high levels of DAB2 in both peritumoral and intratumoral infiltrates had lymph node metastases, high tumor cell proliferation and presence of vascular invasion inside the primary tumor. The direct correlation between DAB2 expression and all these bad prognosis markers is statistically significant.
Moreover, an extremely important result is that both peritumoral and intratumoral DAB2 levels with identified cut-offs inversely correlated with the DFS of patients (Figure 19D).

The results of this preliminary analysis support the idea that the presence of $DAB2^+$ macrophages at the tumor site, in both peritumoral and intratumoral regions, could be considered as a prognostic marker for tumor progression and metastasis formation in patients with primary resected ILC.
The preliminary and exploratory nature of our data, also in consideration of the small sample size, represent a hypothesis that should be prospectively verified and validated in a more extensive series of patients.

DISCUSSION

Tumor spreading and metastatization are the main cause of cancer-associated death. Nevertheless, the pathophysiological and molecular mechanisms supporting them are still to be fully elucidated[9]. The dissemination of malignant cells from the primary tumor to distant organs is a multistep process that requires detachment of cancer cells from the site of origin, remodelling of basement membranes and ECM, migration into blood or lymph vessels, extravasation in an ectopic tissue and proliferation. To spread inside the host, tumor cells have to survive in each one of these phases[10]. Thanks to the intervention of the immune system with both innate and adoptive responses, the metastatic process results to have a very low rate of success. Indeed, considering that a tumor can release in the circulation thousands of CTCs every day, only a few of them are able to generate metastases during the whole time of tumor establishment and progression[64]. However, tumor cells, albeit rarely, manage to reach local vessels in the primary tumor and, after translocation, they invade and colonize the target tissue. It has not been completely understood how this occurs, but it is increasingly clear that tumor cells cannot do it alone, but they are aided by specific stromal cell populations[3]. Both in the primary tumor and in the metastatic site, cancer cells are able to subvert homeostasis by reprogramming the microenvironment from a pro-inflammatory and anti-tumor state to an immunosuppressed and pro-tumor state[24,25].

A plentiful literature in the last years highlighted the presence of tumor-infiltrating immune cells as critical determinants for tumor progression and metastatic spreading[24,25]. Among the immunosuppressive myeloid cell populations that infiltrate the tumor microenvironment, TAMs have a key role in the pathogenesis of cancer, since they are able to sustain many of the known pro-tumor processes[18,78]. Indeed, TAMs have been demonstrated to promote: suppression of $CD8^+$ T-cell infiltration and anti-tumor immunity[76]; activation of neoplastic cells in terms of survival, proliferation, stemness and therapeutic resistance[94,95]; angiogenesis[100]; tumor cell invasion and metastasis formation[24,107]. Despite the numerous studies in support of the pro-metastatic role of myeloid cells and in particular of TAMs, the molecular mechanisms through which they act are not completely known. One of these mechanisms derives from the ability of TAMs to induce tumor cell migration toward intratumoral vessels[105,109,112]. To favour malignant cells in this process, TAMs can degrade and remodel the ECM in a protease-dependent manner[106,107]. The same occurs at the metastatic site, where MAMs are involved in similar mechanisms to aid tumor cells in colonizing the target tissue[78].

Since many years, our group is particularly interested in studying the role of myeloid cells in tumor progression. Gene chip data obtained in our laboratory showed that the *Dab2* gene was upregulated in CD11b$^+$ myeloid cells isolated from tumors in comparison to those from healthy spleens (see the introduction). In the present work, we wondered whether DAB2 expressed in tumor-infiltrating myeloid cells might have a role in tumor progression and in the metastatic process. To this purpose, we generated a transgenic mouse model, the Dab2 KO strain, lacking the protein DAB2 in the hematopoietic lineage[255].

In our model, we demonstrated the pro-metastatic role of DAB2 by injecting mice with MN-MCA or E0771 tumor cells. DAB2 expression in WT mice was associated with a higher number of lung micrometastases in comparison to Dab2 KO mice. Nonetheless, there were no significant differences in primary tumor growth. This suggested us that DAB2 expressed by tumor-infiltrating myeloid cells was not involved in tumor initiation or progression, but rather in promoting tumor cell invasiveness and metastatization into other organs. Considering the possible myeloid cell-dependent processes that can sustain metastasis development[24,107], we tested whether DAB2 depletion was inducing an alteration in the immunosuppressive functions of myeloid cells within the tumor microenvironment. We showed that myeloid CD11b$^+$ cells isolated from MN-MCA tumors co-cultured with OVA-activated OT-I lymphocytes maintained their immunosuppressive functions even if isolated from Dab2 KO mice. Moreover, the accumulation within the tumor microenvironment of different myeloid subpopulations, such as granulocytes, monocytes and TAMs, was similar between WT and Dab2 KO mice. Likewise, metastatic lungs from MN-MCA tumor-bearing WT or Dab2 KO animals showed comparable amounts of granulocytes, monocytes, CD11c$^+$ resident macrophages and MAMs.

Therefore, these initial experiments demonstrated that the pro-metastatic function of DAB2 did not appear to be determined by an imbalance in the accumulation of specific myeloid populations or in their incapacity to act on the CD8-mediated anti-tumor response, as instead reported from our group for the pathway of c/EBPβ, also involved in the metastatic process[255].

To further investigate the metastatic role of DAB2 we tried to understand which myeloid subsets expressed the protein, as well as where and how this protein was activated.

The expression of DAB2 was analysed in different myeloid sub-populations isolated from the tumor microenvironment. We detected the protein mainly in TAMs, but not or much less in other subsets. Importantly, DAB2 was expressed in TAMs isolated from both the transplantable MN-MCA tumor and the more physiological cancer model PyMT. Interestingly, we found DAB2 expressed also in lung MAMs from MN-MCA tumor-bearing mice. Thus, we thought that DAB2 could control a common non-immunosuppressive function of macrophages in both the primary tumor and the metastatic site. This DAB2-dependent activity was tumor-related, since DAB2 activation was not detectable in BM or splenic myeloid precursors from WT mice.

Moreover, we found that the same cytokines able to guide the macrophage differentiation *in vitro* and *in vivo*, M-CSF and GM-CSF[256], upregulated DAB2 expression in both BM and spleen myeloid precursors. Both M-CSF and GM-CSF are abundantly released in the tumor microenvironment and foster the *in vivo* recruitment and proliferation of TAMs[31,257]. Following further experiments on splenocytes cultured in the presence of M-, GM- or G-CSF, we excluded the possibility of an upregulation of DAB2 during granulocyte differentiation. This was supported by the previous data on sorted myeloid populations, showing that the protein was not present in tumor and lung granulocytes. Thus, M-CSF or GM-CSF cytokines are at the same time able to promote macrophage differentiation and DAB2 expression. In accordance with these results, DAB2 had been initially identified in the BAC1.2F5 macrophage cell line, where it was phosphorylated after M-CSF stimulation[134]. Moreover, we demonstrated that during *in vitro* cultures DAB2 upregulation was a consequence of macrophage differentiation induced by these cytokines and that there were no defects in the differentiation and proliferation of macrophages in the absence of the DAB2 protein. Consequently, DAB2 seems not to have an essential role in M- and GM-CSF signal transduction or in the differentiation process occurring in precursor cells. Since in the primary tumor the accumulation of macrophages was comparable between WT and Dab2 KO mice, we did not analyse the amount of these cytokines in the tumor microenvironment and supposed they were comparable, too.

Then, we looked at the localization of DAB2-expressing TAMs and MAMs on tissue slices, since their pro-metastatic function could be related to a specific distribution in the tumor mass. We performed IHC and IF analyses on primary tumor slices from MN-MCA–injected and PyMT mice and observed that $DAB2^+$ TAMs were mainly localized in stromal, peri-lesional areas, at the invasive frontline between the tumor and the surrounding healthy tissue. In MN-MCA tumors these cells accumulated around muscle fibers partially or not-yet reached by invading tumor cells, and in PyMT tumors they were similarly localized around healthy or not completely transformed mammary acini. The amount of $DAB2^+$ TAMs progressively increased from internal areas, where proliferating tumor cells generally reduce stromal regions, toward the border of the tumor, where stroma is still abundant. Interestingly, a similar situation was observable in metastatic lungs from MN-MCA tumor-bearing animals, where $DAB2^+$ MAMs were localized inside metastases in increasing numbers from the centre to the borders. It is worth to note that in tissue slices $DAB2^+$ macrophages were a fraction of the total macrophages: about 30% in PyMT tumors, 50-70% in MN-MCA tumors and 65-70% in lung metastases from MN-MCA tumor-bearing animals. The *in vivo* existence of $DAB2^-$ macrophages explains why BM-derived macrophages from Dab2 KO mice develop and proliferate at the

same manner of that from WT mice. As already mentioned, DAB2 is upregulated as a consequence of macrophage differentiation and it seems not to be essential for their survival and expansion.
In order to understand the extent of DAB2 expression in tumors and metastases, we checked also tissues from healthy mice and we found few DAB2-expressing resident macrophages in breast, lungs and quadriceps. Altogether, these results indicate that DAB2 could have a role also in physiological conditions, but we clearly observed an accumulation of DAB2$^+$ macrophages during tumor progression and a peculiar localization of these cells in both primary tumors and metastatic sites, that is nearby the front of invasion were they can promote tumor spreading.

The expression of DAB2 did not have effects on macrophage differentiation. However, when we looked at the macrophage cell morphology, we found that the shape of cultured BM-derived macrophages from WT mice was significantly more elongated than that from Dab2 KO mice. Nonetheless, when we verified if this phenotype could influence cell migratory abilities *in vitro*, we did not find any difference in the absence of the protein. These results are in line with the literature, since it has been shown that DAB2 in macrophages, fibroblasts and HeLa cells promotes cell adhesion and spreading on the substrate[145,147] and that siRNA-mediated silencing of *Dab2* in SUM159 breast cancer cells does not affect their motility in a monolayer culture[202]. Anyway, further experiments are necessary to understand if DAB2 depletion hampers macrophage migratory ability in more physiological contexts, such as in 3-dimensional organotypic cultures, instead of a monolayer, and in the presence of a chemotactic signal[248].

In addition to the described phenotypic evaluations, our final goal was to identify the specific mechanism of DAB2 activation and function in the tumor microenvironment. Our GSEA showed the interesting correlation between *Dab2* expression in macrophages and the tumor-related YAP signature. YAP is an emerging transcription regulator that acts in mechanotransduction pathways. It has been demonstrated that YAP expression is modulated by the substrate stiffness: soft matrices induce its cytoplasmic retention, while stiff matrices cause its nuclear transfer and activation[233]. YAP is generally upregulated and activated in tumor cells and CAFs (cancer-associated fibroblasts) in response to the high ECM stiffness in tumors[17]. Once activated, YAP promotes cell proliferation, survival and motility[232].
Remarkably, two published works, in the context of extensive bioinformatic analyses, had previously predicted an association between the *Dab2* gene expression and a transcriptional regulation by YAP, although without experimental validation[233,236]. Thus, we investigated a possible role of DAB2$^+$ TAMs in YAP-mediated mechanotransduction. First, we used HeLa

cells as a model because these cells constitutively express both the DAB2 isoform p96 and YAP. We observed that a higher substrate stiffness induced a more intense expression of p96. Since YAP expression is modulated in an analogous manner[233], we had a first hint that DAB2 was associated to the YAP mechanotransduction pathway. The relation between DAB2 and YAP was confirmed by silencing *YAP* in HeLa cells and finding that YAP depletion induced a significant downregulation of DAB2. Therefore, *Dab2* expression appeared to be directly or indirectly regulated by YAP.

In agreement with these results, we detected YAP in DAB2-expressing TAMs from MN-MCA and PyMT tumors by using WB, IHC and IF analyses. Cell imaging allowed us to visualize $DAB2^+$ YAP^+ stromal macrophages in external areas of the tumor and along the invasion frontline. A fraction of these cells had a nuclear localization of YAP, indicating that the transcription regulator was active[233].

To our knowledge, this study correlates for the first time the protein DAB2 expressed by macrophages and the transcription regulator YAP, suggesting that DAB2 may be modulated in a mechanosensitive manner. To definitively prove the transcriptional regulation of DAB2 through YAP, we are going to mutate the potential binding sites for YAP on the enhancers of *Dab2* in the RAW 264.7 macrophage cell line and evaluate DAB2 expression.

As extensively reported in the introduction, DAB2 is known as an endocytic adaptor that is involved also in clathrin-mediated internalization and recycling of membrane integrins. These receptors function as signal transducers in many cellular mechanisms and are particularly important since they mediate the interactions between the cell and the surrounding microenvironment[207]. Cells adhere to the ECM by using integrin-based focal adhesions that are disassembled and re-assembled elsewhere in the membrane during cell migration. In this process, inactive integrins are internalized in a DAB2-dependent manner in order to be subsequently re-allocated in the membrane or degraded[208,209]. To elucidate the mechanism by which $DAB2^+$ macrophages promote metastatization of cancer cells, we considered a pathway related to endocytosis. Thus, we hypothesized that DAB2 absence could compromise the turnover of integrins. Accordingly, we observed a higher accumulation of integrins on the surface of BM-derived macrophages from Dab2 KO mice in comparison to that from WT mice. Likewise, RAW 264.7 cells treated with a *Dab2*-specific shRNA had higher surface levels of integrins than that treated with a scramble shRNA. These results are consistent with previously reported studies in which *DAB2* silencing in HeLa cells led to an increase in integrin surface expression[210,213]. In this way we confirmed that also in macrophages DAB2 is a component of the endocytic apparatus involved in integrin recycling.

We evaluated four integrin subunits able to assemble on the cell surface to form three heterodimers which are α1β1, α5β1 and α6β1 and bind respectively collagens, fibronectin and

laminin[260]. α1β1 and α5β1 had been previously reported as dimers internalized through DAB2 both in fibroblasts and tumor cell lines[147,209-213].

It is known that, when ECM proteins are degraded by matrix proteases, integrins which are recycled inside the cell mediate the uptake of fragments of their ECM ligands. Then, the degradation of these ECM fragments is continued by lysosomal enzymes[144,210].

After having verified the expression of ECM proteins in tumor stroma, as exemplified by collagen I and IV in PyMT tumors, we observed a higher internalization of soluble type I and IV collagens and fibronectin in WT BM-derived macrophages in comparison to the Dab2 KO. Therefore, Dab2 KO macrophages showed both an impaired CME-dependent integrin turnover and a consequent reduced endocytosis of ECM proteins. We also demonstrated that DAB2 was not involved in the phagocytic route since stimulation of this pathway in BM-derived macrophages showed no defects in the absence of the protein.

This is the first demonstration that DAB2 in macrophages participates in CME and also the first report of a DAB2-mediated turnover of the α6β1 integrin.

Moreover, it is worth to note that the more elongated shape observed in WT BM-derived macrophages reflects a higher cellular spreading and can be explained considering the role of DAB2 in CME. Indeed, an efficient recycling of integrins allows the assembly of new focal adhesions where the cell needs to contact the substrate[209,210]. Consequently, Dab2 KO macrophages probably have a smaller number of active adhesions and display a rounder shape. Interestingly, integrins were reported as receptors able to sense substrate stiffness and induce mechanotransduction signalling pathways inside the cells[216]. The consequences of this function are numerous, since it can affect diverse processes such as cellular survival, proliferation, cytoskeletal rearrangement and migration[217,218]. The integrin dimers α1β1, α5β1 and α6β1, which we found to be associated with DAB2-dependent CME, had been previously linked to mechanotransduction[219,222,223]. So, this represents another possible connection between DAB2 and mechanotransduction pathways, in addition to the gene regulation through the YAP transcriptional regulator.

As reviewed in the introduction, tumor cells locally invade the primary site and then move to distant sites if a process of tissue remodelling and ECM degradation precedes their migration[3]. Indeed, it has been demonstrated that tumors are stiffer than normal tissues of origin, due to a tumor growth-derived increase in interstitial tissue pressure[264], fibrosis[265] and an elevated Rho GTPase-dependent cytoskeletal tension in cancer cells[258]. For example, the elastic modulus of healthy mammary glands is about 140-200 Pa, while an average breast tumor is 3000-5000 Pa and tumor-associated stroma is 650-2000 Pa[258]. Since tumor rigidity is very high, malignant cells has to find a way to escape in order to invade surrounding healthy tissues. TAMs and MAMs are already known to support tumor cells through the proteolysis

of the ECM, although the mechanisms remain poorly understood[78,106,107]. In this context, DAB2 seems to have a paramount role. The integrin- and YAP-mediated mechanotransduction pathways could be the systems used by DAB2$^+$ TAMs and MAMs to sense ECM stiffness and induce specific cellular responses that lead to a degradation and remodelling of the ECM. To validate this hypothesis, we performed *in vitro* invasion assays by adding E0771 cancer cells on a macrophage-remodelled Matrigel layer. Matrigel (Corning Inc.) was used to mimic a physiological matrix. Remarkably, tumor cell invasion was significantly higher in the case of WT BM-derived macrophages or scramble shRNA-silenced RAW 264.7 cells as compared to the correspondent DAB2-deficient cells. This suggests that DAB2$^+$ macrophages are able to remodel the ECM in order to assist tumor cell invasion.

Since the healing process is known to depend on tissue remodelling and macrophage intervention[262], we performed wound healing experiments on WT and Dab2 KO mice and found that DAB2 absence in KO mice partially impaired their repair ability in comparison to WT mice. Thus, these results strongly support our hypothesis of a role for DAB2$^+$ TAMs and MAMs in mechanotransduction-driven ECM remodelling and metastasis development.

The proposed idea is further sustained by our observations on the localization of DAB2$^+$ YAP$^+$ macrophages, which were concentrated in external areas and along the borders in both primary tumors and metastases. In this peculiar position, DAB2-mediated ECM remodelling would allow both the reduction of stroma stiffness and the degradation of basement membranes. Indeed, in mammals, ECM and basement membranes are mainly made of collagens I and IV, fibronectin and laminin, the ligands of the three integrin dimers we have above reported[261]. In this way, cancer cells are assisted by DAB2$^+$ TAMs and MAMs in their invasion of surrounding tissues and toward local blood or lymph vessels.

The clinical relevance of these discoveries was assessed by analysing tumor samples from breast cancer patients. First of all, we confirmed that the number of DAB2$^+$ cells with macrophage morphology was significantly higher at invasive frontlines as compared to intratumoral areas and normal peritumoral regions, likewise in mouse models. The comparison with healthy breast samples suggested again that there was an accumulation of DAB2$^+$ TAMs in tumors. In line with animal models, YAP distribution was similar to that of DAB2.

Finally, we quantified peritumoral and intratumoral DAB2-expressing cells with a macrophage morphology in tumors from ILC patients and found a significant correlation with clinicopathological characteristics that indicate a poor prognosis, in particular diagnosis of lymph node metastases, high tumor cell proliferation and presence of vascular invasion inside the primary tumor. Consistently, DAB2 expression inversely correlated with DFS of patients. These very exciting data allow us to consider the expression of DAB2 as a possible, novel prognostic marker for ILC breast cancer, although it will be necessary a further validation in a larger

cohort of patients. We are also extending our analysis to subjects diagnosed with ductal carcinoma to confirm our findings on the lobular carcinoma.

In conclusion, the results obtained in this work demonstrate an unprecedented role for TAMs in DAB2-mediated, mechanotransduction-driven ECM remodelling and cancer promotion. We propose a model in which the *Dab2* gene is activated in TAMs and MAMs during their differentiation from BM precursors, in response to the cytokines M-CSF and GM-CSF, released in the inflamed tumor microenvironment[31,257].

In macrophages the DAB2 protein participates in the CME of plasma membrane integrins, in particular the dimers α1β1, α5β1 and α6β1. During this process, DAB2 mediates integrin turnover and, at the same time, endocytic internalization of fragments from ECM collagens and fibronectin. Indeed, TAMs and MAMs are known to secrete and expose on the cell surface proteases able to degrade the ECM within the primary tumor and metastatic sites and facilitate tumor cell invasion[78,106,107]. This mechanism allows a more efficient degradation of ECM proteins, probably because it is carried out by both surface/extracellular proteases and lysosomal enzymes.

Since integrins are involved in mechanotransduction and are able to sense the stiffness of the surrounding ECM, this information is relayed inside the cell through mechanisms based on changes in cytoskeletal tension and intracellular signalling[216].

We propose that the elevated ECM rigidity of tumors[258] elicits an integrin-dependent activation of YAP, one of the key cellular players in mechanotransduction[233]. In turn, YAP directly or indirectly induces DAB2 expression and subsequently a sustained integrin recycling. Integrins are re-collocated in active focal adhesions and proceed with ECM stiffness sensing, thus fuelling a positive loop inside TAMs and MAMs. This DAB2-mediated integrin turnover allows a continued ECM uptake and degradation by macrophages, that accumulate in the stroma along tumor and metastasis borders. Since it is a mechanosensitive process, it is activated by the high stiffness of tumor stroma and basement membranes; the resultant remodelling and loss of integrity of these matrices allow cancer cell migration toward external, healthy tissues and blood/lymph vessels. Thus, DAB2-expressing TAMs and MAMs assist tumor cells during local invasion and metastatization.

All these interesting discoveries are opening new attractive opportunities of investigation. However, to definitely confirm our mechanistic model, we are now working on different points. First, we are evaluating *in vivo* if tumors from WT mice show signs of a more pronounced ECM degradation than tumors from Dab2 KO mice. We are confirming the role of integrins, DAB2 and YAP in ECM remodelling and tumor cell invasion by silencing their expression with the Crispr/Cas9 system in the RAW 264.7 cell line. These silenced cells will be tested in

invasion assays for their ability to remodel the ECM and promote invasion of cancer cells. An *in vitro* invasion assay will be also performed to understand if DAB2$^+$ macrophages can directly contact and guide tumor cells to further promote their invasiveness (we will consider the 'trailblazer effect' described by Westcott and colleagues to describe the migration of leader and follower breast cancer cell subsets)[202]. We are also determining if the absence of DAB2 in macrophages causes a reduction in the release of matrix proteases since this effect would define another novel role for the protein in mediating ECM remodelling. Finally, the role of YAP in the control of DAB2 expression will be confirmed by checking if Yap KO mice are a phenocopy of Dab2 KO mice in terms of metastasis reduction and ECM remodelling and then we will test Dab2 Yap double KO mice.

It is important to point out that DAB2 or other components of its putative pathway could be considered as potential therapeutic targets against the pro-metastatic functions of TAMs. As illustrated in the introduction, targeting of TAMs produces favourable therapeutic effects, as in the recent studies on CSF-1 signalling blockade with pharmacological inhibitors or blocking antibodies. These strategies result in reduced tumor growth, angiogenesis and metastasis formation as well as in enhanced efficacy of chemotherapy and ACT treatment, CD8$^+$ T cell response and mice survival[40,72,129,130]. Furthermore, Ries and colleagues described the clinical benefits of an anti-CSF-1R antibody-based treatment in patients diagnosed with diffuse-type giant-cell tumors, thus showing that targeting TAMs can be a promising therapeutic approach[131].

Several macrophage-targeting drugs have been developed and clinical trials are ongoing[74]. Some examples are an anti-CD204 immunotoxin[266], an immunotoxin targeted to FRβ (folate receptor β)[267], a TIM-3 (T cell immunoglobulin and mucin domain-containing molecule-3) blocking antibody[268] and corosolic acid[269], that were found to kill TAMs, inhibit their recruitment or block their differentiation into the M2 pro-tumor phenotype. In all these cases evident effects on tumor progression were observed. However, current therapies are likely to have a limited application as they target all macrophages or pathways shared with other cell types[24].

Another possible therapeutic intervention is the inhibition of the macrophage support to the metastatic process. Only a few studies regarding this approach have been published, since little is known on the pro-tumor mechanisms used by macrophages to sustain migratory and metastatic abilities of neoplastic cells. An interesting target would be the CCL2-CCR2 axis, because it mediates TAM recruitment at metastatic sites, but it has been shown that a CCL2-neutralizing antibody was ineffective in suppressing tumour progression[270].

Thus, in light of the few existing therapeutic approaches to target TAMs and especially their pro-metastatic functions, further investigation on the detailed mechanisms of the pro-tumor

activation of TAMs and MAMs is necessary to develop new and more precise macrophage-targeted anti-tumor therapies.

For this reason, our work acquires a particular significance. The mechanotransduction- and DAB2-dependent ECM remodelling model that we propose seems to be a cancer-specific mechanism that has never been described before and offers suitable candidates for immunotherapeutic targeting. This approach, also in the context of combinatorial therapies, would allow to block or contain tumor spreading and reduce the risk of metastasis formation in the host.

Abbreviations

ACT: adoptive cell therapy
APC(-cy7): allophycocyanin (-cyanin 7)
APC: antigen presenting cell
ARG1: arginase 1
AU: arbitrary unit
BM: bone marrow
BSA: bovine serum albumin
CAF: cancer-associated fibroblast
CD: cluster of differentiation
CME: clathrin-mediated endocytosis
CSF-1: colony-stimulating factor 1
CSFE: carboxyfluorescein diacetate succinimidyl ester
CTC: circulating tumor cell
CTL: cytotoxic T lymphocytes
Da: Dalton
DAB: 3,3'-diaminobenzidine
DAB2/Dab2: disabled 2, mitogen-responsive phosphoprotein (human/murine gene)
DAB2: disabled homolog 2 (human and murine protein)
DAPI: 4',6-diamidino-2-phenylindole
DC: dendritic cell
DFS: disease-free survival
DMEM: Dulbecco's modified Eagle medium
ECM: extracellular matrix
EDTA: ethylenediaminetetraacetic acid
EGF: epidermal growth factor
FACS: fluorescence-activated cell sorting
FBS: fetal bovine serum
FDR: false discovery rate
FITC: fluorescein isothiocyanate
FSC: forward scatter
GAPDH: glyceraldehyde-3-phosphate dehydrogenase (human protein)
G-CSF: granulocyte colony-stimulating factor
GM-CSF: granulocyte-macrophage colony-stimulating factor

GSEA: gene set enrichment analysis
HEPES: 4-(2-hydroxyethyl)-1-piperazineethanesulfonic acid
HPF: high power field
HRP: horse radish peroxidase
IF: immunofluorescence
IFN: interferon
IHC: immunohistochemistry
IL: interleukin
ILC: invasive lobular carcinoma
IM: intra-muscle
iNOS: inducible nitric oxide synthase
KO: knock out
LPS: lipopolysaccharide
MAM: metastasis-associated macrophage
M-CSF: macrophage colony-stimulating factor
MDSC: myeloid-derived suppressor cell
MFI: mean fluorescence intensity
MHC: major histocompatibility complex
MLPC: mixed leucocyte-peptide culture
MMP: matrix metalloproteinase
MOI: multiplicity of infection
MTM: mammary tissue macrophage
NK: natural killer cell
NT: not treated
OT: orthotopic
OVA: ovalbumin
p: p-value
Pa: Pascal
PBS: phosphate buffered saline
PE: phycoerythrin
PerCP-Cy5.5: peridinin-chlorophyll-protein complex-cyanin 5.5
PVDF: polyvinylidene fluoride
PyMT: polyomavirus middle T-antigen
RNS: reactive nitrogen species
ROC: receiver operating characteristic
ROS: reactive oxygen species

RPMI: Roswell Park Memorial Institute

RT: room temperature

SCR: scramble

SD: standard deviation

SE: standard error

shRNA: short hairpin RNA

siRNA: small interfering RNA

SSC: side scatter

TAM: tumor-associated macrophage

TAZ: transcriptional coactivator with PDZ-binding motif (human and murine protein)

TCR: T cell receptor

TDSF: tumor-derived soluble factor

TGF: tumor growth factor

T_h: T helper cell

TLR: Toll-like receptor

TNF: tumor necrosis factor

Treg: regulatory T lymphocyte

VEGF: vascular endothelial growth factor

VI: vascular invasion

WB: Western blot

WT: wild type

YAP/Yap: Yes-associated protein (human/murine gene)

YAP: Yes-associated protein (human and murine protein)

References

1 Hanahan, D. & Weinberg, R. A. The hallmarks of cancer. *Cell* 100, 57-70 (2000).
2 Hanahan, D. & Weinberg, R. A. Hallmarks of cancer: the next generation. *Cell* 144, 646-674, doi:10.1016/j.cell.2011.02.013 (2011).
3 Hanahan, D. & Coussens, L. M. Accessories to the crime: functions of cells recruited to the tumor microenvironment. *Cancer Cell* 21, 309-322, doi:10.1016/j.ccr.2012.02.022 (2012).
4 Lunt, S. Y. & Vander Heiden, M. G. Aerobic glycolysis: meeting the metabolic requirements of cell proliferation. *Annu Rev Cell Dev Biol* 27, 441-464, doi:10.1146/annurev-cellbio-092910-154237 (2011).
5 Schreiber, R. D., Old, L. J. & Smyth, M. J. Cancer immunoediting: integrating immunity's roles in cancer suppression and promotion. *Science* 331, 1565-1570, doi:10.1126/science.1203486 (2011).
6 Cho, R. W. & Clarke, M. F. Recent advances in cancer stem cells. *Curr Opin Genet Dev* 18, 48-53, doi:10.1016/j.gde.2008.01.017 (2008).
7 Singh, A. & Settleman, J. EMT, cancer stem cells and drug resistance: an emerging axis of evil in the war on cancer. *Oncogene* 29, 4741-4751, doi:10.1038/onc.2010.215 (2010).
8 Lobo, N. A., Shimono, Y., Qian, D. & Clarke, M. F. The biology of cancer stem cells. *Annu Rev Cell Dev Biol* 23, 675-699, doi:10.1146/annurev.cellbio.22.010305.104154 (2007).
9 Chaffer, C. L. & Weinberg, R. A. A perspective on cancer cell metastasis. *Science* 331, 1559-1564, doi:10.1126/science.1203543 (2011).
10 Nguyen, D. X., Bos, P. D. & Massague, J. Metastasis: from dissemination to organ-specific colonization. *Nat Rev Cancer* 9, 274-284, doi:10.1038/nrc2622 (2009).
11 Hanahan, D. & Folkman, J. Patterns and emerging mechanisms of the angiogenic switch during tumorigenesis. *Cell* 86, 353-364 (1996).
12 Tammela, T. & Alitalo, K. Lymphangiogenesis: Molecular mechanisms and future promise. *Cell* 140, 460-476, doi:10.1016/j.cell.2010.01.045 (2010).
13 Bergers, G. & Song, S. The role of pericytes in blood-vessel formation and maintenance. *Neuro Oncol* 7, 452-464, doi:10.1215/s1152851705000232 (2005).
14 Gaengel, K., Genove, G., Armulik, A. & Betsholtz, C. Endothelial-mural cell signaling in vascular development and angiogenesis. *Arterioscler Thromb Vasc Biol* 29, 630-638, doi:10.1161/atvbaha.107.161521 (2009).
15 Kalluri, R. & Zeisberg, M. Fibroblasts in cancer. *Nat Rev Cancer* 6, 392-401, doi:10.1038/nrc1877 (2006).
16 Shimoda, M., Mellody, K. T. & Orimo, A. Carcinoma-associated fibroblasts are a rate-limiting determinant for tumour progression. *Semin Cell Dev Biol* 21, 19-25, doi:10.1016/j.semcdb.2009.10.002 (2010).
17 Calvo, F. *et al.* Mechanotransduction and YAP-dependent matrix remodelling is required for the generation and maintenance of cancer-associated fibroblasts. *Nat Cell Biol* 15, 637-646, doi:10.1038/ncb2756 (2013).
18 Ugel, S., De Sanctis, F., Mandruzzato, S. & Bronte, V. Tumor-induced myeloid deviation: when myeloid-derived suppressor cells meet tumor-associated macrophages. *J Clin Invest* 125, 3365-3376, doi:10.1172/JCI80006 (2015).
19 Pages, F. *et al.* Immune infiltration in human tumors: a prognostic factor that should not be ignored. *Oncogene* 29, 1093-1102, doi:10.1038/onc.2009.416 (2010).
20 Nelson, B. H. The impact of T-cell immunity on ovarian cancer outcomes. *Immunol Rev* 222, 101-116, doi:10.1111/j.1600-065X.2008.00614.x (2008).
21 Restifo, N. P. *et al.* Identification of human cancers deficient in antigen processing. *J Exp Med* 177, 265-272, doi:10.1084/jem.177.2.265 (1993).
22 Hicklin, D. J. *et al.* beta2-Microglobulin mutations, HLA class I antigen loss, and tumor progression in melanoma. *J Clin Invest* 101, 2720 (1998).
23 Balkwill, F., Charles, K. A. & Mantovani, A. Smoldering and polarized inflammation in the initiation and promotion of malignant disease. *Cancer Cell* 7, 211-217, doi:10.1016/j.ccr.2005.02.013 (2005).
24 Kitamura, T., Qian, B. Z. & Pollard, J. W. Immune cell promotion of metastasis. *Nat Rev Immunol* 15, 73-86, doi:10.1038/nri3789 (2015).
25 Gabrilovich, D. I., Ostrand-Rosenberg, S. & Bronte, V. Coordinated regulation of myeloid cells by tumours. *Nat Rev Immunol* 12, 253-268, doi:10.1038/nri3175 (2012).
26 Zitvogel, L., Tesniere, A., Apetoh, L., Ghiringhelli, F. & Kroemer, G. [Immunological aspects of anticancer chemotherapy]. *Bull Acad Natl Med* 192, 1469-1487; discussion 1487-1469 (2008).
27 Nagaraj, S. *et al.* Altered recognition of antigen is a mechanism of CD8+ T cell tolerance in cancer. *Nat Med* 13, 828-835, doi:10.1038/nm1609 (2007).
28 Ugel, S. *et al.* Immune tolerance to tumor antigens occurs in a specialized environment of the spleen. *Cell Rep* 2, 628-639, doi:10.1016/j.celrep.2012.08.006 (2012).
29 Swiecki, M. & Colonna, M. Unraveling the functions of plasmacytoid dendritic cells during viral infections, autoimmunity, and tolerance. *Immunol Rev* 234, 142-162, doi:10.1111/j.0105-2896.2009.00881.x (2010).
30 Rotta, G. *et al.* Lipopolysaccharide or whole bacteria block the conversion of inflammatory monocytes into dendritic cells in vivo. *J Exp Med* 198, 1253-1263, doi:10.1084/jem.20030335 (2003).
31 Gabrilovich, D. Mechanisms and functional significance of tumour-induced dendritic-cell defects. *Nat Rev Immunol* 4, 941-952, doi:10.1038/nri1498 (2004).
32 Yang, M. *et al.* HIF-dependent induction of adenosine receptor A2b skews human dendritic cells to a Th2-stimulating phenotype under hypoxia. *Immunol Cell Biol* 88, 165-171, doi:10.1038/icb.2009.77 (2010).
33 Gottfried, E. *et al.* Tumor-derived lactic acid modulates dendritic cell activation and antigen expression. *Blood* 107, 2013-2021, doi:10.1182/blood-2005-05-1795 (2006).

34 Herber, D. L. *et al.* Lipid accumulation and dendritic cell dysfunction in cancer. *Nat Med* 16, 880-886, doi:10.1038/nm.2172 (2010).
35 Norian, L. A. *et al.* Tumor-infiltrating regulatory dendritic cells inhibit CD8+ T cell function via L-arginine metabolism. *Cancer Res* 69, 3086-3094, doi:10.1158/0008-5472.CAN-08-2826 (2009).
36 Watkins, S. K. *et al.* FOXO3 programs tumor-associated DCs to become tolerogenic in human and murine prostate cancer. *J Clin Invest* 121, 1361-1372, doi:10.1172/jci44325 (2011).
37 Baban, B. *et al.* IDO activates regulatory T cells and blocks their conversion into Th17-like T cells. *J Immunol* 183, 2475-2483, doi:10.4049/jimmunol.0900986 (2009).
38 Janco, J. M. T., Lamichhane, P., Karyampudi, L. & Knutson, K. L. Tumor-infiltrating dendritic cells in cancer pathogenesis. *J Immunol* 194, 2985-2991 (2015).
39 Miyagawa, S. *et al.* Prognostic significance of mature dendritic cells and factors associated with their accumulation in metastatic liver tumors from colorectal cancer. *Hum Pathol* 35, 1392-1396, doi:http://dx.doi.org/10.1016/j.humpath.2004.07.018 (2004).
40 Marigo, I. *et al.* T Cell Cancer Therapy Requires CD40-CD40L Activation of Tumor Necrosis Factor and Inducible Nitric-Oxide-Synthase-Producing Dendritic Cells. *Cancer Cell* 30, 377-390, doi:10.1016/j.ccell.2016.08.004 (2016).
41 Coffelt, S. B., Wellenstein, M. D. & de Visser, K. E. Neutrophils in cancer: neutral no more. *Nat Rev Cancer* 16, 431-446, doi:10.1038/nrc.2016.52 (2016).
42 Fridlender, Z. G. *et al.* Polarization of tumor-associated neutrophil phenotype by TGF-beta: "N1" versus "N2" TAN. *Cancer Cell* 16, 183-194, doi:10.1016/j.ccr.2009.06.017 (2009).
43 Granot, Z. *et al.* Tumor entrained neutrophils inhibit seeding in the premetastatic lung. *Cancer Cell* 20, 300-314, doi:10.1016/j.ccr.2011.08.012 (2011).
44 Shojaei, F. *et al.* G-CSF-initiated myeloid cell mobilization and angiogenesis mediate tumor refractoriness to anti-VEGF therapy in mouse models. *Proc Natl Acad Sci U S A* 106, 6742-6747, doi:10.1073/pnas.0902280106 (2009).
45 Kowanetz, M. *et al.* Granulocyte-colony stimulating factor promotes lung metastasis through mobilization of Ly6G+Ly6C+ granulocytes. *Proc Natl Acad Sci U S A* 107, 21248-21255, doi:10.1073/pnas.1015855107 (2010).
46 De Sanctis, F. *et al.* MDSCs in cancer: Conceiving new prognostic and therapeutic targets. *Biochim Biophys Acta* 1865, 35-48, doi:10.1016/j.bbcan.2015.08.001 (2016).
47 Youn, J. I., Nagaraj, S., Collazo, M. & Gabrilovich, D. I. Subsets of myeloid-derived suppressor cells in tumor-bearing mice. *J Immunol* 181, 5791-5802 (2008).
48 Gallina, G. *et al.* Tumors induce a subset of inflammatory monocytes with immunosuppressive activity on CD8+ T cells. *J Clin Invest* 116, 2777-2790, doi:10.1172/jci28828 (2006).
49 Dolcetti, L. *et al.* Hierarchy of immunosuppressive strength among myeloid-derived suppressor cell subsets is determined by GM-CSF. *Eur J Immunol* 40, 22-35, doi:10.1002/eji.200939903 (2010).
50 Bronte, V. & Zanovello, P. Regulation of immune responses by L-arginine metabolism. *Nat Rev Immunol* 5, 641-654, doi:10.1038/nri1668 (2005).
51 Molon, B. *et al.* Chemokine nitration prevents intratumoral infiltration of antigen-specific T cells. *J Exp Med* 208, 1949-1962, doi:10.1084/jem.20101956 (2011).
52 Serafini, P., Mgebroff, S., Noonan, K. & Borrello, I. Myeloid-derived suppressor cells promote cross-tolerance in B-cell lymphoma by expanding regulatory T cells. *Cancer Res* 68, 5439-5449, doi:10.1158/0008-5472.can-07-6621 (2008).
53 Mussai, F. *et al.* Acute myeloid leukemia creates an arginase-dependent immunosuppressive microenvironment. *Blood* 122, 749-758 (2013).
54 Mussai, F. *et al.* Neuroblastoma arginase activity creates an immunosuppressive microenvironment that impairs autologous and engineered immunity. *Cancer Res* 75, 3043-3053 (2015).
55 Corzo, C. A. *et al.* HIF-1alpha regulates function and differentiation of myeloid-derived suppressor cells in the tumor microenvironment. *J Exp Med* 207, 2439-2453, doi:10.1084/jem.20100587 (2010).
56 Kitamura, T. *et al.* SMAD4-deficient intestinal tumors recruit CCR1+ myeloid cells that promote invasion. *Nat Genet* 39, 467-475, doi:10.1038/ng1997 (2007).
57 Toh, B. *et al.* Mesenchymal transition and dissemination of cancer cells is driven by myeloid-derived suppressor cells infiltrating the primary tumor. *PLoS Biol* 9, e1001162, doi:10.1371/journal.pbio.1001162 (2011).
58 Franklin, R. A. *et al.* The cellular and molecular origin of tumor-associated macrophages. *Science* 344, 921-925, doi:10.1126/science.1252510 (2014).
59 Movahedi, K. *et al.* Different Tumor Microenvironments Contain Functionally Distinct Subsets of Macrophages Derived from Ly6C(high) Monocytes. *Cancer Res* 70, 5728-5739, doi:10.1158/0008-5472.can-09-4672 (2010).
60 Schulz, C. *et al.* A Lineage of Myeloid Cells Independent of Myb and Hematopoietic Stem Cells. *Science* 336, 86-90, doi:10.1126/science.1219179 (2012).
61 Hoeffel, G. *et al.* Adult Langerhans cells derive predominantly from embryonic fetal liver monocytes with a minor contribution of yolk sac-derived macrophages. *J Exp Med* 209, 1167-1181, doi:10.1084/jem.20120340 (2012).
62 Guilliams, M. *et al.* Alveolar macrophages develop from fetal monocytes that differentiate into long-lived cells in the first week of life via GM-CSF. *J Exp Med* 210, 1977-1992, doi:10.1084/jem.20131199 (2013).
63 Mosser, D. M. & Edwards, J. P. Exploring the full spectrum of macrophage activation. *Nat Rev Immunol* 8, 958-969, doi:10.1038/nri2448 (2008).
64 Qian, B. Z. & Pollard, J. W. Macrophage diversity enhances tumor progression and metastasis. *Cell* 141, 39-51, doi:10.1016/j.cell.2010.03.014 (2010).
65 Gordon, S. & Taylor, P. R. Monocyte and macrophage heterogeneity. *Nat Rev Immunol* 5, 953-964, doi:10.1038/nri1733 (2005).
66 Biswas, S. K. & Mantovani, A. Macrophage plasticity and interaction with lymphocyte subsets: cancer as a paradigm. *Nat Immunol* 11, 889-896, doi:10.1038/ni.1937 (2010).
67 Sica, A. & Mantovani, A. Macrophage plasticity and polarization: in vivo veritas. *J Clin Invest* 122, 787-795, doi:10.1172/jci59643 (2012).

68 Savage, N. D. *et al.* Human anti-inflammatory macrophages induce Foxp3+ GITR+ CD25+ regulatory T cells, which suppress via membrane-bound TGFbeta-1. *J Immunol* 181, 2220-2226 (2008).
69 Mantovani, A., Sozzani, S., Locati, M., Allavena, P. & Sica, A. Macrophage polarization: tumor-associated macrophages as a paradigm for polarized M2 mononuclear phagocytes. *Trends Immunol* 23, 549-555 (2002).
70 Pollard, J. W. Trophic macrophages in development and disease. *Nat Rev Immunol* 9, 259-270, doi:10.1038/nri2528 (2009).
71 O'Sullivan, T. *et al.* Cancer immunoediting by the innate immune system in the absence of adaptive immunity. *J Exp Med* 209, 1869-1882, doi:10.1084/jem.20112738 (2012).
72 DeNardo, D. G. *et al.* Leukocyte complexity predicts breast cancer survival and functionally regulates response to chemotherapy. *Cancer Discov* 1, 54-67, doi:10.1158/2159-8274.cd-10-0028 (2011).
73 Steidl, C. *et al.* Tumor-associated macrophages and survival in classic Hodgkin's lymphoma. *N Engl J Med* 362, 875-885, doi:10.1056/NEJMoa0905680 (2010).
74 Komohara, Y., Fujiwara, Y., Ohnishi, K. & Takeya, M. Tumor-associated macrophages: Potential therapeutic targets for anti-cancer therapy. *Adv Drug Deliv Rev* 99, 180-185, doi:10.1016/j.addr.2015.11.009 (2016).
75 Sica, A. *et al.* Autocrine Production of IL-10 Mediates Defective IL-12 Production and NF- B Activation in Tumor-Associated Macrophages. *J Immunol* 164, 762-767, doi:10.4049/jimmunol.164.2.762 (2000).
76 DeNardo, D. G. *et al.* CD4(+) T cells regulate pulmonary metastasis of mammary carcinomas by enhancing protumor properties of macrophages. *Cancer Cell* 16, 91-102, doi:10.1016/j.ccr.2009.06.018 (2009).
77 Murai, M. *et al.* Interleukin 10 acts on regulatory T cells to maintain expression of the transcription factor Foxp3 and suppressive function in mice with colitis. *Nat Immunol* 10, 1178-1184, doi:10.1038/ni.1791 (2009).
78 Noy, R. & Pollard, J. W. Tumor-associated macrophages: from mechanisms to therapy. *Immunity* 41, 49-61, doi:10.1016/j.immuni.2014.06.010 (2014).
79 Curiel, T. J. *et al.* Specific recruitment of regulatory T cells in ovarian carcinoma fosters immune privilege and predicts reduced survival. *Nat Med* 10, 942-949, doi:10.1038/nm1093 (2004).
80 Biswas, S. K. *et al.* A distinct and unique transcriptional program expressed by tumor-associated macrophages (defective NF-kappaB and enhanced IRF-3/STAT1 activation). *Blood* 107, 2112-2122, doi:10.1182/blood-2005-01-0428 (2006).
81 Liou, G. Y. *et al.* Macrophage-secreted cytokines drive pancreatic acinar-to-ductal metaplasia through NF-kappaB and MMPs. *J Cell Biol* 202, 563-577, doi:10.1083/jcb.201301001 (2013).
82 Liu, J. *et al.* Tumor-associated macrophages recruit CCR6+ regulatory T cells and promote the development of colorectal cancer via enhancing CCL20 production in mice. *PLoS One* 6, e19495, doi:10.1371/journal.pone.0019495 (2011).
83 Tiemessen, M. M. *et al.* CD4+ CD25+ Foxp3+ regulatory T cells induce alternative activation of human monocytes/macrophages. *Proc Natl Acad Sci USA* 104, 19446-19451 (2007).
84 Summers, C. *et al.* Neutrophil kinetics in health and disease. *Trends Immunol* 31, 318-324 (2010).
85 Murai, M. *et al.* Interleukin 10 acts on regulatory T cells to maintain expression of the transcription factor Foxp3 and suppressive function in mice with colitis. *Nat Immunol* 10, 1178-1184 (2009).
86 Belai, E. B. *et al.* PD-1 blockage delays murine squamous cell carcinoma development. *Carcinogenesis* 35, 424-431, doi:10.1093/carcin/bgt305 (2014).
87 Kuang, D. M. *et al.* Activated monocytes in peritumoral stroma of hepatocellular carcinoma foster immune privilege and disease progression through PD-L1. *J Exp Med* 206, 1327-1337, doi:10.1084/jem.20082173 (2009).
88 Kratochvill, F. *et al.* TNF Counterbalances the Emergence of M2 Tumor Macrophages. *Cell Rep* 12, 1902-1914, doi:10.1016/j.celrep.2015.08.033 (2015).
89 Vlaicu, P. *et al.* Monocytes/macrophages support mammary tumor invasivity by co-secreting lineage-specific EGFR ligands and a STAT3 activator. *BMC Cancer* 13, 197, doi:10.1186/1471-2407-13-197 (2013).
90 Garner, J. M. *et al.* Constitutive activation of signal transducer and activator of transcription 3 (STAT3) and nuclear factor kappaB signaling in glioblastoma cancer stem cells regulates the Notch pathway. *J Biol Chem* 288, 26167-26176, doi:10.1074/jbc.M113.477950 (2013).
91 Rao, G. *et al.* Reciprocal Interactions between Tumor-Associated Macrophages and CD44-Positive Cancer Cells via Osteopontin/CD44 Promote Tumorigenicity in Colorectal Cancer. *Clin Cancer Res* 19, 785-797, doi:10.1158/1078-0432.ccr-12-2788 (2013).
92 Lu, H. *et al.* A breast cancer stem cell niche supported by juxtacrine signalling from monocytes and macrophages. *Nat Cell Biol* 16, 1105-1117, doi:10.1038/ncb3041 http://www.nature.com/ncb/journal/v16/n11/abs/ncb3041.html #supplementary-information (2014).
93 Wan, S. *et al.* Tumor-Associated Macrophages Produce Interleukin 6 and Signal via STAT3 to Promote Expansion of Human Hepatocellular Carcinoma Stem Cells. *Gastroenterology* 147, 1393-1404, doi:http://dx.doi.org/10.1053/j.gastro.2014.08.039 (2014).
94 Hughes, R. *et al.* Perivascular M2 Macrophages Stimulate Tumor Relapse after Chemotherapy. *Cancer Res* 75, 3479-3491, doi:10.1158/0008-5472.CAN-14-3587 (2015).
95 Komohara, Y. *et al.* Clinical significance of CD163(+) tumor-associated macrophages in patients with adult T-cell leukemia/lymphoma. *Cancer Sci* 104, 945-951, doi:10.1111/cas.12167 (2013).
96 Chen, W., Lou, J., Evans, E. A. & Zhu, C. Observing force-regulated conformational changes and ligand dissociation from a single integrin on cells. *J Cell Biol* 199, 497-512 (2012).
97 Lin, E. Y. *et al.* Macrophages regulate the angiogenic switch in a mouse model of breast cancer. *Cancer Res* 66, 11238-11246, doi:10.1158/0008-5472.can-06-1278 (2006).
98 Lin, E. Y. & Pollard, J. W. Tumor-associated macrophages press the angiogenic switch in breast cancer. *Cancer Res* 67, 5064-5066, doi:10.1158/0008-5472.can-07-0912 (2007).
99 Yeo, E. J. *et al.* Myeloid WNT7b mediates the angiogenic switch and metastasis in breast cancer. *Cancer Res* 74, 2962-2973, doi:10.1158/0008-5472.can-13-2421 (2014).

100 Mazzieri, R. *et al.* Targeting the ANG2/TIE2 axis inhibits tumor growth and metastasis by impairing angiogenesis and disabling rebounds of proangiogenic myeloid cells. *Cancer Cell* 19, 512-526, doi:10.1016/j.ccr.2011.02.005 (2011).
101 Coffelt, S. B. *et al.* Angiopoietin-2 regulates gene expression in TIE2-expressing monocytes and augments their inherent proangiogenic functions. *Cancer Res* 70, 5270-5280, doi:10.1158/0008-5472.can-10-0012 (2010).
102 Kessenbrock, K., Plaks, V. & Werb, Z. Matrix metalloproteinases: regulators of the tumor microenvironment. *Cell* 141, 52-67, doi:10.1016/j.cell.2010.03.015 (2010).
103 Gocheva, V. *et al.* IL-4 induces cathepsin protease activity in tumor-associated macrophages to promote cancer growth and invasion. *Genes Dev* 24, 241-255, doi:10.1101/gad.1874010 (2010).
104 Almholt, K. *et al.* Reduced metastasis of transgenic mammary cancer in urokinase-deficient mice. *Int J Cancer* 113, 525-532, doi:10.1002/ijc.20631 (2005).
105 Wyckoff, J. B. *et al.* Direct visualization of macrophage-assisted tumor cell intravasation in mammary tumors. *Cancer Res* 67, 2649-2656, doi:10.1158/0008-5472.CAN-06-1823 (2007).
106 Gocheva, V. *et al.* Distinct roles for cysteine cathepsin genes in multistage tumorigenesis. *Genes Dev* 20, 543-556, doi:10.1101/gad.1407406 (2006).
107 Joyce, J. A. & Pollard, J. W. Microenvironmental regulation of metastasis. *Nat Rev Cancer* 9, 239-252, doi:10.1038/nrc2618 (2009).
108 Egeblad, M. & Werb, Z. New functions for the matrix metalloproteinases in cancer progression. *Nat Rev Cancer* 2, 161-174, doi:10.1038/nrc745 (2002).
109 Wyckoff, J. *et al.* A paracrine loop between tumor cells and macrophages is required for tumor cell migration in mammary tumors. *Cancer Res* 64, 7022-7029, doi:10.1158/0008-5472.CAN-04-1449 (2004).
110 Wyckoff, J. B. *et al.* Direct Visualization of Macrophage-Assisted Tumor Cell Intravasation in Mammary Tumors. *Cancer Res* 67, 2649-2656, doi:10.1158/0008-5472.can-06-1823 (2007).
111 Sangaletti, S. *et al.* Macrophage-derived SPARC bridges tumor cell-extracellular matrix interactions toward metastasis. *Cancer Res* 68, 9050-9059, doi:10.1158/0008-5472.can-08-1327 (2008).
112 Condeelis, J. & Segall, J. E. Intravital imaging of cell movement in tumours. *Nat Rev Cancer* 3, 921-930, doi:10.1038/nrc1231 (2003).
113 Hanna, R. N. *et al.* The transcription factor NR4A1 (Nur77) controls bone marrow differentiation and the survival of Ly6C- monocytes. *Nat Immunol* 12, 778-785, doi:10.1038/ni.2063 (2011).
114 Kaplan, R. N. *et al.* VEGFR1-positive haematopoietic bone marrow progenitors initiate the pre-metastatic niche. *Nature* 438, 820-827, doi:10.1038/nature04186 (2005).
115 Kim, S. *et al.* Carcinoma-produced factors activate myeloid cells through TLR2 to stimulate metastasis. *Nature* 457, 102-106, doi:10.1038/nature07623 (2009).
116 Hiratsuka, S., Watanabe, A., Aburatani, H. & Maru, Y. Tumour-mediated upregulation of chemoattractants and recruitment of myeloid cells predetermines lung metastasis. *Nat Cell Biol* 8, 1369-1375, doi:10.1038/ncb1507 (2006).
117 Hoshino, A. *et al.* Tumour exosome integrins determine organotropic metastasis. *Nature* 527, 329-335, doi:10.1038/nature15756 (2015).
118 Gil-Bernabe, A. M. *et al.* Recruitment of monocytes/macrophages by tissue factor-mediated coagulation is essential for metastatic cell survival and premetastatic niche establishment in mice. *Blood* 119, 3164-3175, doi:10.1182/blood-2011-08-376426 (2012).
119 Ferjancic, S. *et al.* VCAM-1 and VAP-1 recruit myeloid cells that promote pulmonary metastasis in mice. *Blood* 121, 3289-3297, doi:10.1182/blood-2012-08-449819 (2013).
120 Qian, B. Z. *et al.* CCL2 recruits inflammatory monocytes to facilitate breast-tumour metastasis. *Nature* 475, 222-225, doi:10.1038/nature10138 (2011).
121 Qian, B. *et al.* A distinct macrophage population mediates metastatic breast cancer cell extravasation, establishment and growth. *PLoS One* 4, e6562, doi:10.1371/journal.pone.0006562 (2009).
122 Zhao, L. *et al.* Recruitment of a myeloid cell subset (CD11b/Gr1 mid) via CCL2/CCR2 promotes the development of colorectal cancer liver metastasis. *Hepatology* 57, 829-839, doi:10.1002/hep.26094 (2013).
123 Hiratsuka, S. *et al.* MMP9 induction by vascular endothelial growth factor receptor-1 is involved in lung-specific metastasis. *Cancer Cell* 2, 289-300 (2002).
124 Hussell, T. & Bell, T. J. Alveolar macrophages: plasticity in a tissue-specific context. *Nat Rev Immunol* 14, 81-93, doi:10.1038/nri3600 (2014).
125 Chen, Q., Zhang, X. H. & Massague, J. Macrophage binding to receptor VCAM-1 transmits survival signals in breast cancer cells that invade the lungs. *Cancer Cell* 20, 538-549, doi:10.1016/j.ccr.2011.08.025 (2011).
126 Lin, E. Y., Nguyen, A. V., Russell, R. G. & Pollard, J. W. Colony-stimulating factor 1 promotes progression of mammary tumors to malignancy. *J Exp Med* 193, doi:10.1084/jem.193.6.727 (2001).
127 Strachan, D. C. *et al.* CSF1R inhibition delays cervical and mammary tumor growth in murine models by attenuating the turnover of tumor-associated macrophages and enhancing infiltration by CD8+ T cells. *Oncoimmunology* 2, e26968, doi:10.4161/onci.26968 (2013).
128 Coussens, L. M., Zitvogel, L. & Palucka, A. K. Neutralizing tumor-promoting chronic inflammation: a magic bullet? *Science* 339, 286-291, doi:10.1126/science.1232227 (2013).
129 Mitchem, J. B. *et al.* Targeting tumor-infiltrating macrophages decreases tumor-initiating cells, relieves immunosuppression, and improves chemotherapeutic responses. *Cancer Res* 73, 1128-1141, doi:10.1158/0008-5472.can-12-2731 (2013).
130 Quail, D. F. & Joyce, J. A. Microenvironmental regulation of tumor progression and metastasis. *Nat Med* 19, 1423-1437, doi:10.1038/nm.3394 (2013).
131 Ries, C. H. *et al.* Targeting tumor-associated macrophages with anti-CSF-1R antibody reveals a strategy for cancer therapy. *Cancer Cell* 25, 846-859, doi:10.1016/j.ccr.2014.05.016 (2014).

132 Maurer, M. E. & Cooper, J. A. The adaptor protein Dab2 sorts LDL receptors into coated pits independently of AP-2 and ARH. *J Cell Sci* 119, 4235-4246, doi:10.1242/jcs.03217 (2006).
133 Liang, P. & Pardee, A. Differential display of eukaryotic messenger RNA by means of the polymerase chain reaction. *Science* 257, 967-971, doi:10.1126/science.1354393 (1992).
134 Xu, X. X., Yang, W., Jackowski, S. & Rock, C. O. Cloning of a novel phosphoprotein regulated by colony-stimulating factor 1 shares a domain with the Drosophila disabled gene product. *J Biol Chem* 270, 14184-14191 (1995).
135 Sheng, Z. *et al.* Chromosomal location of murine disabled-2 gene and structural comparison with its human ortholog. *Gene* 268, 31-39 (2001).
136 Albertsen, H. M. *et al.* Sequence, genomic structure, and chromosomal assignment of human DOC-2. *Genomics* 33, 207-213 (1996).
137 Gertler, F. B., Bennett, R. L., Clark, M. J. & Hoffmann, F. M. Drosophila abl tyrosine kinase in embryonic CNS axons: a role in axonogenesis is revealed through dosage-sensitive interactions with disabled. *Cell* 58, 103-113 (1989).
138 Gertler, F. B., Hill, K. K., Clark, M. J. & Hoffmann, F. M. Dosage-sensitive modifiers of Drosophila abl tyrosine kinase function: prospero, a regulator of axonal outgrowth, and disabled, a novel tyrosine kinase substrate. *Genes Dev* 7, 441-453 (1993).
139 Hoffmann, F. M. Drosophila abl and genetic redundancy in signal transduction. *Trends Genet* 7, 351-355 (1991).
140 Xu, X.-X., Yi, T., Tang, B. & Lambeth, J. D. Disabled-2 (Dab2) is an SH3 domain-binding partner of Grb2. *Oncogene* 16, 1561-1569 (1998).
141 Traub, L. M. Sorting it out: AP-2 and alternate clathrin adaptors in endocytic cargo selection. *J Cell Biol* 163, 203-208, doi:10.1083/jcb.200309175 (2003).
142 Maurer, M. E. & Cooper, J. A. Endocytosis of megalin by visceral endoderm cells requires the Dab2 adaptor protein. *J Cell Sci* 118, 5345-5355, doi:10.1242/jcs.02650 (2005).
143 Morris, S. M. & Cooper, J. A. Disabled-2 colocalizes with the LDLR in clathrin-coated pits and interacts with AP-2. *Traffic* 2, 111-123 (2001).
144 Caswell, P. T., Vadrevu, S. & Norman, J. C. Integrins: masters and slaves of endocytic transport. *Nat Rev Mol Cell Biol* 10, 843-853, doi:10.1038/nrm2799 (2009).
145 Rosenbauer, F. *et al.* Disabled-2 is transcriptionally regulated by ICSBP and augments macrophage spreading and adhesion. *EMBO J* 21, 211-220, doi:10.1093/emboj/21.3.211 (2002).
146 Huang, C. L. *et al.* Disabled-2 is a negative regulator of integrin alpha(IIb)beta(3)-mediated fibrinogen adhesion and cell signaling. *J Biol Chem* 279, 42279-42289, doi:10.1074/jbc.M402540200 (2004).
147 Chetrit, D., Ziv, N. & Ehrlich, M. Dab2 regulates clathrin assembly and cell spreading. *Biochem J* 418, 701-715, doi:10.1042/BJ20081288 (2009).
148 Chetrit, D. *et al.* Negative regulation of the endocytic adaptor disabled-2 (Dab2) in mitosis. *J Biol Chem* 286, 5392-5403, doi:10.1074/jbc.M110.161851 (2011).
149 Morris, S. M., Tallquist, M. D., Rock, C. O. & Cooper, J. A. Dual roles for the Dab2 adaptor protein in embryonic development and kidney transport. *EMBO J* 21, 1555-1564, doi:10.1093/emboj/21.7.1555 (2002).
150 Spudich, G. *et al.* Myosin VI targeting to clathrin-coated structures and dimerization is mediated by binding to Disabled-2 and PtdIns(4,5)P2. *Nat Cell Biol* 9, 176-183, doi:10.1038/ncb1531 (2007).
151 Šamaj, J. *et al.* Endocytosis, actin cytoskeleton, and signaling. *Plant Physiol* 135, 1150-1161 (2004).
152 Doherty, G. J. & McMahon, H. T. Mechanisms of endocytosis. *Annu Rev Biochem* 78, 857-902, doi:10.1146/annurev.biochem.78.081307.110540 (2009).
153 McMahon, H. T. & Boucrot, E. Molecular mechanism and physiological functions of clathrin-mediated endocytosis. *Nat Rev Mol Cell Biol* 12, 517-533, doi:10.1038/nrm3151 (2011).
154 Kirkham, M. & Parton, R. G. Clathrin-independent endocytosis: new insights into caveolae and non-caveolar lipid raft carriers. *Biochim Biophys Acta* 1746, 349-363 (2005).
155 Han, B., Copeland, C. A., Tiwari, A. & Kenworthy, A. K. Assembly and Turnover of Caveolae: What Do We Really Know? *Front Cell Dev Biol* 4, 68, doi:10.3389/fcell.2016.00068 (2016).
156 Parton, R. G. & Richards, A. A. Lipid rafts and caveolae as portals for endocytosis: new insights and common mechanisms. *Traffic* 4, 724-738 (2003).
157 Cheng, J. P. & Nichols, B. J. Caveolae: One Function or Many? *Trends Cell Biol* 26, 177-189, doi:10.1016/j.tcb.2015.10.010 (2016).
158 Gordon, S. Phagocytosis: An Immunobiologic Process. *Immunity* 44, 463-475, doi:http://dx.doi.org/10.1016/j.immuni.2016.02.026 (2016).
159 Lundmark, R. *et al.* The GTPase-Activating Protein GRAF1 Regulates the CLIC/GEEC Endocytic Pathway. *Curr Biol* 18, 1802-1808, doi:10.1016/j.cub.2008.10.044 (2008).
160 Hopkins, C. R., Miller, K. & Beardmore, J. M. Receptor-mediated endocytosis of transferrin and epidermal growth factor receptors: a comparison of constitutive and ligand-induced uptake. *J Cell Sci Suppl* 3, 173-186 (1985).
161 Stimpson, H. E., Toret, C. P., Cheng, A. T., Pauly, B. S. & Drubin, D. G. Early-arriving Syp1p and Ede1p function in endocytic site placement and formation in budding yeast. *Mol Biol Cell* 20, 4640-4651, doi:10.1091/mbc.E09-05-0429 (2009).
162 Henne, W. M. *et al.* FCHo proteins are nucleators of clathrin-mediated endocytosis. *Science* 328, 1281-1284, doi:10.1126/science.1188462 (2010).
163 Ferguson, S. M. *et al.* Coordinated actions of actin and BAR proteins upstream of dynamin at endocytic clathrin-coated pits. *Dev Cell* 17, 811-822, doi:10.1016/j.devcel.2009.11.005 (2009).
164 Sundborger, A. *et al.* An endophilin-dynamin complex promotes budding of clathrin-coated vesicles during synaptic vesicle recycling. *J Cell Sci* 124, 133-143, doi:10.1242/jcs.072686 (2011).
165 Sweitzer, S. M. & Hinshaw, J. E. Dynamin undergoes a GTP-dependent conformational change causing vesiculation. *Cell* 93, 1021-1029 (1998).

166 Fujimoto, L. M., Roth, R., Heuser, J. E. & Schmid, S. L. Actin assembly plays a variable, but not obligatory role in receptor-mediated endocytosis in mammalian cells. *Traffic* 1, 161-171 (2000).
167 Boucrot, E., Saffarian, S., Massol, R., Kirchhausen, T. & Ehrlich, M. Role of lipids and actin in the formation of clathrin-coated pits. *Exp Cell Res* 312, 4036-4048, doi:10.1016/j.yexcr.2006.09.025 (2006).
168 Aghamohammadzadeh, S. & Ayscough, K. R. Differential requirements for actin during yeast and mammalian endocytosis. *Nat Cell Biol* 11, 1039-1042, doi:10.1038/ncb1918 (2009).
169 Mooren, O. L., Galletta, B. J. & Cooper, J. A. Roles for actin assembly in endocytosis. *Annu Rev Biochem* 81, 661-686, doi:10.1146/annurev-biochem-060910-094416 (2012).
170 Merrifield, C. J. & Kaksonen, M. Endocytic accessory factors and regulation of clathrin-mediated endocytosis. *Cold Spring Harb Perspect Biol* 6, a016733 (2014).
171 Traub, L. M. Tickets to ride: selecting cargo for clathrin-regulated internalization. *Nat Rev Mol Cell Biol* 10, 583-596, doi:10.1038/nrm2751 (2009).
172 Cheng, Y., Boll, W., Kirchhausen, T., Harrison, S. C. & Walz, T. Cryo-electron tomography of clathrin-coated vesicles: structural implications for coat assembly. *J Mol Biol* 365, 892-899, doi:10.1016/j.jmb.2006.10.036 (2007).
173 Garcia, C. K. *et al.* Autosomal recessive hypercholesterolemia caused by mutations in a putative LDL receptor adaptor protein. *Science* 292, 1394-1398, doi:10.1126/science.1060458 (2001).
174 Santolini, E. *et al.* Numb is an endocytic protein. *J Cell Biol* 151, 1345-1352 (2000).
175 Pryor, P. R. *et al.* Molecular basis for the sorting of the SNARE VAMP7 into endocytic clathrin-coated vesicles by the ArfGAP Hrb. *Cell* 134, 817-827, doi:10.1016/j.cell.2008.07.023 (2008).
176 Haucke, V. & De Camilli, P. AP-2 recruitment to synaptotagmin stimulated by tyrosine-based endocytic motifs. *Science* 285, 1268-1271 (1999).
177 Yang, D. H., Cai, K. Q., Roland, I. H., Smith, E. R. & Xu, X. X. Disabled-2 is an epithelial surface positioning gene. *J Biol Chem* 282, 13114-13122, doi:10.1074/jbc.M611356200 (2007).
178 Yang, D. H. *et al.* Disabled-2 is essential for endodermal cell positioning and structure formation during mouse embryogenesis. *Dev Biol* 251, 27-44 (2002).
179 Sheng, Z. *et al.* Restoration of positioning control following Disabled-2 expression in ovarian and breast tumor cells. *Oncogene* 19, 4847-4854, doi:10.1038/sj.onc.1203853 (2000).
180 Moore, R., Cai, K. Q., Tao, W., Smith, E. R. & Xu, X. X. Differential requirement for Dab2 in the development of embryonic and extra-embryonic tissues. *BMC Dev Biol* 13, 39, doi:10.1186/1471-213X-13-39 (2013).
181 Tsai, H.-J. *et al.* Disabled-2 is required for efficient hemostasis and platelet activation by thrombin in mice. *Arterioscler Thromb Vasc Biol* 34, 2404-2412 (2014).
182 Hannigan, A. *et al.* Epigenetic downregulation of human disabled homolog 2 switches TGF-beta from a tumor suppressor to a tumor promoter. *J Clin Invest* 120, 2842-2857, doi:10.1172/jci36125 (2010).
183 Zhang, Z., Chen, Y., Tang, J. & Xie, X. Frequent loss expression of dab2 and promotor hypermethylation in human cancers: A meta-analysis and systematic review. *Pak J Med Sci* 30, 432 (2014).
184 Mok, S. C. *et al.* DOC-2, a candidate tumor suppressor gene in human epithelial ovarian cancer. *Oncogene* 16, 2381-2387, doi:10.1038/sj.onc.1201769 (1998).
185 Fazili, Z., Sun, W., Mittelstaedt, S., Cohen, C. & Xu, X.-X. Disabled-2 inactivation is an early step in ovarian tumorigenicity. *Oncogene* 18, 3104-3113 (1999).
186 Kleeff, J. *et al.* Down-Regulation of DOC-2 in Colorectal Cancer Points to Its Role as a Tumor Suppressor in This Malignancy. *Dis Colon Rectum* 45, 1242-1248, doi:10.1007/s10350-004-6399-2 (2002).
187 Bagadi, S. A. *et al.* Frequent loss of Dab2 protein and infrequent promoter hypermethylation in breast cancer. *Breast Cancer Res Treat* 104, 277-286, doi:10.1007/s10549-006-9422-6 (2007).
188 Schwahn, D. J. & Medina, D. p96, a MAPK-related protein, is consistently downregulated during mouse mammary carcinogenesis. *Oncogene* 17, 1173-1178, doi:10.1038/sj.onc.1202038 (1998).
189 Martin, J. C., Herbert, B. S. & Hocevar, B. A. Disabled-2 downregulation promotes epithelial-to-mesenchymal transition. *Br J Cancer* 103, 1716-1723, doi:10.1038/sj.bjc.6605975 (2010).
190 Tseng, C. P. *et al.* The role of DOC-2/DAB2 protein phosphorylation in the inhibition of AP-1 activity. An underlying mechanism of its tumor-suppressive function in prostate cancer. *J Biol Chem* 274, 31981-31986 (1999).
191 Anupam, K., Tusharkant, C., Gupta, S. D. & Ranju, R. Loss of disabled-2 expression is an early event in esophageal squamous tumorigenesis. *World J Gastroenterol* 12, 6041-6045 (2006).
192 Karam, J. A. *et al.* Decreased DOC-2/DAB2 expression in urothelial carcinoma of the bladder. *Clin Cancer Res* 13, 4400-4406, doi:10.1158/1078-0432.ccr-07-0287 (2007).
193 Tong, J. H. *et al.* Putative tumour-suppressor gene DAB2 is frequently down regulated by promoter hypermethylation in nasopharyngeal carcinoma. *BMC Cancer* 10, 253, doi:10.1186/1471-2407-10-253 (2010).
194 Tseng, C. P., Ely, B. D., Li, Y., Pong, R. C. & Hsieh, J. T. Regulation of rat DOC-2 gene during castration-induced rat ventral prostate degeneration and its growth inhibitory function in human prostatic carcinoma cells. *Endocrinology* 139, 3542-3553, doi:10.1210/endo.139.8.6159 (1998).
195 He, J., Smith, E. R. & Xu, X. X. Disabled-2 exerts its tumor suppressor activity by uncoupling c-Fos expression and MAP kinase activation. *J Biol Chem* 276, 26814-26818, doi:10.1074/jbc.M101820200 (2001).
196 Zhou, J. & Hsieh, J. T. The inhibitory role of DOC-2/DAB2 in growth factor receptor-mediated signal cascade. DOC-2/DAB2-mediated inhibition of ERK phosphorylation via binding to Grb2. *J Biol Chem* 276, 27793-27798, doi:10.1074/jbc.M102803200 (2001).
197 Zuber, J. *et al.* A genome-wide survey of RAS transformation targets. *Nat Genet* 24, 144-152, doi:10.1038/72799 (2000).
198 Hocevar, B. A., Prunier, C. & Howe, P. H. Disabled-2 (Dab2) mediates transforming growth factor beta (TGFbeta)-stimulated fibronectin synthesis through TGFbeta-activated kinase 1 and activation of the JNK pathway. *J Biol Chem* 280, 25920-25927, doi:10.1074/jbc.M501150200 (2005).
199 Prunier, C. & Howe, P. H. Disabled-2 (Dab2) is required for transforming growth factor beta-induced epithelial to mesenchymal transition (EMT). *J Biol Chem* 280, 17540-17548, doi:10.1074/jbc.M500974200 (2005).

200 Xu, S., Zhu, J. & Wu, Z. Loss of Dab2 expression in breast cancer cells impairs their ability to deplete TGF-beta and induce Tregs development via TGF-beta. *PLoS One* 9, e91709, doi:10.1371/journal.pone.0091709 (2014).
201 Jiang, Y., He, X. & Howe, P. H. Disabled-2 (Dab2) inhibits Wnt/beta-catenin signalling by binding LRP6 and promoting its internalization through clathrin. *EMBO J* 31, 2336-2349, doi:10.1038/emboj.2012.83 (2012).
202 Westcott, J. M. *et al.* An epigenetically distinct breast cancer cell subpopulation promotes collective invasion. *J Clin Invest* 125, 1927-1943 (2015).
203 Xie, Y. *et al.* Disabled homolog 2 is required for migration and invasion of prostate cancer cells. *Front Med* 9, 312-321, doi:10.1007/s11684-015-0401-3 (2015).
204 Cheong, S. M., Choi, H., Hong, B. S., Gho, Y. S. & Han, J. K. Dab2 is pivotal for endothelial cell migration by mediating VEGF expression in cancer cells. *Exp Cell Res* 318, 550-557, doi:10.1016/j.yexcr.2012.01.013 (2012).
205 Adamson, S. E. *et al.* Disabled homolog 2 controls macrophage phenotypic polarization and adipose tissue inflammation. *J Clin Invest* 126, 1311-1322 (2016).
206 Ahmed, M. S. *et al.* Dab2, a negative regulator of DC immunogenicity, is an attractive molecular target for DC-based immunotherapy. *Oncoimmunology* 4, e984550 (2015).
207 De Franceschi, N., Hamidi, H., Alanko, J., Sahgal, P. & Ivaska, J. Integrin traffic - the update. *J Cell Sci* 128, 839-852, doi:10.1242/jcs.161653 (2015).
208 Paul, N. R., Jacquemet, G. & Caswell, P. T. Endocytic Trafficking of Integrins in Cell Migration. *Curr Biol* 25, R1092-1105, doi:10.1016/j.cub.2015.09.049 (2015).
209 Chao, W. T. & Kunz, J. Focal adhesion disassembly requires clathrin-dependent endocytosis of integrins. *FEBS Lett* 583, 1337-1343, doi:10.1016/j.febslet.2009.03.037 (2009).
210 Teckchandani, A. *et al.* Quantitative proteomics identifies a Dab2/integrin module regulating cell migration. *J Cell Biol* 186, 99-111, doi:10.1083/jcb.200812160 (2009).
211 Ezratty, E. J., Partridge, M. A. & Gundersen, G. G. Microtubule-induced focal adhesion disassembly is mediated by dynamin and focal adhesion kinase. *Nat Cell Biol* 7, 581-590, doi:10.1038/ncb1262 (2005).
212 Ezratty, E. J., Bertaux, C., Marcantonio, E. E. & Gundersen, G. G. Clathrin mediates integrin endocytosis for focal adhesion disassembly in migrating cells. *J Cell Biol* 187, 733-747, doi:10.1083/jcb.200904054 (2009).
213 Teckchandani, A., Mulkearns, E. E., Randolph, T. W., Toida, N. & Cooper, J. A. The clathrin adaptor Dab2 recruits EH domain scaffold proteins to regulate integrin beta1 endocytosis. *Mol Biol Cell* 23, 2905-2916, doi:10.1091/mbc.E11-12-1007 (2012).
214 Eskova, A. *et al.* An RNAi screen identifies KIF15 as a novel regulator of the endocytic trafficking of integrin. *J Cell Sci* 127, 2433-2447, doi:10.1242/jcs.137281 (2014).
215 Yu, C.-h. *et al.* Integrin-beta3 clusters recruit clathrin-mediated endocytic machinery in the absence of traction force. *Nat Commun* 6 (2015).
216 Ross, T. D. *et al.* Integrins in mechanotransduction. *Curr Opin Cell Biol* 25, 613-618, doi:10.1016/j.ceb.2013.05.006 (2013).
217 Engler, A. J., Sen, S., Sweeney, H. L. & Discher, D. E. Matrix Elasticity Directs Stem Cell Lineage Specification. *Cell* 126, 677-689, doi:http://dx.doi.org/10.1016/j.cell.2006.06.044 (2006).
218 Butcher, D. T., Alliston, T. & Weaver, V. M. A tense situation: forcing tumour progression. *Nat Rev Cancer* 9, 108-122 (2009).
219 Jalali, S. *et al.* Integrin-mediated mechanotransduction requires its dynamic interaction with specific extracellular matrix (ECM) ligands. *Proc Natl Acad Sci U S A* 98, 1042-1046, doi:10.1073/pnas.031562998 (2001).
220 Waitkus-Edwards, K. R. alpha4beta1 Integrin Activation of L-Type Calcium Channels in Vascular Smooth Muscle Causes Arteriole Vasoconstriction. *Circ Res* 90, 473-480, doi:10.1161/hh0402.105899 (2002).
221 Loufrani, L. *et al.* Key role of α1β1-integrin in the activation of PI3-kinase-Akt by flow (shear stress) in resistance arteries. *Am J Physiol Heart Circ Physiol* 294, H1906-H1913 (2008).
222 Roca-Cusachs, P., Gauthier, N. C., Del Rio, A. & Sheetz, M. P. Clustering of alpha(5)beta(1) integrins determines adhesion strength whereas alpha(v)beta(3) and talin enable mechanotransduction. *Proc Natl Acad Sci U S A* 106, 16245-16250, doi:10.1073/pnas.0902818106 (2009).
223 Kurakawa, T. *et al.* Functional impact of integrin alpha5beta1 on the homeostasis of intervertebral discs: a study of mechanotransduction pathways using a novel dynamic loading organ culture system. *Spine J* 15, 417-426, doi:10.1016/j.spinee.2014.12.143 (2015).
224 Chen, F. *et al.* An essential role for TH2-type responses in limiting acute tissue damage during experimental helminth infection. *Nat Med* 18, 260-266, doi:10.1038/nm.2628 (2012).
225 Katsumi, A., Naoe, T., Matsushita, T., Kaibuchi, K. & Schwartz, M. A. Integrin activation and matrix binding mediate cellular responses to mechanical stretch. *J Biol Chem* 280, 16546-16549 (2005).
226 Thodeti, C. K. *et al.* TRPV4 Channels Mediate Cyclic Strain–Induced Endothelial Cell Reorientation Through Integrin-to-Integrin Signaling. *Circ Res* 104, 1123-1130, doi:10.1161/circresaha.108.192930 (2009).
227 Grashoff, C. *et al.* Measuring mechanical tension across vinculin reveals regulation of focal adhesion dynamics. *Nature* 466, 263-266, doi:http://www.nature.com/nature/journal/v466/n7303/abs/nature09198.html#supplementaryinformation (2010).
228 Plotnikov, S. V., Pasapera, A. M., Sabass, B. & Waterman, C. M. Force fluctuations within focal adhesions mediate ECM-rigidity sensing to guide directed cell migration. *Cell* 151, 1513-1527, doi:10.1016/j.cell.2012.11.034 (2012).
229 Kong, F. *et al.* Cyclic mechanical reinforcement of integrin–ligand interactions. *Mol Cell* 49, 1060-1068 (2013).
230 Nemir, S. & West, J. L. Synthetic Materials in the Study of Cell Response to Substrate Rigidity. *Ann Biomed Eng* 38, 2-20, doi:10.1007/s10439-009-9811-1 (2010).
231 Wada, K., Itoga, K., Okano, T., Yonemura, S. & Sasaki, H. Hippo pathway regulation by cell morphology and stress fibers. *Development* 138, 3907-3914, doi:10.1242/dev.070987 (2011).
232 Piccolo, S., Dupont, S. & Cordenonsi, M. The biology of YAP/TAZ: hippo signaling and beyond. *Physiol Rev* 94, 1287-1312, doi:10.1152/physrev.00005.2014 (2014).
233 Dupont, S. *et al.* Role of YAP/TAZ in mechanotransduction. *Nature* 474, 179-183, doi:10.1038/nature10137 (2011).

234 Zanconato, F., Cordenonsi, M. & Piccolo, S. YAP/TAZ at the Roots of Cancer. *Cancer Cell* 29, 783-803, doi:10.1016/j.ccell.2016.05.005 (2016).
235 Halder, G., Dupont, S. & Piccolo, S. Transduction of mechanical and cytoskeletal cues by YAP and TAZ. *Nat Rev Mol Cell Biol* 13, 591-600, doi:10.1038/nrm3416 (2012).
236 Zanconato, F. *et al.* Genome-wide association between YAP/TAZ/TEAD and AP-1 at enhancers drives oncogenic growth. *Nat Cell Biol* 17, 1218-1227, doi:10.1038/ncb3216 (2015).
237 Zhao, B. *et al.* Cell detachment activates the Hippo pathway via cytoskeleton reorganization to induce anoikis. *Genes Dev* 26, 54-68, doi:10.1101/gad.173435.111 (2012).
238 Dong, J. *et al.* Elucidation of a universal size-control mechanism in Drosophila and mammals. *Cell* 130, 1120-1133, doi:10.1016/j.cell.2007.07.019 (2007).
239 García-Prat, L. *et al.* Autophagy maintains stemness by preventing senescence. *Nature* 529, 37-42, doi:10.1038/nature16187 http://www.nature.com/nature/journal/v529/n7584/abs/nature16187.html#supplementary- information (2016).
240 Hayashi, H. *et al.* An Imbalance in TAZ and YAP Expression in Hepatocellular Carcinoma Confers Cancer Stem Cell–like Behaviors Contributing to Disease Progression. *Cancer Res* 75, 4985-4997, doi:10.1158/0008-5472.can-15-0291 (2015).
241 Song, S. *et al.* Hippo Coactivator YAP1 Upregulates SOX9 and Endows Esophageal Cancer Cells with Stem-like Properties. *Cancer Res* 74, 4170-4182, doi:10.1158/0008-5472.can-13-3569 (2014).
242 Wang, G. *et al.* Targeting YAP-Dependent MDSC Infiltration Impairs Tumor Progression. *Cancer Discov* 6, 80-95, doi:10.1158/2159-8290.cd-15-0224 (2016).
243 Johnstone, C. N. *et al.* Functional and molecular characterisation of EO771.LMB tumours, a new C57BL/6-mouse-derived model of spontaneously metastatic mammary cancer. *Dis Model Mech* 8, 237-251, doi:10.1242/dmm.017830 (2015).
244 Campbell, L., Saville, C. R., Murray, P. J., Cruickshank, S. M. & Hardman, M. J. Local arginase 1 activity is required for cutaneous wound healing. *J Invest Dermatol* 133, 2461-2470, doi:10.1038/jid.2013.164 (2013).
245 Quintanilla-Dieck, M. J., Codriansky, K., Keady, M., Bhawan, J. & Runger, T. M. Cathepsin K in melanoma invasion. *J Invest Dermatol* 128, 2281-2288, doi:10.1038/jid.2008.63 (2008).
246 Kjøller, L. *et al.* uPARAP/endo180 directs lysosomal delivery and degradation of collagen IV. *Exp Cell Res* 293, 106-116, doi:10.1016/j.yexcr.2003.10.008 (2004).
247 Martinez-Pomares, L. *et al.* Carbohydrate-independent recognition of collagens by the macrophage mannose receptor. *Eur J Immunol* 36, 1074-1082, doi:10.1002/eji.200535685 (2006).
248 Gaggioli, C. *et al.* Fibroblast-led collective invasion of carcinoma cells with differing roles for RhoGTPases in leading and following cells. *Nat Cell Biol* 9, 1392-1400, doi:10.1038/ncb1658 (2007).
249 Pixley, F. J., Lee, P. S., Condeelis, J. S. & Stanley, E. R. Protein tyrosine phosphatase phi regulates paxillin tyrosine phosphorylation and mediates colony-stimulating factor 1-induced morphological changes in macrophages. *Mol Cell Biol* 21, 1795-1809, doi:10.1128/MCB.21.5.1795-1809.2001 (2001).
250 Tse, J. R. & Engler, A. J. Preparation of hydrogel substrates with tunable mechanical properties. *Curr Protoc Cell Biol* Chapter 10, Unit 10 16, doi:10.1002/0471143030.cb1016s47 (2010).
251 Morsut, L. *et al.* Negative control of Smad activity by ectodermin/Tif1gamma patterns the mammalian embryo. *Development* 137, 2571-2578, doi:10.1242/dev.053801 (2010).
252 Sasso, M. S. *et al.* Low dose gemcitabine-loaded lipid nanocapsules target monocytic myeloid-derived suppressor cells and potentiate cancer immunotherapy. *Biomaterials* 96, 47-62 (2016).
253 Haverkamp, Jessica M. *et al.* Myeloid-Derived Suppressor Activity Is Mediated by Monocytic Lineages Maintained by Continuous Inhibition of Extrinsic and Intrinsic Death Pathways. *Immunity* 41, 947-959, doi:http://dx.doi.org/10.1016/j.immuni.2014.10.020 (2014).
254 Shuster, J. J. Median follow-up in clinical trials. *J Clin Oncol* 9, 191-192, doi:10.1200/jco.1991.9.1.191 (1991).
255 Marigo, I. *et al.* Tumor-induced tolerance and immune suppression depend on the C/EBPbeta transcription factor. *Immunity* 32, 790-802, doi:10.1016/j.immuni.2010.05.010 (2010).
256 Hamilton, J. A. Colony-stimulating factors in inflammation and autoimmunity. *Nat Rev Immunol* 8, 533-544, doi:10.1038/nri2356 (2008).
257 Laoui, D., Van Overmeire, E., De Baetselier, P., Van Ginderachter, J. A. & Raes, G. Functional relationship between tumor-associated macrophages and macrophage colony-stimulating factor as contributors to cancer progression. *Front Immunol* 8, 102 (2014).
258 Paszek, M. J. *et al.* Tensional homeostasis and the malignant phenotype. *Cancer Cell* 8, 241-254, doi:10.1016/j.ccr.2005.08.010 (2005).
259 Levental, I., Georges, P. C. & Janmey, P. A. Soft biological materials and their impact on cell function. *Soft Matter* 3, 299-306 (2007).
260 Humphries, J. D., Byron, A. & Humphries, M. J. Integrin ligands at a glance. *J Cell Sci* 119, 3901-3903 (2006).
261 Hynes, R. O. & Naba, A. Overview of the matrisome--an inventory of extracellular matrix constituents and functions. *Cold Spring Harb Perspect Biol* 4, a004903, doi:10.1101/cshperspect.a004903 (2012).
262 Li, Z. *et al.* Transforming growth factor-beta and substrate stiffness regulate portal fibroblast activation in culture. *Hepatology* 46, 1246-1256, doi:10.1002/hep.21792 (2007).
263 Arpino, G., Bardou, V. J., Clark, G. M. & Elledge, R. M. Infiltrating lobular carcinoma of the breast: tumor characteristics and clinical outcome. *Breast Cancer Res* 6, R149-156, doi:10.1186/bcr767 (2004).
264 Padera, T. P. *et al.* Pathology: cancer cells compress intratumour vessels. *Nature* 427, 695, doi:10.1038/427695a (2004).
265 Paszek, M. J. & Weaver, V. M. The tension mounts: mechanics meets morphogenesis and malignancy. *J Mammary Gland Biol Neoplasia* 9, 325-342, doi:10.1007/s10911-004-1404-x (2004).

266 Bak, S. P., Walters, J. J., Takeya, M., Conejo-Garcia, J. R. & Berwin, B. L. Scavenger Receptor-A–Targeted Leukocyte Depletion Inhibits Peritoneal Ovarian Tumor Progression. *Cancer Res* 67, 4783-4789, doi:10.1158/0008-5472.can-06-4410 (2007).
267 Nagai, T. *et al.* Targeting tumor-associated macrophages in an experimental glioma model with a recombinant immunotoxin to folate receptor β. *Cancer Immunol Immunother* 58, 1577-1586, doi:10.1007/s00262-009-0667-x (2009).
268 Komohara, Y., Niino, D., Ohnishi, K., Ohshima, K. & Takeya, M. Role of tumor-associated macrophages in hematological malignancies. *Pathol Int* 65, 170-176, doi:10.1111/pin.12259 (2015).
269 Horlad, H. *et al.* Corosolic acid impairs tumor development and lung metastasis by inhibiting the immunosuppressive activity of myeloid-derived suppressor cells. *Mol Nutr Food Res* 57, 1046-1054, doi:10.1002/mnfr.201200610 (2013).
270 Pienta, K. J. *et al.* Phase 2 study of carlumab (CNTO 888), a human monoclonal antibody against CC-chemokine ligand 2 (CCL2), in metastatic castration-resistant prostate cancer. *Invest New Drugs* 31, 760-768, doi:10.1007/s10637-012-9869-8 (2013).

Acknowledgements

I want to thank the director of the PhD course in Clinical and Experimental Oncology and Immunology, Prof. Paola Zanovello, who gave me the possibility to carry out my PhD in an educative, self-growth promoting and young environment.

I thank Prof. Vincenzo Bronte for having accommodated my request to work in his group at the Veneto Institute of Oncology (IOV) and for having entrusted me with such an exciting, yet challenging, research project.

I am grateful to my PhD supervisor, Ilaria Marigo, for having believed in me despite the initial difficulties, for the determination in bringing out the best one can do, for her educative contribution with scientific advices and the hours spent to review all my presentations, posters and, of course, this thesis.

I thank all my colleagues and in particular those who contributed to this work with their experiments, setups, good ideas and suggestions, always with helpfulness: Giada Pace, Stefano Ugel, Rosalinda Trovato, Francesco De Sanctis, Giacomo Desantis, Laura Morbiato, Giulio Fracasso, Cristina Anselmi, Stefania Canè.

I also thank all the collaborators who worked on parts of this project: Prof. Silvio Bicciato (University of Modena and Reggio Emilia), Matteo Fassan and Vincenza Guzzardo (University of Padova), Prof. Emilio Bria and Luisa Carbognin (University of Verona).

Within my group, I want to warmly thank Giada Pace for being a good colleague and a lovely friend who makes me laugh a lot with her spontaneity, as well as Rosalinda Trovato and Alessandra Fiore for the friendship and the memorable (mis)adventures at international conferences.

I thank all the PhD students and the people at IOV for the friendship, the laughs, the moral support in difficult moments and scientific advices, in particular Anna D.P., Anna P., Francesco C., Silvia D.S., Anna T., Vittoria R., Samantha S., Laura P., Marina V., Elena M.

I finally address a special acknowledgement to my parents for their daily support, caring about me and patience during these three years.